UNDERSTANDING AROMATASE: A MECHANISTIC BASIS FOR DRUG INTERACTIONS AND NEW INHIBITORS

Wenjie Lu

Submitted to the faculty of the University Graduate School
in partial fulfillment of the requirements
for the degree
Doctor of Philosophy
in the Department of Pharmacology and Toxicology,
Indiana University

January 2012

Accepted by the Faculty of Indiana University, in partial fulfillment of the requirements for the degree of Doctor of Philosophy.

_____

David A. Flockhart, M.D., Ph.D., Chair

_____

Zeruesenay Desta, Ph.D.

Doctoral Committee

_____

Sherry F. Queener, Ph.D.

November 17, 2011

_____

Michael R. Vasko, Ph.D.

_____

Jian-Ting Zhang, Ph.D.

ACKNOWLEDGEMENTS

I am grateful for having the opportunity to complete my Ph.D. journey in a scientifically diverse environment, where I have been able to learn from many senior scientists, especially from my mentor Dr. David Flockhart, to interact with lots of peers, including my colleagues in the Division of Clinical Pharmacology and the Department of Pharmacology & Toxicology, and also to collaborate with investigators within and outside of Indiana University. This journey would not have been possible without the support from all these people during the maturation of my research project and of my philosophy for both research and life. I am thankful to everyone who spent time with me every step of the way.

In particular, I would like to thank other members of my thesis committee, Dr. Zeruesenay Desta, Dr. Sherry Queener, Dr. Michael Vasko and Dr. Jiang-Ting Zhang for their generous advice and honest evaluation. There is no word I can find to express how deeply I appreciate their scientific guidance. The education I was fortunate to receive from these great teachers will be a tremendous resource of skills and ideas for my future career. This kind of influence has been true in my whole life, and I would like to officially thank two of my dearest old friends, my Biology teachers from elementary school and high school in my hometown: Ms. Zhang and Mr. Yao. They inspired me. They inspired me with knowledge and passion to build a lifetime basis that is the key to my devotion to Biological Sciences.

From the eighth day of August in 2007 to the end of 2011, living in Indianapolis is a significantly memorable time of my life. I feel lucky that I have met many very kind people and a lot of good friends in this unique place.

ABSTRACT

Wenjie Lu

Understanding Aromatase:

A Mechanistic Basis for Drug Interactions and New Inhibitors

Aromatase is the cytochrome P450 enzyme that converts androgens to estrogens. Aromatase is the target of the aromatase inhibitor class of drugs widely used to treat estrogen-mediated conditions including breast cancer. Little is known about the role of this enzyme in drug metabolism or in drug interactions. Since this lack of knowledge has been an impediment to optimal therapy, it is important to understand these roles of aromatase. Therefore, a comprehensive series of studies was carried out to characterize its ability to metabolize drugs and its susceptibility to inhibition by xenobiotics. The overall objective of this work was to better understand the interactions of small molecules with aromatase and to use this new knowledge to predict aromatase-mediated drug interactions and anticipate novel molecular structures that interact with the enzyme.

Aromatase was shown to be a drug metabolizing enzyme able to metabolize methadone both in vitro (K_m of 314 μM) and in vivo (22% of methadone clearance). A number of novel aromatase inhibitors that employ diverse kinetic mechanisms were identified. These include a potent competitive inhibitor: norendoxifen (K_i of 35 nM), two non-competitive inhibitors: endoxifen (K_i of 4.0 μM) and N-desmethyl-tamoxifen (K_i of 15.9 μM), a mechanism-based inhibitor: methadone (K_I of 40.6 ± 2.8 μM; k_{inact} of 0.061 ± 0.001 min^{-1}), and a stereoselective inhibitor: naringenin (IC_{50}s of 2.8 μM for (R)-enatiomer and 1.4 μM for (S)-enatiomer). Through investigation of the structure-potency

relationships so discovered, a series of new biochemical structures to be exploited as aromatase inhibitors were identified.

These studies have identified new roles for aromatase as a catalyst for methadone metabolism and as a mediator of the effects of tamoxifen by demonstrating that a number of its metabolites can act as aromatase inhibitors. This work also provides a new mechanistic framework for the design of novel aromatase inhibitors that can be used in breast cancer. Overall, the data suggest ways to more consistently treat breast cancer with current medications, to better anticipate drug interactions, and therefore to improve the quality of life of patients in ways that minimize side effects, while optimizing therapeutic benefits, in each person treated.

David A. Flockhart, M.D., Ph.D., Chair

TABLE OF CONTENTS

LIST OF TABLES

LIST OF FIGURES

ABBREVIATIONS

Φ	tissue binding factor
4HT	(Z)-4-hydroxy-tamoxifen
AAG	α_1-acid-glycoprotein
AI	aromatase inhibitor
AMISS	AI-associated musculoskeletal syndrome
AMMC	3-[2-(N,N-diethyl-N-methylamino)ethyl]-7-methoxy-4-methylcoumarin
AUC	area under the plasma concentration-time curve
BMI	body mass index
C	concentration
C_0	extrapolated initial plasma drug concentration at the time of dosing
cc	cubic centimeter
CEC	3-cyano-7-ethoxycoumarin
CL	clearance
CL_{IV}	systemic clearance of intravenously administered drug
CL_r	renal clearance of administered drug
CYP	cytochrome P450 enzyme
CYP19	aromatase
dl	deciliter
ECF	volume of the extracellular fluid
EDDP	2-ethylidene-1, 5-dimethyl-3, 3-diphenylpyrrolidine
EMDP	2-ethyl-5-methyl-3, 3-diphenylpyrroline

Endoxifen	4-hydroxy-N-desmethyl-tamoxifen
f_u	fraction unbound
FDA	food and drug administration
GWA	genome-wide association
HFC	7-hydroxytrifluoromethylcoumarin
HLMs	pooled human liver microsomes
HPLC	high performance liquid chromatography
IC_{50}	the half maximal inhibitory concentration
ICRC	Indiana University School of Medicine Clinical Research Center
ICF	volume of the intracellular fluid
kb	kilo-base pair
K_i	the equilibrium dissociation constant of the inhibitor
K_m	the Michaelis constant
K_{Sapp}	the apparent Michaelis constant
LC-MS/MS	HPLC with tandem mass spectrometry detection
LOQ	limit of quantification
MFC	7-methoxy-4-trifluoromethylcoumarin
MTD	methadone
NADPH	reduced nicotinamide adenine dinucleotide phosphate
NDMT	N-desmethyl-tamoxifen
Norendoxifen	N,N-didesmethyl-4-hydroxytamoxifen
NSAID	non-steroidal anti-inflammatory drug
rac	racemic

SD	standard deviation
SERM	selective estrogen receptor modulator
Subject “ADR”	the subject who experienced the adverse drug reaction
Subject “N”	the unaffected subject
$t_{½}$	half-life
t_{max}	time of maximum concentration
UV	ultraviolet
V_d	volume of distribution
V_{max}	the maximum reaction rate
V_{maxi}	the apparent maximum reaction rate in the presence of the inhibitor

CHAPTER ONE

Introduction and Literature Review

The cytochrome P450 enzyme family

The cytochrome P450s (CYPs) are a superfamily of enzymes. These enzymes all contain a molecule of heme non-covalently bound to the polypeptide chain. CYPs use O_2 and H^+, which is derived from the cofactor reduced nicotinamide adenine dinucleotide phosphate (NADPH), to carry out the oxidative metabolism of a number of endogenous and exogenous compounds like steroids, bile acids and drugs. In humans, there are more than 50 individual CYP isoforms (Gonzalez and Tukey 2006). The CYP genes with known functions are expressed in the endoplasmic reticulum of a number of tissues (Nelson et al. 2004). Human liver expresses important drug-metabolizing CYPs, including CYP1A1, CYP1A2, CYP2B6, CYP2C8, CYP2C9, CYP2C19, CYP2D6, CYP2E1, CYP3A4 and CYP3A5. These are the most actively studied of the drug-metabolizing enzymes since they are the responsible for metabolizing the vast majority of therapeutic xenobiotics (Gonzalez and Tukey 2006).

The activities of these CYPs determine the rate of biotransformation of a parent substrate into active and/or inactive metabolites. This process influences several subsequent outcomes including the concentration of the substrate and its metabolites that will be achieved in the body and the rate of their elimination from the body. The CYPs that catalyze steroid and bile acid synthesis have very specific substrate preferences. In contrast, the CYPs that carry out xenobiotic metabolism have the capacity to bind and metabolize a large number of structurally diverse chemicals. A single compound can also

be metabolized by different CYPs. This extensive overlapping of substrate specificities is one of the underlying causes for the predominant clinical pharmacokinetic drug-drug interactions. For example, when two coadministrated drugs are both metabolized by the active site of the same CYP, they compete for the binding site. As a result, the metabolism of one or both drugs may be inhibited and this can lead to increased clinical exposure to the parent drug and decreased exposure to the metabolites. The activity of CYPs can also be influenced by factors other than co-medication, including environmental and genetic factors.

Aromatase and its role in steroidogenesis

The CYP that converts androgens to estrogens is CYP19, also known as aromatase (Chen 1998). Aromatase has been recognized as a key enzyme in steroidogenesis as it is the only enzyme responsible for the demethylation and subsequent aromatization of testosterone to estradiol and androstenedione to estrone.

Aromatase expression and variability in aromatase activity

Unlike most of the important CYPs, aromatase is not highly expressed in healthy human livers (Carruba 2009) and hepatic aromatase activity is minimal. In premenopausal women, aromatase activity is high in the ovaries. Estrogens produced in the ovaries are important hormones that can circulate and act on distal estrogen receptors in the target tissues. In postmenopausal women and men, estradiol is primarily synthesized in extragonadal tissues where it also serves locally as a paracrine, autocrine or intracrine factor. Aromatase is expressed in these extragonadal sites including

osteoblasts and chondrocytes of bone, mesenchymal cells of breast and other adipose tissue, the vascular endothelium, aortic smooth muscle cells, and numerous sites in the brain (Simpson 2003).

Aromatase is coded by the gene *CYP19A1*, which is located on chromosome 15q21.1 in humans. This gene spans 120 kb and it has a large and complex upstream regulatory unit comprising untranslated exon I and a number of promoters, and a 30 kb coding region consisting of nine translated exons II to X (Simpson 2003). Untranslated exon I is associated with at least 10 different tissue–specific promoters. Since the exon I is not translated, the translated protein product are identical in all the tissues. Each tissues utilizes its own promoters and associated enhancers and suppressors to express a unique untranslated first exon 5'-UTR (Simpson and Davis 2001; Sebastian and Bulun 2001; Bulun et al. 2003). This differential splicing process leads to different amounts of mRNA transcripts, differences in mRNA stability and protein translation (Simpson and Davis 2001; Santen et al. 2009; Wang, Li, and Hu 2009). As a result, this process defines the tissue-specific regulation of aromatase activity and estrogen biosynthesis.

Since aromatase expression is present in many tissues and its regulation is complex, the enzyme activity has been shown to vary with a lot of factors including gender (Labrie et al. 1997), menstrual cycle (Sano et al. 1981), age (Labrie et al. 1997; Grow 2002), weight (Yousefi et al. 2011) and ethnicity (Marsh et al. 2011). The enzyme activity is also influenced by genetic variants. The most widely studied is a tetranucleotide (TTTA)n tandem repeat polymorphism located in intron 4 of the human *CYP19A1* gene, and it has been reported that the number of TTTA repeats is associated with estrogen concentrations and risks for several estrogen-regulated diseases (Somner et

al. 2004; Gennari et al. 2004; Ahsan et al. 2005; Kristensen et al. 2000; Masi et al. 2001). There have also been a few reports of a rare autosomal recessive disease, human aromatase deficiency, caused by loss-of-function mutations in the *CYP19A1* gene (Bulun 2000; Belgorosky et al. 2009; Rochira and Carani 2009). In addition, aromatase activity may be influenced by many extrinsic factors such as herbal supplements (Wang et al. 2009), red wine (Eng et al. 2003), calcitriol (Krishnan and Feldman 2011), myosmine (Doering and Richter 2009), and environmental toxins like phthalates (Toda et al. 2003).

Aromatase as a target of endocrine therapy for breast cancer

Aromatase expression and activity has been shown to be enhanced in various cancers, including breast tumors, hepatocellular carcinoma, adrenocortical tumors and testicular tumors (Bulun and Simpson 2008; Jongen et al. 2006; Carruba 2009; Bulun et al. 1997; Young et al. 1996; Aiginger et al. 1981). Local paracrine and/or intracrine estrogen signaling is believed to stimulate the progression and recurrence of the disease, particularly in the case of breast cancer. About 70 - 80% of all newly diagnosed breast cancers are positive for the estrogen receptor (Hammond et al. 2010). The total number worldwide is more than one million every year. Peripheral estrogen synthesis by aromatase is the primary pathway for the production of estrogen in women after ovarian function subsides during menopause or after another pathological change or medical intervention that reduces or eliminates ovarian function. For this reason, the enzyme aromatase represents an important target of many therapies that are designed to treat post-menopausal estrogen-dependent breast cancer by reducing estrogen concentrations, and thereby reducing the growth of breast tumors and patients' risk for recurrent breast

cancer. Of note, in premenopausal women aromatase inhibitors do not suppress estrogen concentrations because their ovarian-pituitary feedback loop prevents effective suppression of the enzyme activity. In fact, aromatase inhibition has been an effective endocrine therapy for other estrogen-mediated conditions. For example, the enzyme can be valuably targeted as part of treatments for infertility in premenopausal women in whom reduction of systemic estrogen is used to stimulate pituitary function and increase ovarian function (Pritts 2010).

Two classes of drugs have been effective and widely used in treating hormone receptor positive breast cancer (Burstein et al. 2010; Osborne, Zhao, and Fuqua 2000): aromatase inhibitors (AIs) and selective estrogen receptor modulators (SERMs). While AIs operate by reducing peripheral estrogen generation, SERMs reduce estrogenic effects by antagonism of estrogen binding to the estrogen receptors (Figure 1.1). The most widely used SERM, tamoxifen, reduces the risk for recurrence and mortality in women with estrogen-sensitive breast cancer by 40% (Early Breast Cancer Trialists' Collaborative Group 2005). Over the last decade, large definitive trials have demonstrated that therapy with AIs is more effective than tamoxifen treatment in both the metastatic and adjuvant settings, but the absolute benefit relative to tamoxifen is only 2-4% (Cuzick et al. 2010). On the basis of trials such as these, AIs have become the standard of care for the treatment of endocrine-responsive breast cancer in post-menopausal women.

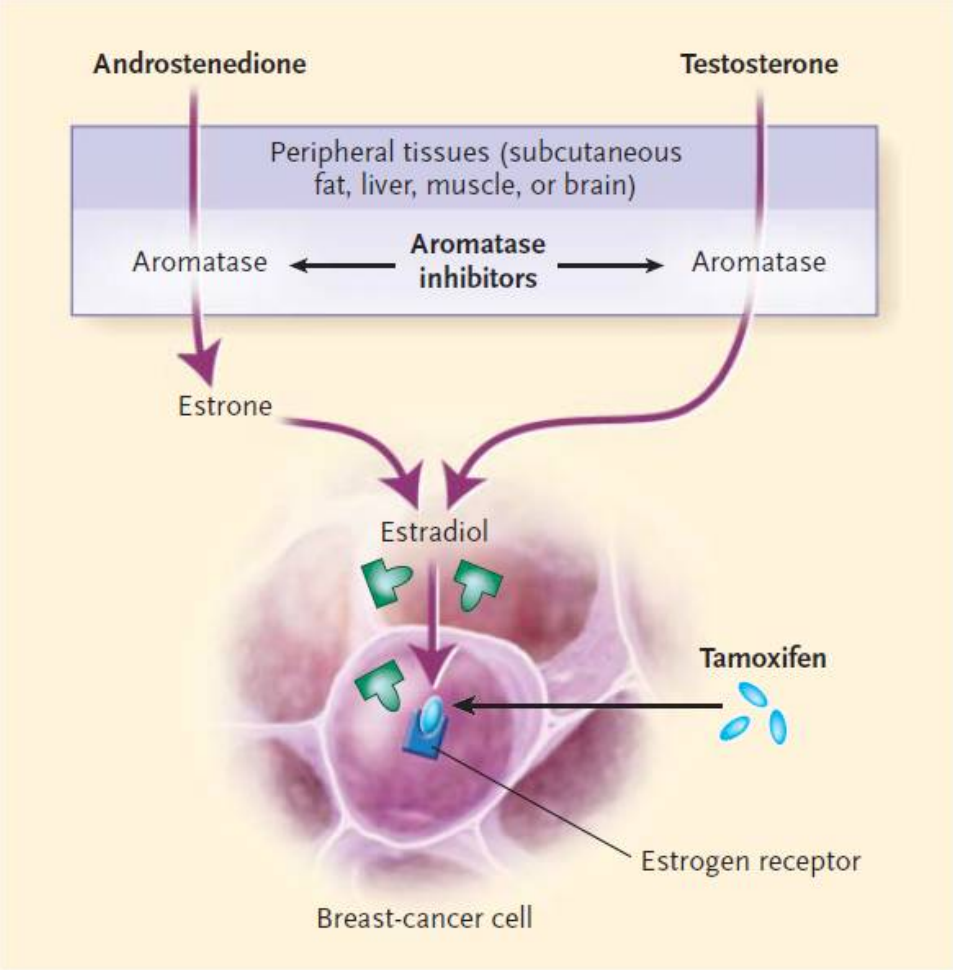

Figure 1.1. Mechanism of action of aromatase inhibitors and SERM tamoxifen.

The AIs reduce peripheral estrogen generation by blocking aromatase activity. The SERMs reduce estrogenic signaling by antagonism of estrogen binding to the estrogen receptors. Source: with permission from Smith et al. 2003 (see Appendix).

Efficacy and toxicity profiles of current aromatase inhibitors

There are three aromatase inhibitors currently on the market: the azoles, anastrozole (Arimidex™) and letrozole (Femara™), which are potent competitive inhibitors, and the steroidal compound, exemestane (Aromasin™), which is a

mechanism-based inhibitor. These are the third-generation AIs. They are more selective and more clinically efficacious than the first-generation AI aminoglutethimide and the second-generation AIs formestane, fadrozole and rogletimide (Smith and Dowsett 2003). All third generation AIs decrease circulating estrogen concentrations by at least ten-fold compared to concentrations before treatment in untreated postmenopausal women. They have also been shown in large clinical trials to reduce the risk for breast cancer recurrence in post-menopausal women with estrogen-sensitive breast cancer by about 50% (Cuzick et al. 2010).

Despite their efficacy, therapy with current AIs results in marked side effects that make the drugs difficult to tolerate for the 2 - 5 years required for effective breast cancer treatment (Figure 1.2). Toxicities are one of the major reasons for discontinuation of AIs, and the most common adherence-limiting toxicity is the AI-associated musculoskeletal syndrome, or AIMSS (Henry et al. 2008; Henry, Giles, and Stearns 2008; Crew et al. 2007; Morales et al. 2004; Land et al. 2006). This syndrome consists of a constellation of musculoskeletal symptoms, including generalized arthralgias, trigger finger, digital stiffness, carpal tunnel syndrome, or tendinitis/tendinopathy that occur in the absence of any alternative reason for development of these symptoms, such as trauma, pre-existing rheumatoid arthritis, or other definable causes. Earlier studies suggest that AIMSS is the reason for recorded discontinuation in 10 - 20% of all patients taking an aromatase inhibitor (Henry et al. 2008; Land et al. 2006). In a more recent survey (1,199 women), about 60% patients experienced debilitating side effects and AIMSS was the reason for discontinuation in ~ 75% of those who stopped the drug (Zivian and Salgado 2008).

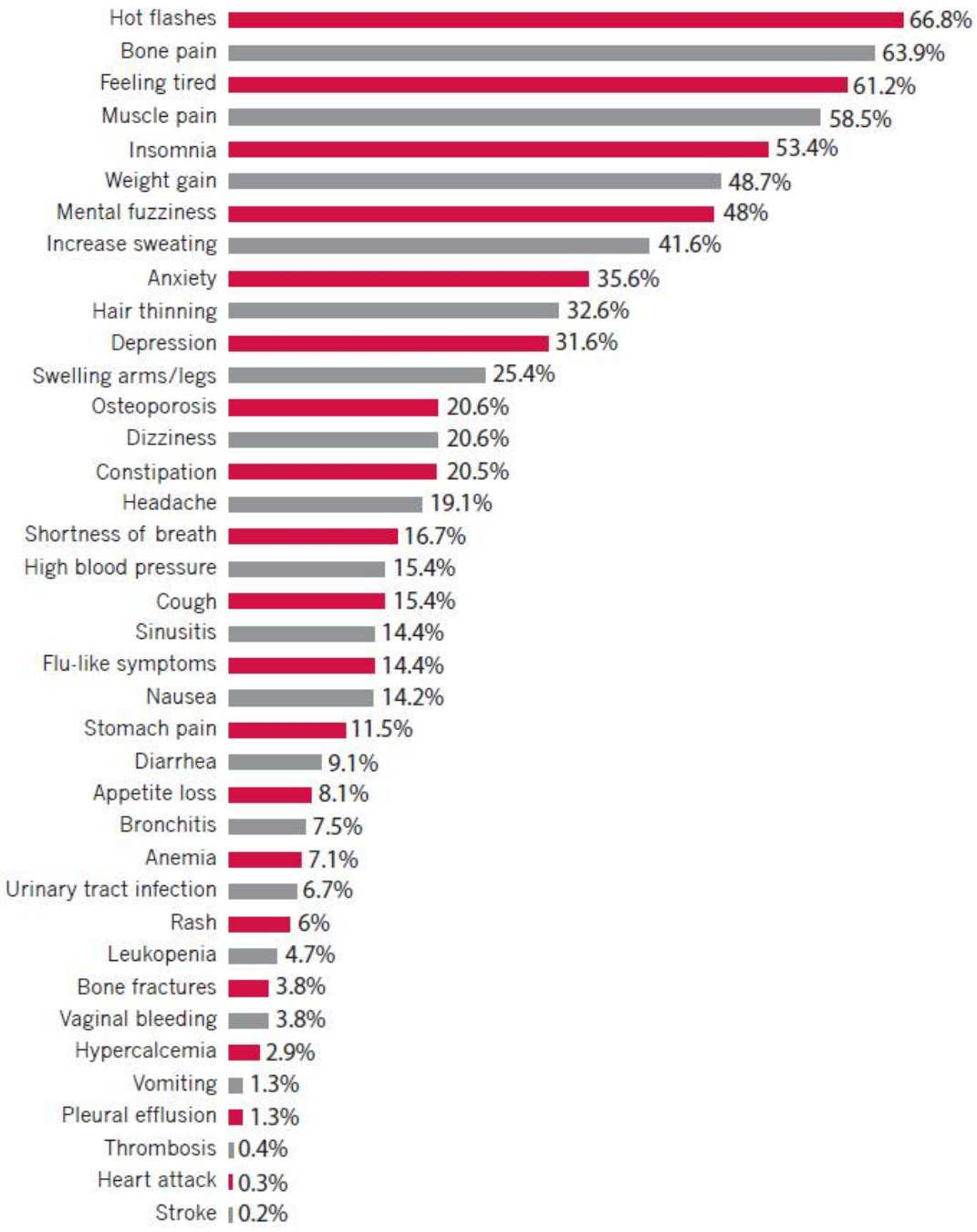

Figure 1.2. Side effects of current AIs reported by breast cancer patients.

The AI-associated musculoskeletal toxicities such as muscle pain and bone pain were the reason for discontinuation in ~ 75% of those who stopped taking the drug. Source: with permission from Zivian and Salgado 2008 (see Appendix).

While the available AIs reduce the recurrence of breast cancer, they do not eliminate recurrence. About 50% of patients treated with AIs still developed recurrent cancer (Cuzick et al. 2010). Furthermore, the positive effects of AIs come at the price of numerous side effects, which reduce compliance with therapy, reduce the quality of life of breast cancer patients and also decrease overall disease-free survival (Oberguggenberger et al. 2011; Zivian and Salgado 2008; Ziller et al. 2009; Partridge et al. 2008; Hershman et al. 2010). In a recent systemic review and meta-analysis of seven randomized controlled trials that compared AIs with tamoxifen as primary adjuvant endocrine therapy in postmenopausal women (a total of 30023 patients), treatment with current AIs was found to be associated with increased odds of developing cardiovascular disease and bone fractures that were major causes of death in this patient population (Amir et al. 2011). These cumulative toxicities of current AIs significantly reduced the survival benefit to this therapy despite improvements in cancer-free survival. Thus, there remains a need for developing more tolerable and effective drugs with better risk/benefit profile as the next generation of AIs.

Aromatase inhibition therapy has also been shown to be effective in the prevention of the first occurrence of breast cancer. In a study of 4560 postmenopausal women who were at moderately increased risk for breast cancer, therapy with one of the available AIs, exemestane, was associated with a 65% relative reduction in the annual incidence of invasive breast cancer (Goss et al. 2011). It follows that improved AIs that are less toxic and easier to take could be better treatment options in a preventive setting for women at risk.

In addition, aromatase inhibitors are being explored as therapies for a number of other estrogen-related conditions. A recent study suggested that aromatase inhibition could be utilized as a better therapy for refractory endometriosis-related chronic pelvic pain than conventional treatments (Abushahin et al. 2011).

Evidence suggesting a broader role for aromatase in xenobiotic disposition

The conversion of androgens to estrogens by aromatase is a key step in steroidogenesis, but this may not be the only important role that this enzyme plays in humans. Although aromatase has been widely recognized as an enzyme that "has strict substrate requirements and does not participate in xenobiotic or drug metabolism" (quoted from Gonzalez and Tukey 2006), emerging evidence suggests that this enzyme may also interact with xenobiotics, such as medications, dietary compounds and even environmental toxins. The clinical relevance of these interactions remains unclear.

Possible involvement in drug metabolism and drug interactions

Placental aromatase is able to metabolize methadone (Nanovskaya et al. 2004), cocaine (Osawa et al. 1993), and buprenorphine (Deshmukh, Nanovskaya, and Ahmed 2003) in vitro, but the role of aromatase in drug metabolism in general has not been carefully investigated. The biochemical mechanism by which aromatase catalyzes the metabolism of testosterone or androstenedione employs 3 moles of O_2 and 3 moles of NADPH for every mole of estrogen generated, and it involves three successive hydroxylations of the 19-methyl group of the androgens followed by the removal of this methyl group (Simpson et al. 2002) (Figure 1.3). Since it has been shown that aromatase

is able to remove a methyl group from cocaine and buprenorphine, it follows that other medications of similar structure and class may also be aromatase substrates.

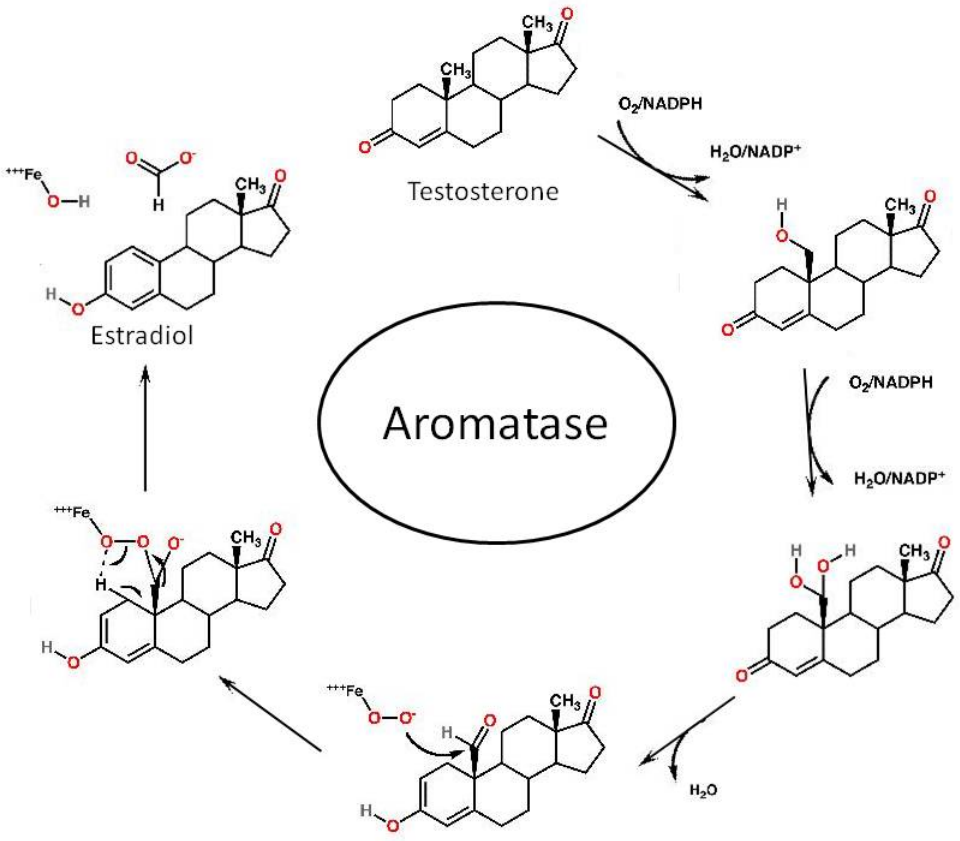

Figure 1.3. Demethylation of testosterone by aromatase.

Source: modified from Vaz 2003.

Aromatase has activity in many tissues. Therefore it is possible that the aggregate of this activity contributes significantly to drug metabolism in vivo. For example, methadone is a drug that undergoes demethylation and that has large inter-individual variability in its clearance, and the enzymatic route by which this reaction occurs in the human body is controversial (Shiran et al. 2009). Women metabolize methadone faster

than men (Baselt and Casarett 1972), and methadone clearance is significantly increased during pregnancy, when placental aromatase has high activity (Flockhart et al. 2009; Nanovskaya et al. 2004). This evidence all points to a possible role for aromatase in the metabolism of methadone and other drugs subject to demethylation.

Since it is possible that aromatase contributes to human drug metabolism, co-administration of aromatase inhibitors, particularly in patients with breast cancer, may result in pharmacokinetic drug-drug interactions that decrease the elimination of those drugs metabolized by aromatase and thereby lead to unfavorable pharmacodynamic effects at standard doses.

Aromatase inhibition may also alter the metabolism of endogenous testosterone and androstenedione. This change might lead to indirect effects on up- or down-regulation of gene expression brought about by changes in the androgen and estrogen signaling pathways. These effects include the regulation of the expression of other drug metabolizing enzymes, drug transporters and even receptors, all of which might in turn contribute to undesirable drug side effects and/or alterations in drug disposition. It follows that aromatase may play an important role in drug metabolism and drug interactions.

The active search for new aromatase inhibitors

Since the current AIs are drugs that inhibit aromatase activity in the human body by binding to the active site of the enzyme, it is possible that other xenobiotics might also affect the enzyme activity in the similar way. The currently available AIs (letrozole, anastrozole, and exemestane) bring about side effects that limit patients' compliance with

treatment (Hershman et al. 2010; Ziller et al. 2009; Partridge et al. 2008), and thus cause higher rates of breast cancer recurrence (Thompson et al. 2010). As a result, there is a recognized need for next generation inhibitors (Muftuoglu and Mustata 2010).

A large number of investigators have invested significant effort in the search for novel structures and mechanisms that bring about adequate aromatase inhibition, while limiting side effects. More than a decade ago, a chemopreventive synthetic retinoid was reported to inhibit aromatase activity (Ciolino, Wang, and Sathyamoorthy 2000). Later, researchers found that phytochemicals in white button mushrooms, especially the unsaturated fatty acids linoleic acid and linolenic acid, have anti-aromatase activity (Chen et al. 2006). More and more studies have emerged in the last two years. Ellagitannins, a class of compounds found in pomegranate fruit, were extracted and tested, and derivatives were reported as potential aromatase inhibitors (Adams et al. 2010). Retinol and all-trans retinoic acid and several 7-substituted-4-imidazolylflavans based on the structure of natural flavonoids were shown to interact with aromatase (Yahiaoui et al. 2011; Ciolino, Dai, and Nair 2011). Resveratrol and a series of synthesized new resveratrol analogues were characterized for their ability to inhibit aromatase, and one compound was suggested as a new promising aromatase inhibitor (Sun et al. 2010). This search remains active, and in contrast to conventional thinking, it is clear that aromatase, a catalyst of endogenous steroid metabolism, has the structural ability to interact with a large number of xenobiotics.

Summary

Aromatase is an important cytochrome P450 enzyme that converts androgens to estrogens. Since estrogens drive breast cancer proliferation, aromatase is also the target of the aromatase inhibitor class of drugs used to treat breast cancer. While the available AIs are effective, they bring about severe side effects that reduce the quality of life of breast cancer patients, reduce compliance with therapy and also cause cardiovascular and musculoskeletal toxicities, which bring down the overall survival of breast cancer patients. There is a need for effective and more tolerable drugs with better risk/benefit profile as the next generation of aromatase inhibitors. In addition, little is known about the role of aromatase in xenobiotic drug metabolism, or in drug interactions. As a result, optimal therapy with AIs could be compromised by unpredictable adverse events and reductions in efficacy that result.

Research aims

My *long-term goal* is to improve the treatment of breast cancer by optimizing the use of medications in ways that minimize side effects, while optimizing therapeutic benefits, in each person treated. The primary objective of my work is to better understand the interactions of small molecules with aromatase and to use this new knowledge to predict aromatase-mediated drug interactions and anticipate novel molecular structures that interact with the enzyme. Since aromatase is able to remove a methyl group from androgens to generate estrogens, I selected for study a group of drugs that (1) similarly undergo demethylation, and (2) are commonly prescribed to breast cancer patients and therefore are clinically relevant.

The *overall hypothesis* of this work is that aromatase interacts with a group of selected xenobiotics and therefore plays important roles in xenobiotic disposition and action in breast cancer. The *specific objective* of this research is to investigate 1) the ability of aromatase to metabolize drugs and possible involvement in pharmacokinetic drug-drug interactions that may result in significant clinical effects; 2) the effects of a selected series of xenobiotic compounds and their metabolites on aromatase activity. The specific objective will be tested through the following *specific aims*:

Specific aim 1: To test the ability of aromatase to metabolize methadone and determine its quantitative contribution to methadone clearance in humans.

Specific aim 2: To test the ability of a select group of compounds to inhibit aromatase activity.

Significance

The studies described herein may have clinical implications. Breast cancer is the most common cancer in women and one of the leading causes of death worldwide (Ferlay et al. 2010), and aromatase inhibitors are widely used as effective agents in the treatment of this disease. The translational relevance of this work includes new insights into drugs that are metabolized by aromatase, and that interact with it as inhibitors, and these findings have the potential to improve the use of methadone, and of the AI class of drugs, both of which are commonly co-prescribed with a wide range of other medications. As a result, it may be possible to more consistently treat breast cancer with current medications, and to better anticipate drug interactions. It also provides new insights into xenobiotic-aromatase interactions that illuminate potential alternative AIs.

Overall, this study could allow a better understanding of the involvement of aromatase in xenobiotic disposition and effects. This research will create a robust scientific knowledge base upon which to build future studies that address the importance of aromatase as a target for drug interactions, and that improve the rational prescribing database involving aromatase inhibitors.

CHAPTER TWO

Metabolism of Methadone by Aromatase In Vitro

Introduction

Methadone is a synthetic analgesic that is distinguished by its long duration of action, a property that makes it ideal for the treatment of chronic pain and for opioid withdrawal (Fredheim et al. 2008). Prescriptions in the United States have grown by 1300% between 1997 and 2006 (Kharasch et al. 2009), primarily as the result of increasing use as a first-line analgesic. In addition, methadone maintenance therapy is the mainstay for the treatment of opioid addiction, but it is estimated that fewer than 10% of individuals who are addicted to heroin and prescription opioids are actually receiving methadone (Kleber 2008).

Despite its advantages and widespread utility, the use of methadone is limited by complex pharmacokinetic characteristics that include a long elimination half-life and susceptibility to pharmacokinetic drug-drug interactions (Weschules, Bain, and Richeimer 2008). The goal of predictable, reproducible and effective dosing is confounded by considerable inter-individual variability in methadone pharmacokinetics, particularly in its clearance (up to 100-fold, Totah et al. 2008). This variability is further complicated by stereoselectivity in methadone pharmacokinetics. While methadone is generally administered as a racemic mixture, consisting of equal amount of two enantiomers; the (R)-, levo-, 1-or (+) and the (S)-, dextro-, d- or (-) methadone, these enantiomers differ in pharmacokinetic and pharmacodynamic properties. The unpredictability of methadone's effects due to these multiple characteristics results in a

high incidence of over- and under-dosing. Inappropriate dosing can clearly cause severe adverse events such as withdrawal symptoms, respiratory depression, and electrocardiographic QT interval prolongation that can result in sudden cardiac death (Sims, Snow, and Porucznik 2007; Kharasch et al. 2009; Kalgutkar, Obach, and Maurer 2007; Krantz et al. 2003).

Although methadone has been used for more than seventy years, the metabolism of methadone in the human body is still not fully understood and the effective and safe dose among patients is highly variable. It is suspected that the variability in methadone clearance and the frequent under- or over-dosing are results of a wide distribution of the rate of methadone metabolism. The metabolism of methadone to its primary demethylated metabolite, EDDP, and then to its secondary metabolite, EMDP (Figure 2.1), is well documented as the major metabolic pathway (Pohland, Boaz, and Sullivan 1971; Sullivan and Due 1973), but the enzymatic route by which these reactions occur in the body is controversial (Shiran et al. 2009). Since understanding of the metabolic pathways responsible for drug interactions or environmental effects is incomplete (Weschules, Bain, and Richeimer 2008), it is difficult to predict methadone pharmacokinetics, and adverse events during methadone therapy are frequent. Patients taking methadone are often co-prescribed many other medications and are therefore vulnerable to drug-drug interactions (Weschules, Bain, and Richeimer 2008). Poorly understood drug-drug interactions may thus contribute to the notable increase in methadone-related deaths (Sims, Snow, and Porucznik 2007) that has attended the increase in the drug's use over the past decade (Kharasch et al. 2009).

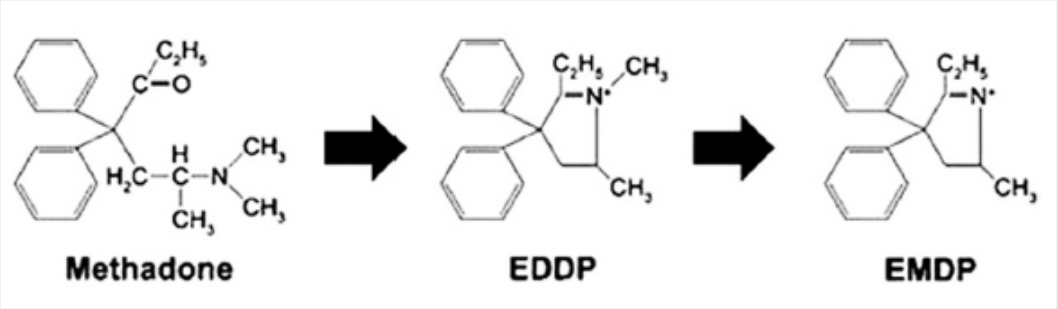

Figure 2.1. Dominant route of methadone metabolism.

Methadone is N-demethylated to the primary metabolite, EDDP, and EDDP is further N-demethylated to the secondary metabolite, EMDP. Source: drawn based on results from (Sullivan and Due 1973).

There is a need to improve our understanding of methadone metabolic pathways. While potential interactions with methadone via CYP3A and CYP2B6 have been carefully studied in vitro (Iribarne et al. 1997; Foster, Somogyi, and Bochner 1999; Wang and DeVane 2003; Kharasch et al. 2004) and in vivo (Eap, Buclin, and Baumann 2002; Totah et al. 2008), it is clear that these enzymes cannot fully explain the large variability in methadone pharmacokinetics. Other potential routes of metabolism may be important. Previous studies suggested that placental aromatase may be responsible for the increased methadone clearance in pregnant women (Hieronymus et al. 2006; Nanovskaya et al. 2004). However, drug interactions involving drugs that alter methadone clearance via aromatase have not been described or tested for. Patients with metastatic breast cancer who are in pain may often be co-prescribed methadone with a potent aromatase inhibitor, and may therefore be at risk for interactions between these two drugs. To better understand the role aromatase plays in methadone metabolism, I tested the hypothesis that aromatase is able to metabolize methadone to its primary metabolite, EDDP.

Results

The ability of recombinant human aromatase to metabolize methadone was tested using microsomal incubations in vitro. The metabolism of methadone by pooled human liver microsomes (HLMs) was used as a positive control. Metabolism of methadone (1000 μM) to EDDP by both recombinant human aromatase and HLMs was observed (Figure 2.2). A selective aromatase inhibitor, letrozole, was used to completely block aromatase activity as a control. In human liver microsomes, letrozole (50 nM) lowered EDDP formation from methadone (10 μM) by ~ 7%, whereas in recombinant aromatase letrozole at this concentration reduced EDDP formation by ~ 65%. Most important of all, the enzyme in the recombinant aromatase microsomal preparation that converts methadone to EDDP was confirmed to be aromatase because the conversion of methadone to EDDP was completely inhibited by 1 μM of letrozole.

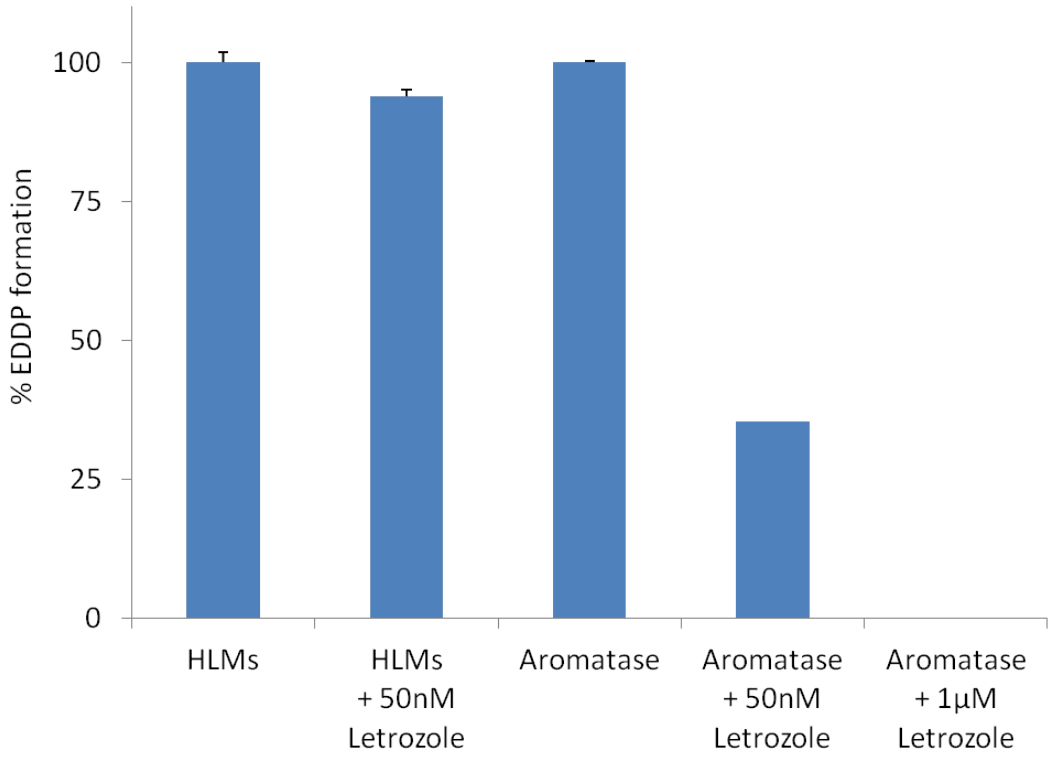

Figure 2.2. Both human liver CYP enzymes and aromatase can contribute to the primary metabolism of methadone.

Percent of EDDP formation from methadone relative to controls without letrozole (Columns 1 and 3 from the left). Human liver or recombinant aromatase microsomal preparations were incubated with methadone (10 µM) for 30 min at 37 ^{o}C and the amount of EDDP generated was determined by LC-MS/MS.

The logical next step was to characterize the metabolism of methadone by aromatase and these experiments were then carried out under conditions where secondary metabolism from EDDP to EMDP was not detected. Figure 2.3 depicts the rate of EDDP generation from methadone across a range of methadone concentrations (0 - 2000 µM). These data indicate metabolism of methadone to EDDP by recombinant human

aromatase with a K_m of 314 µM and a V_{max} of 7.6 pmol/min/pmol of P450. When the (R)- and (S)-enantiomers of methadone were separately tested, no stereoselectivity was observed (Figure 2.4).

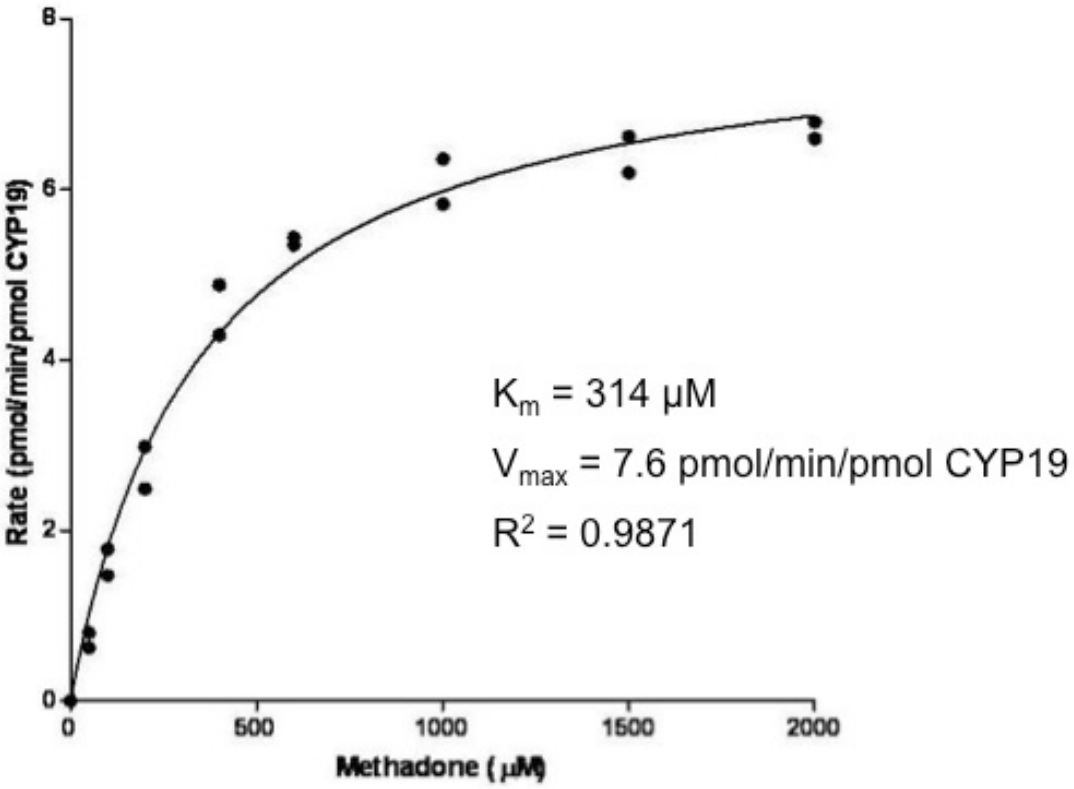

Figure 2.3. Michaelis-Menten kinetics of methadone metabolism by recombinant human aromatase.

A range of racemic methadone concentrations was incubated with recombinant aromatase (0.05 µM) for 30 min, and the amounts of EDDP generated were determined using HPLC in three independent experiments. Individual points represent the mean of duplicate incubations.

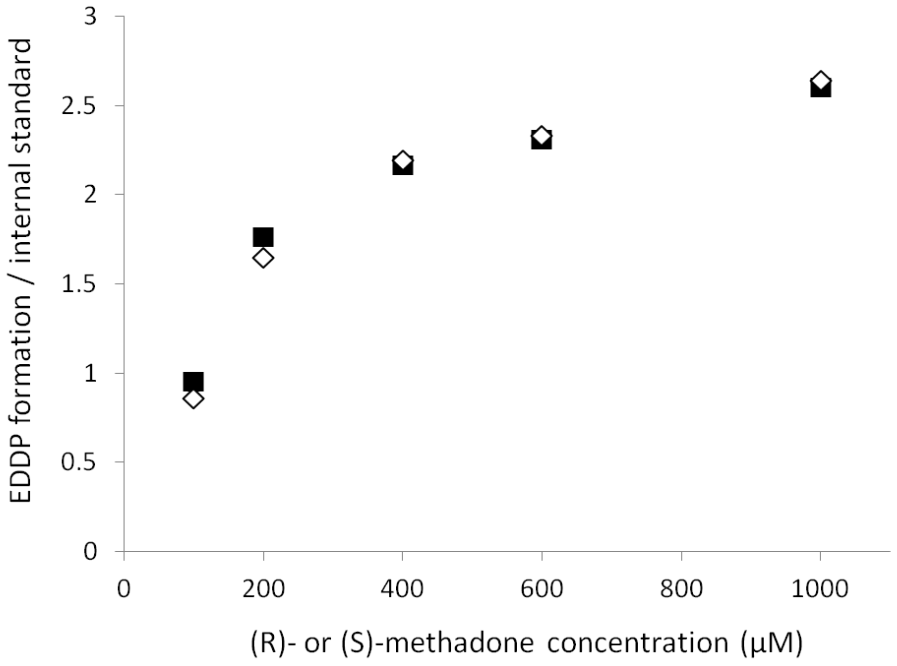

Figure 2.4. Metabolism of methadone by human aromatase was not stereoselective.

A range of (R)-methadone (dark square) or (S)-methadone (open diamond) concentrations was incubated with recombinant aromatase (0.05 μM) for 30 min, and the amounts of EDDP generated were determined using HPLC. Individual points represent the mean of duplicate incubations.

Discussion

The effective use of methadone in the treatment of pain and heroin addiction is compromised by poor understanding of the metabolic routes involved in its disposition. One direct consequence is the inability to anticipate drug interactions in patient populations who are commonly co-prescribed multiple medications. For years, methadone metabolism has been widely attributed to CYP3A4 (Iribarne et al. 1997), and

this body of science is reflected in the current FDA-approved label for methadone, which states in part:

> "Since the metabolism of methadone is mediated primarily by the CYP3A4 isozyme, coadministration of drugs that inhibit CYP3A4 activity may cause decreased clearance of methadone. Thus, methadone-treated patients coadministered strong inhibitors of CYP3A4, such as azole antifungal agents (e.g., ketoconazole) and macrolide antibiotics (e.g., erythromycin), with methadone should be carefully monitored and dosage adjustment should be undertaken if warranted."

The scientific basis of this recommendation has been challenged by recent clinical data that provide strong and unambiguous evidence against the involvement of this enzyme (Kharasch et al. 2008; Kharasch et al. 2009). An assessment of clinical CYP3A activity and methadone clearance in normal volunteers showed that CYP3A inhibition by ritonavir (a potent CYP3A4 inhibitor that caused > 90% inhibition) had no effect on methadone plasma concentrations or clearance (Kharasch et al. 2008). Variability in CYP3A4 activity also had modest influence on the oral clearance of methadone and its enantiomers (Shiran et al. 2009). Most notably, there was no correlation between intravenous methadone clearance and hepatic CYP3A activity, and none between oral methadone apparent clearance and first-pass CYP3A activity (Kharasch et al. 2009). This in vivo evidence strongly supports the notion that the role of CYP3A in clinical methadone clearance is not critical and that other CYPs may be more important.

In our study, aromatase has been demonstrated as an alternative enzyme that is able to metabolize methadone. We showed that human recombinant aromatase metabolized methadone to the dominant metabolites that are observed in humans and that this conversion can be completely blocked by the selective aromatase inhibitor letrozole. These data are consistent with the earlier reports that suggest methadone metabolism by

human placental aromatase (Nanovskaya et al. 2004; Hieronymus et al. 2006). This finding may be important. First, it is possible that aromatase contributes to the clearance of methadone in vivo. However, our observed K_m value in the recombinant system is high compared to plasma methadone concentrations within therapeutic range in patients (Eap, Buclin, and Baumann 2002), the clinical relevance of aromatase and the extent to which aromatase metabolizes methadone in general is unclear. Second, the data showing that methadone metabolism by HLMs was not substantially inhibited by letrozole are consistent with the fact that aromatase is expressed at a low level in human liver (Carruba 2009). However, aromatase does have high activity in many other tissues (Simpson et al. 2002), and methadone has a high volume of distribution that varies from 1.0 to 8.0 L/kg (FDA label for methadone) reflecting its distribution to many tissues. Therefore, metabolism of methadone by aromatase in tissues where methadone accumulates in vivo would seem possible. Fourth, since withdrawal from methadone is often idiosyncratic and is poorly understood, the possibility of patients having variable aromatase activity that leads to different rate of methadone elimination deserves further studies. With that said, methadone metabolism by other liver CYP450 enzymes could be largely responsible for the variability seen in methadone clearance, and the role of aromatase might be important in patients who either have low liver metabolism of methadone or have relatively high aromatase activity. In addition, since the biochemical aromatization of testosterone by aromatase is initiated by the removal of a methyl group, and since aromatase is also able to remove methyl groups from methadone, cocaine (Osawa et al. 1997), and buprenorphine (Deshmukh, Nanovskaya, and Ahmed 2003), it is possible that aromatase is involved in the demethylation of other drugs.

In summary, this study has shown that aromatase is able to demethylate methadone in vitro. The clinical relevance of this metabolic pathway, its quantitative contribution to methadone clearance in humans, and the involvement of aromatase in overall methadone disposition are unclear, and further studies that are designed to address these questions are discussed in the next chapter.

Methods

Methadone metabolism in vitro by recombinant aromatase

All incubations were carried out as described in "Chapter Ten: General Methods / Testosterone and methadone metabolism in vitro by recombinant aromatase".

Quantification of EDDP formation

High performance liquid chromatography (HPLC) assays with ultraviolet (UV) detection were developed for the quantification of methadone conversion to EDDP as described in "Chapter Ten: General Methods / HPLC-UV assays for the quantifications of estradiol and EDDP formation".

Kinetic analyses

Formation rates of metabolite at different substrate concentrations were fit to appropriate enzyme kinetic models using SigmaPlot (Version 10.0, Systat software, Port Richmond, CA). Data were best fit to a one site Michaelis-Menten equation.

Note: The work described in this chapter has been published (Lu et al. 2010).

CHAPTER THREE

Metabolism of Methadone by Aromatase in Humans

Introduction

Methadone is of particular value to patients who require long-term treatment of chronic pain and opioid addiction. Despite its acknowledged value, methadone is subject to highly variable pharmacokinetics (Weschules, Bain, and Richeimer 2008; Eap, Buclin, and Baumann 2002). As a result initial dosing requirements and subsequent adjustments are difficult to anticipate, and inappropriate dosing can clearly cause severe adverse events (Modesto-Lowe, Brooks, and Petry 2010; Corkery et al. 2004; Latowsky 2006; Krantz et al. 2003). A rational approach to methadone dose estimation or adjustment during therapy based on the understanding of the pathways of methadone disposition still needs to be developed. Improved understanding of methadone disposition requires knowledge of the enzymes involved in its metabolism in humans. Many enzymes have been proposed to be involved, including CYP1A2, CYP2B6, CYP2C8, CYP2C9, CYP2C19, CYP2D6, CYP3A and aromatase (Kharasch et al. 2008; Kharasch et al. 2009; Shiran et al. 2009; Totah et al. 2008; Chang et al. 2011; Wang and DeVane 2003; Hieronymus et al. 2006), but few of these has been definitively demonstrated to be involved in vivo. For example, CYP2B6 plays an important role in methadone metabolism (Totah et al. 2008; Crettol et al. 2005; Wang et al. 2011) but CYP3A does not (Kharasch et al. 2008; Kharasch et al. 2009); yet, it is equally clear that CYP2B6 cannot explain all of the variability in methadone disposition and effects (Chang et al. 2011; Crettol et al. 2005). For this reason, other possibilities have been explored and a

number of lines of evidence point to the involvement of aromatase (Chapter One, this dissertation), an enzyme previously thought to be involved exclusively in endogenous steroidogenesis.

My previous work has shown that methadone can be metabolized by recombinant human aromatase in vitro (Chapter Two, this dissertation). The metabolic routes involved in methadone disposition are unclear and previous studies in vitro suggest that metabolism by aromatase may contribute (K_m of 314 μM, V_{max} of 7.6 pmol/min/pmol of P450; single-site Michaels-Menden model). These data were determined in a recombinant system. It is difficult to extrapolate in vitro binding affinity to clinical predictions, especially with drugs such as methadone that are concentrated in tissues (Inturrisi et al. 1987). The contribution, if any, of aromatase to the metabolism of methadone in clinical settings has not been determined. The possibility exists that aromatase contributes significantly to the metabolism of methadone, and that the inter-individual variability seen in methadone pharmacokinetics may be explained in part by variability in aromatase activity.

Aromatase activity is highly variable. It is the enzyme responsible for the conversion of endogenous androgens to estrogens, and its regulation and expression have been the subjects of intense study (Simpson et al. 2002; Simpson 2003; Czajka-Oraniec and Simpson 2010). The activity of the enzyme varies considerably between men and women (Labrie et al. 1997), with age (Grow 2002; Labrie et al. 1997), with the menstrual cycle (Sano et al. 1981) and with weight (Yousefi et al. 2011). In addition, its activity may be influenced by many extrinsic factors including herbal supplements (Wang et al. 2009), and calcitriol (Krishnan and Feldman 2011). In order to address whether or not

aromatase can metabolize methadone in humans, the ability of aromatase to demethylate methadone in tissues should be examined. Since aromatase is present in many tissues including adipose tissue, breast, bone, brain, liver and blood vessels (Simpson et al. 2002), it is difficult, if not impossible, to assess the overall contribution of this enzyme to systemic drug clearance using in vitro studies conducted in any individual tissue. For this reason, clinical studies are the ideal means with which to address the involvement of aromatase in the elimination of methadone in a quantitative manner.

Aromatase is the target of the aromatase inhibitor class of drugs now routinely used to reduce circulating estrogens in the treatment of breast cancer and a number of other conditions. The availability of these potent and selective aromatase inhibitors presents a valuable opportunity to study the disposition of drugs that might be metabolized by aromatase. Our study was designed to use the clinically available aromatase inhibitor, letrozole, to test the hypothesis that the metabolism of methadone in humans is altered by essentially complete aromatase inhibition.

We designed a clinical trial and then carried it out in a group of postmenopausal women. We chose to study postmenopausal women because aromatase activity in general is higher in women than in men and aromatase inhibitors do not fully block aromatase activity in premenopausal women, in whom the ovarian-pituitary feedback loop prevents effective suppression of enzyme activity (Pritts 2010). After analysis of blood and urine samples collected during this trial, I present here the resulting data on the effects of letrozole on the disposition of methadone in this group.

Results

The effects of aromatase inhibition on single dose methadone pharmacokinetics (2 mg, intravenous) were studied in 15 healthy, post-menopausal women. The subjects studied were all healthy female and post-menopausal, with a mean age of 54, a mean weight of 84 kg and BMI of 30 (Table 3.1). The mean QTc (Bazette) interval at screening before their participation in the study was 413 msec. All 15 subjects enrolled completed the study according to the protocol. No serious adverse events or significant changes in vital signs (blood pressure, pulse, respiratory rate and pulse oximetry) were recorded.

Table 3.1. Demographics of study population (n = 15).

Variable	Mean ± SD / frequency
Age	54 ± 4.4
Years since last menstrual period	> 3
Height	165 ± 3.8
Weight	83.8 ± 14.9
BMI	30.1 ± 5.2
Ethnicity	
White	9 (60 %)
African American	6 (40 %)
Smoker	3 (20 %)

A sequential design was employed, involving a control period followed by treatment with letrozole (2.5 mg/day, 10 days) in which each subject served as her own control (see “Methods” section). The disposition of methadone after intravenous administration (2.0 mg) was altered by the treatment of letrozole. Mean plasma

concentrations of methadone and its primary metabolite, EDDP, before and after letrozole treatment, are shown in Figure 3.1. The calculated methadone and EDDP pharmacokinetic parameters derived from these data are displayed in Table 3.2. Methadone systemic clearance, plasma AUC, elimination half-life, and the ratio of plasma AUC of methadone to plasma AUC of EDDP during letrozole treatment were all significantly different from those derived from the data obtained after the first dose of methadone, administered during the control period. In contrast, there was no appreciable change in the methadone distribution half-life, volume of distribution or its estimated apparent 0 - 12 h renal clearance between the control and letrozole-treated periods. When the metabolite data from the two periods were compared, no appreciable difference was observed in the AUC of plasma EDDP concentrations, or in its estimated apparent 0 - 12 h renal clearance (Table 3.2). The secondary metabolite of methadone, EMDP, was present at concentrations at least ten-fold lower than that of EDDP, and was not consistently detected in all plasma samples and so pharmacokinetic parameters for this metabolite could not be calculated.

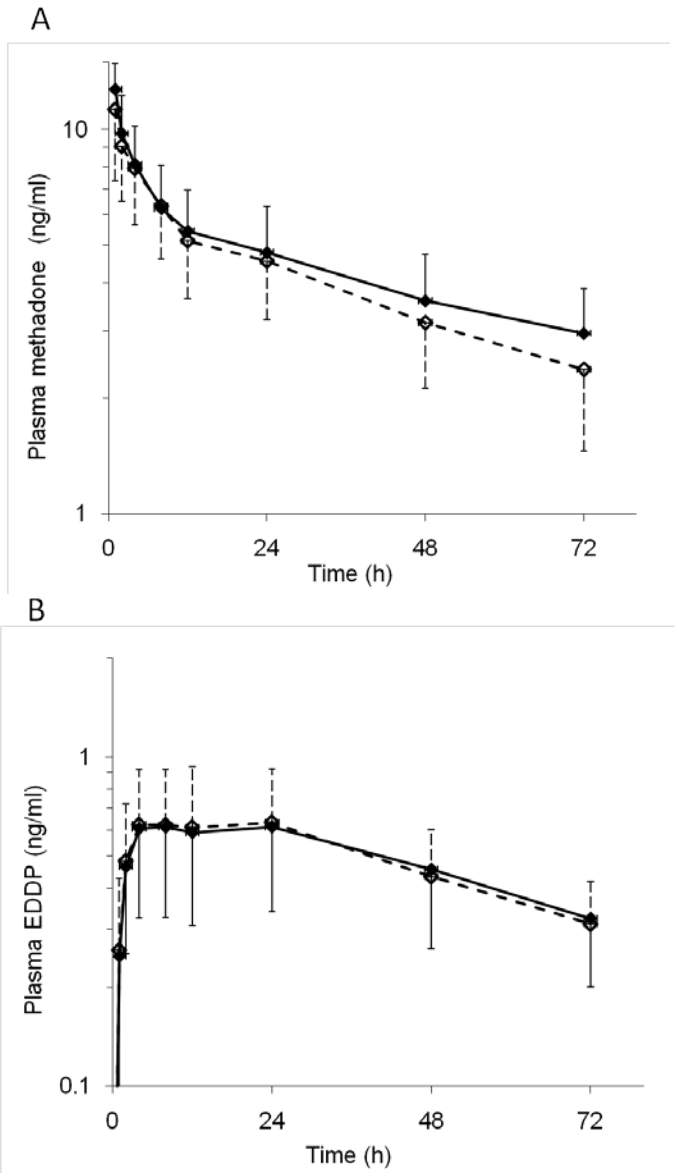

Figure 3.1. Effects of letrozole treatment on intravenous methadone disposition.

Plasma methadone (A) and EDDP (B) concentrations in the control (open diamond, dash line) and letrozole (closed diamond, solid line) periods are shown as the mean ± SD (n = 15) on a logarithmic scale (base 10). Subjects received 2.0 mg intravenous methadone HCl (1.8 mg free base) in both periods. Variation in the actual time of plasma sampling was less than 5%.

Table 3.2. Pharmacokinetic parameters in the letrozole-treated period compared to control.

	Control	Letrozole	Ratio of Means (letrozole/control)	P value
		Methadone		
CL_{IV} (ml kg^{-1} min^{-1})	0.95 ± 0.54	0.74 ± 0.40 *	0.78	0.001
AUC_{0-72h} (ng h ml^{-1})	305 ± 83	335 ± 91 *	1.10	0.003
$AUC_{0-\infty}$ (ng h ml^{-1})	536 ± 227	659 ± 224 *	1.23	0.007
Distribution $t_{½}$ (h)	11.6 ± 3.34	11.0 ± 4.29	0.95	
Elimination $t_{½}$ (h)	60.6 ± 31.7	73.3 ± 24.7 *	1.21	0.042
V_d (L/kg)	4.10 ± 1.36	4.17 ± 1.42	1.02	
Apparent 0-12 h CL_r (ml kg^{-1} min^{-1})	0.17 ± 0.15	0.17 ± 0.13	1.02	
		EDDP		
AUC_{0-72h} (ng h ml^{-1})	35.76 ± 14.38	35.81 ± 14.57	1.00	
Apparent 0-12 h CL_r (ml kg^{-1} min^{-1})	2.67 ± 1.72	2.53 ± 2.16	0.95	
		Methadone / EDDP		
AUC_{0-72h} Ratio	9.43 ± 3.60	10.42 ± 3.86 *	1.10	0.009
Urinary Ratio (total mole/mole)	0.84 ± 0.47	1.00 ± 0.38	1.20	
		Letrozole		
$C_{baseline}$ (ng/ml)	0	157 ± 49		

Note: Data are presented as mean ± SD (n = 15). $CL_{IV,}$ systemic clearance; AUC, area under the plasma concentration-time curve; $t_{½}$, half life; V_d, volume of distribution; CL_r, renal clearance; $C_{baseline}$, plasma concentration at baseline before methadone dosing. *, significantly different from control; P values were calculated using paired t-test (control-letrozole).

Plasma concentrations of methadone during letrozole treatment were higher than those during the control period, with significant differences being noted after 48 h (Figure 3.1.A). The concentration of EDDP was notably lower than that of methadone itself at all time points. There was no appreciable difference in plasma concentrations of the metabolite EDDP, before and after letrozole treatment (Figure 3.1.B). Both methadone and EDDP concentrations appeared to have large inter-individual variability (up to 3.0-fold for methadone $AUC_{0-\infty}$ and 4.7-fold for EDDP $AUC_{0-72\ h}$, Figure 3.1 and Table 3.2).

The effect of letrozole on systemic methadone clearance was highly variable. While one subject actually experienced a 17% increase in methadone clearance during letrozole treatment, three out of fifteen subjects changed 3% or less, and the majority (eleven) experienced decreases in methadone clearance that ranged from 11% to 51% with a mean of 27% (Figure 3.2). On average, letrozole treatment significantly reduced methadone clearance by 22% ($p = 0.001$, Figure 3.2.B and Table 3.2). Methadone clearance during the untreated control period ranged from 0.45 to 2.42 ml kg^{-1} min^{-1} (a 5.4-fold variation, Figure 3.2.B), but there was no appreciable relationship between this control methadone clearance and the magnitude of the treatment effect that was observed (data not shown).

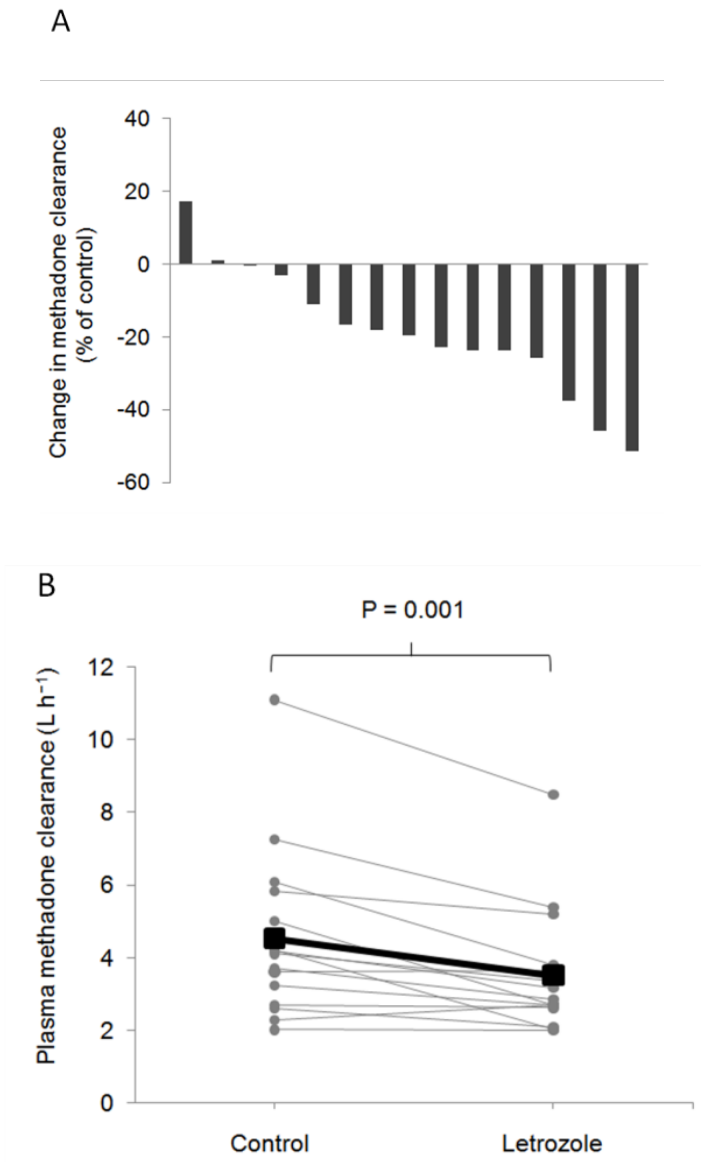

Figure 3.2. Effects of letrozole treatment on methadone systemic clearance.

(A) Each column represents the percent change of methadone clearance for an individual subject during letrozole treatment. (B) Data representing individual subjects are shown as grey circles, with lines connecting the control and letrozole periods. The means are shown as black squares (n = 15). Methadone systemic clearance was significantly different between the two periods ($P < 0.05$, paired t-test).

Changes in methadone $AUC_{0-\infty}$ and elimination half-life observed during letrozole treatment were also highly variable (Table 3.2). The $AUC_{0-\infty}$ increased an average of 23% ($p = 0.007$) and the elimination half-life increased an average of 21% ($p = 0.042$, Table 3.2). In these subjects, methadone elimination half-life during the control period ranged from as short as 34 h to as long as 124 h (a 3.7-fold variation). The largest effect brought about by letrozole on elimination half-life was a 2.2-fold increase in one subject, from 34 to 77 h.

Over the 72 hours after methadone administration, the plasma AUC of methadone increased significantly during letrozole treatment ($p = 0.003$), while the plasma AUC of EDDP did not change (Table 3.2). The ratio of plasma $AUC_{0-72\ h}$ values (methadone / EDDP) increased significantly during letrozole treatment compared to control ($p = 0.009$, Table 3.2). There was also an increase on average in the methadone to EDDP ratio in the urine collected over the first 12 h after methadone administration, but the difference was not significant due to large interindividual variability (Table 3.2). When the observed change in the ratio of plasma $AUC_{0-72\ h}$ values (methadone / EDDP) was plotted against the observed change in plasma methadone $AUC_{0-\infty}$, there was a linear relationship with a R^2 value of 0.74 (Figure 3.3.A), suggesting an association between the decreased rate of methadone metabolism and its decreased systemic clearance. These data indicate that the metabolism of methadone to EDDP was diminished during letrozole treatment. In contrast, there was no obvious association between change in plasma methadone $AUC_{0-\infty}$ and change in apparent 0 - 12 h urinary methadone clearance (Figure 3.3.B), suggesting that alterations in renal elimination rate of methadone were not the primary cause of the observed decrease in methadone clearance.

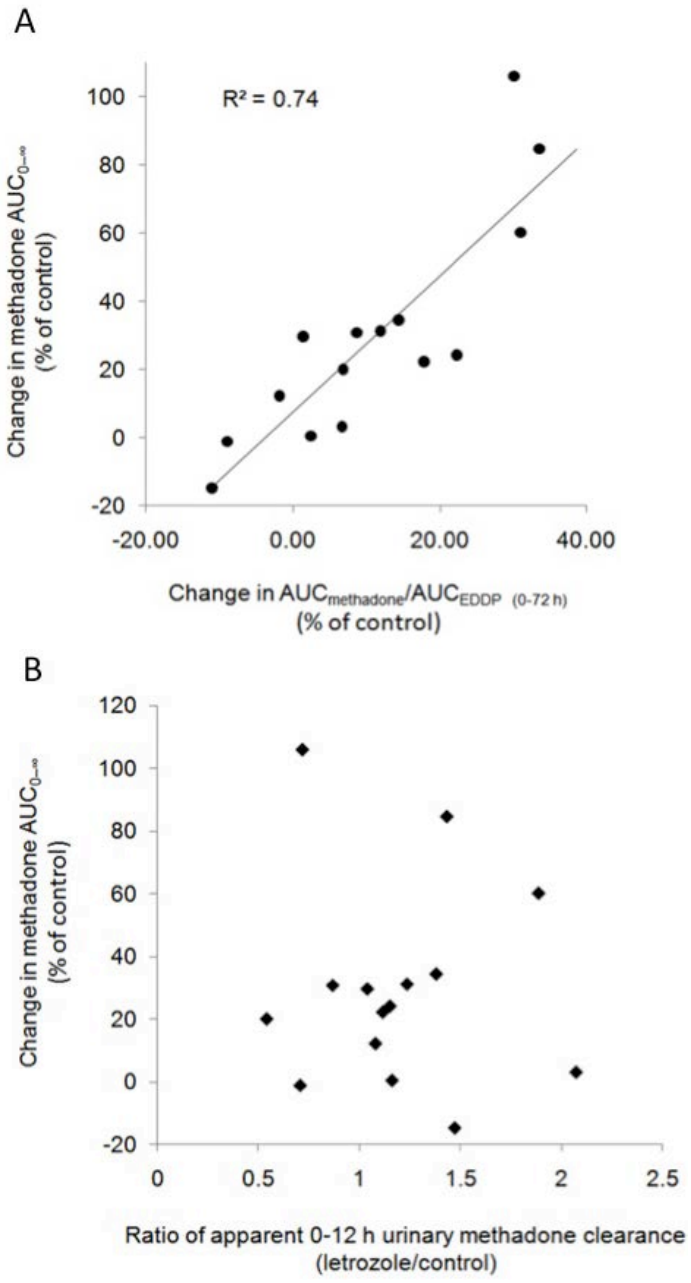

Figure 3.3. Letrozole treatment decreased methadone clearance via inhibition of the metabolism of methadone to EDDP.

(A) Association (R^2 = 0.74) between change in plasma methadone $AUC_{0-\infty}$ and change in the ratio of plasma methadone to EDDP ($AUC_{methadone,\ 0\text{-}72\ h}$ / $AUC_{EDDP,\ 0\text{-}72\ h}$). (B) No association between change in plasma methadone $AUC_{0-\infty}$ and change in apparent 0 - 12 h urinary methadone clearance.

Plasma letrozole concentrations at baseline before the administration of the second methadone dose were measured. After taking 2.5 mg letrozole daily for 8 days, all subjects had letrozole concentrations within the expected range, indicating that no subjects were non compliant. The average plasma letrozole concentration was 157 ng/ml, with a minimum of 80 ng/ml and a maximum of 257 ng/ml (Table 3.2). There was no appreciable association between letrozole concentration and any of the observed changes in methadone pharmacokinetics (data not shown).

Discussion

In this study we observed a significant decrease in the clearance of methadone during the coadministration of letrozole. This decrease was accompanied by significant increases in the methadone AUC, in its half-life and in the parent to metabolite ratio in plasma. These effects are all consistent with a decrease in methadone metabolism brought about by letrozole. Since letrozole is a highly selective inhibitor of aromatase at the given dosage, these data are also consistent with the possibility that some fraction of methadone metabolism is mediated via aromatase.

Aromatase has been implicated in the metabolism and specifically the demethylation of a number of drugs in vitro, including methadone (Chapter Two, this dissertation), buprenorphine (Deshmukh, Nanovskaya, and Ahmed 2003) and cocaine (Osawa et al. 1997), but the role that this enzyme plays in the metabolism of xenobiotic medications in humans has not been directly examined before in a clinical study. Our clinical trial presented here directly examined the involvement of this enzyme in methadone metabolism using selective aromatase inhibition as a tool. While aromatase is

already well recognized as being important in steroidogenesis, these data suggest for the first time a broader clinical role for this enzyme in the disposition of xenobiotic medications. Specifically, the ability of aromatase to catalyze N-demethylation of methadone in vivo suggests that it may be able to mediate the clearance of other drugs via a similar biochemical mechanism.

Our data indicate that aromatase is responsible for ~ 22% of the clearance of a 2 mg dose of methadone on average in a group of post-menopausal women (Table 3.2). Since aromatase may be a high capacity and low affinity enzyme for methadone metabolism, the quantitative contribution of aromatase to methadone disposition at higher doses remain unclear and deserves further studies. These findings suggest that breast cancer patients taking methadone who also take aromatase inhibitors may need appropriate dose adjustment to prevent methadone overexposure. Aromatase may also be important in the disposition of methadone in other populations, and may be in part responsible for the large and unpredictable variability in methadone clearance. Higher aromatase activity in premenopausal women may result in greater methadone clearance as a result. Men have less aromatase than premenopausal women and may consequently have lower clearance and higher exposure. Lastly, a quantitatively important role for aromatase in drug metabolism raises the possibility of clinically meaningful drug-drug interactions with aromatase inhibitors that would not otherwise have been anticipated. Such interactions might reasonably occur in patients taking aromatase inhibitors for a wide range of indications, including breast cancer, the treatment of infertility (Pritts 2010) and their off-label use in testosterone augmentation regimes (Leder et al. 2004; Saylam, Efesoy, and Cayan 2011).

Alternative explanations for these findings exist. First, although letrozole is a potent and selective aromatase inhibitor at low concentrations, it is metabolized by CYP2A6 (Kamden et al. 2011) and has been shown to be able to inhibit CYP2A6 in vitro (Jeong et al. 2009). This inhibition has not been demonstrated in vivo. While it is possible that letrozole might inhibit CYP2A6 activity in vivo, a change in methadone metabolism due to inhibition of CYP2A6 seems unlikely because potent inhibition of CYP2A6 by coumarin in human liver microsomes did not inhibit methadone metabolism (Foster, Somogyi, and Bochner 1999). It seems unlikely that CYP2A6 plays a role in methadone metabolism in vivo. Second, it is possible that the effect of letrozole is not simply the result of direct inhibition of aromatase, but is rather the result of indirect transcriptional down regulation of either aromatase itself, or of CYP2B6 brought about via reductions in estrogen. Although CYP2B6 has been reported to be sensitive to estrogen-receptor dependent regulation in vitro, this has not been consistently reported across all cell lines (Lo et al. 2010; Mnif et al. 2007). It remains possible that CYP2B6 is down-regulated in the presence of low estrogen concentrations, and that this results in alterations in methadone pharmacokinetics, but this important possibility has not been investigated either in human hepatic preparations or in vivo.

Of note, the effects of letrozole on methadone clearance were highly variable (Figure 3.2.A). Since aromatase activity varies among people, the variable response we observed may be in part due to variability in the contribution of aromatase to overall methadone metabolism. We also observed large variability in urinary methadone elimination (Figure 3.3.B). In particular, one subject who experienced a 17% increase in methadone systemic clearance during letrozole treatment also experienced a large

increase in urinary methadone elimination. Surprisingly, this subject had an increase in the parent to metabolite ratio in the urine, consistent with decreased metabolism. These data suggest that variability in both metabolism and urinary elimination contribute to the overall variability in methadone clearance.

The data illuminate a number of possible underlying mechanisms. First, a number of mechanisms could contribute to variability in the inhibitory effects of letrozole on methadone metabolism. While variability in plasma letrozole concentrations could in theory bring about variability in inhibitory effect, our data indicate no relationship between letrozole plasma concentration and the extent of change in methadone pharmacokinetics. We would expect this to be the case given the documented high potency of letrozole. In addition, no relationship was observed between the initial methadone clearance during the control period and the extent of change observed, suggesting that the quantitative contribution of aromatase to methadone metabolism in individual subjects does not associate with the undisturbed metabolic rate. It is likely that there is a balance between aromatase and other enzymes suggested to be important in the metabolism of methadone, including particularly CYP2B6. This balance can vary among people, and therefore variability in the percent contribution of aromatase to overall methadone clearance might exist. It remains possible that the difference in response could be explained by pharmacogenomic variability in aromatase, or of CYP2B6 (Payne et al. 2009; Mao et al. 2011; Ma et al. 2005; Ma et al. 2010; Crettol et al. 2005; Wang et al. 2011). While the current study does not have sufficient power to ascertain the influence of such genetic factors, this possibility deserves further study.

Second, variability in urinary methadone elimination could be due to the well documented influence of urinary pH on the renal elimination of methadone (Nilsson et al. 1982), but may also be the result of effects of letrozole on renal transporters as yet undescribed. In addition, both metabolic and renal clearance could also be influenced by the presence of other drugs or herbal medications taken by the subjects under study via mechanisms as yet unknown. Our current inability to predict methadone dose may thus be due to poor understanding of factors that influence a complex series of methadone elimination mechanisms, including at least two metabolic pathways: aromatase and CYP2B6 as well as variable renal elimination.

Third, it is also possible that variability in the clinical disposition of drugs like methadone during concomitant treatment of aromatase inhibitors can be explained in part by genetic polymorphisms in the estrogen signaling pathways downstream of aromatase. Since estrogen is key to the regulation of the expression of a wide range of proteins, medications that directly affect estrogen synthesis by inhibiting aromatase may result in pharmacokinetic drug interactions via changes in proteins responsible for the absorption, distribution, metabolism and elimination of a specific drug, such as methadone. This estrogen-mediated influence on methadone disposition may be highly variable because of clinical effects of genetic polymorphisms in estrogen receptors and/or in the subsequent regulation of the expression of drug transporters, enzymes, binding proteins or drug receptors. The use of aromatase inhibitors therefore needs to be cautious not only in situations where alterations in direct metabolism of another drug by aromatase can happen. Indirect alterations in the expression of the proteome as the result of estrogen depletion may also lead to changes in drug clearance and exposure.

This trial has the following limitations. First, although methadone was given as a racemic mixture, we did not measure the individual (R)- and (S)-enantiomers. Although it is possible that changes in individual enantiomers may be obscured by this approach, our prior in vitro data using recombinant human aromatase clearly indicated that the metabolism of methadone by aromatase is not stereoselective, and we would therefore expect both enantiomers to be affected equally by the inhibition of aromatase in the subjects studied. Second, the urinary collection time was short (12 hours) relative to the long half-life of methadone, and this limits our ability to most accurately measure the urinary clearance of methadone or EDDP. While this is an important caveat, it does not compromise our ability to accurately determine the other pharmacokinetic parameters, all of which are internally consistent, and indicate a decrease in systemic clearance, and a prolongation of methadone half-life associated with reduced metabolism to EDDP.

In summary, aromatase seems to account for ~ 22% of methadone clearance when the drug is given at a low dose in post-menopausal women. An involvement of aromatase in the metabolism of methadone suggests a broader role for this catalyst of endogenous steroid metabolism in xenobiotic drug disposition, and may help explain the difficulty in dosing methadone. Mechanisms underlying the variability in methadone clearance in response to letrozole treatment merit future studies. It is likely that human methadone metabolism is carried out by both aromatase and CYP2B6. Variability in methadone metabolism could thus be vulnerable to genetic factors that influence the activity or the regulation of either or both of these enzymes.

Methods

Clinical protocol

The study was approved by the Indiana University Institutional Review Board, and was conducted in the Indiana Clinical Research Center. All subjects signed informed consent before participation in the trial, and all procedures were conducted in accordance with the guidelines of the Declaration of Helsinki. Subjects enrolled in this clinical trial were healthy post-menopausal women 45 to 70 years of age who weighed at least 110 lbs, and who agreed to avoid the use of alcohol during the period of the study. Potential subjects were excluded from the study if they had a history of intolerance or allergy to methadone or letrozole, had a known history of addiction to drugs, had a diagnosis of asthma, chronic obstructive pulmonary disease, cor pulmonale, severe obesity with a weight over 300 lbs, or sleep apnea syndrome. Subjects were also excluded if they were anemic (hematocrit below 30%), suffered from renal insufficiency (serum creatinine greater than 1.4) or had elevation of serum liver enzymes, had low serum potassium, a prolonged electrocardiographic QTc interval of more than 480 msecs (Bazette), were taking drugs know to prolong the QT interval or participated in a study within the last two months.

	Period 1 Control				Washout										Period 2 Letrozole			
Study Day	01	02	03	04	05	06	07	08	09	10	11	12	13	14	15	16	17	18
Methadone dose 2 mg, IV	X														X			
Letrozole dose 2.5 mg, PO								X	X	X	X	X	X	X	X	X	X	X
Blood draw , 0, 1, 2, 4, 8, 12, 48, 72 h	X	X	X	X											X	X	X	X
Urine sampling, 0 -12 h	X														X			

Figure 3.4. Clinical trial design and schedule of activities (n = 15).

Blood samples (10 ml each) were collected before and at 1, 2, 4, 8, 12, 24, 48 and 72 hours after every methadone dose. Urine samples were collected at baseline and over the first 12 hours after every methadone dose.

The study protocol was a single-site, acute dose, 2-period sequential design with each subject as their own control (Figure 3.4, control period first). (1) Control period: Subjects were instructed to fast overnight for at least 8 hours before the first day of the study. On study day 1, following predose blood and urine sampling and the insertion of a forearm intravenous catheter, subjects were administered a single intravenous dose of methadone HCl (2.0 mg, 1.8 mg free base). Venous blood samples were collected over the next 72 hours from day 1 to day 4 according to the following schedule: 1, 2, 4, 8, 12, 24, 48, and 72 hours after the dose. Plasma samples were immediately separated and stored at – 80 °C for later analysis. Continuous urine samples were collected over the first 12 hours after the methadone dose, and stored at – 80 °C. Subject received a standard breakfast 2 hours after methadone and free access to food thereafter. (2) Letrozole-treated period: on study day 8, subjects began taking a daily oral dose of letrozole (2.5 mg/day) each morning at the same time, and continuing through study day 18. Before study day

15, subjects were instructed to fast overnight again. On study day 15, the same procedures as that on day 1 of the control period involving a single intravenous dose of methadone, pre- and post-dosing blood and urine pharmacokinetic sampling were repeated from day 15 to day 18. In order to assess patient compliance with daily letrozole dosing, the blood drawn immediately before the dose of methadone on study day 15 was used to measure plasma letrozole concentrations. Plasma methadone concentrations were also measured in these samples to ensure that no methadone remained in the blood before the second pharmacokinetic investigation done in the letrozole-treated period. More detailed clinical procedures are described in "Chapter Ten: General Methods / Protocol for clinical trial: effects of aromatase inhibition on methadone disposition".

Sample analysis

HPLC with tandem mass spectrometry detection (LC-MS/MS) assays were developed for the quantification of plasma and urinary methadone and its major metabolites, EDDP and EMDP. All samples were analyzed as described in "Chapter Ten: General Methods / LC-MS/MS assays for plasma and urinary methadone, EDDP and EMDP". Plasma letrozole concentrations were measured using HPLC assays with ultraviolet and fluorescence detection as described in "Chapter Ten: General Methods / HPLC-UV-fluorescence assays for plasma letrozole".

Pharmacokinetic analysis

Data on methadone and its metabolites including area under the concentration-time curve (AUC), half-life ($t_{½}$), clearance (CL) and volume of distribution (V_d) were

estimated using a two-compartment model (Phoenix™ WinNonlin® 6.1, Pharsight Corporation, Cary, NC). Systemic clearance of intravenous methadone was CL_{IV} = dose / $AUC_{0-\infty}$, $t_{½}$ estimated based on the terminal elimination rate constant, volume of distribution based on the terminal phase was $V_d = CL_{IV} \cdot t_{½} / 0.693$, and apparent 0 - 12 h renal clearance of methadone and its primary metabolite EDDP was estimated as $CL_{r,\ 0\text{-}12h}$ = total amount excreted in urine during the first 12 hours / the corresponding $AUC_{0\text{-}12\ h}$.

Note: Equations are quoted from (Rowland and Tozer 1995).

Statistical analysis

Differences between control and letrozole treatment periods for pharmacokinetic parameters including methadone AUC, $t_{½}$, CL_{IV}, and the ratios of methadone to EDDP both in plasma and in urine were analyzed by two-tailed paired t-test (Microsoft Office Excel 2007). Statistical significance was assigned at $p < 0.05$. Relationships between pharmacokinetic changes were evaluated by linear regression analysis.

Note: The work described in this chapter has been submitted for publication (Lu, Thong, and Flockhart 2011).

CHAPTER FOUR

Screening Select Xenobiotics for Aromatase Inhibition

Introduction

Studies presented in the last two chapters indicate that aromatase is able to metabolize methadone, suggesting that aromatase is not only involved in steroidogenesis, but is also a drug-metabolizing enzyme with potential important roles in drug disposition and drug interactions. Based on these findings, it is possible that aromatase interacts with a broad range of xenobiotic medication. These interactions may in turn affect aromatase activity.

Important drug-metabolizing CYPs, such as CYP1A1, CYP1A2, CYP2B6, CYP2C8, CYP2C9, CYP2C19, CYP2D6, CYP2E1 and CYP3A, have been extensively studied for their involvements in drug interactions, and the knowledge resulted from these studies provides useful guidance for clinical prescription. In contrast, aromatase is much less studied. To date, due to the lack of understanding of its role in drug metabolism, the possibility of altered clinical drug disposition and the resultant adverse drug reaction via aromatase inhibition has not been widely considered. This understanding is important not only in the prediction and prevention of pharmacokinetic drug-drug interactions, but more so in the treatment of a critical disease that causes high fatality and heavy healthcare burden worldwide: breast cancer. The peripheral conversion of testosterone to estradiol by aromatase is the primary source of endogenous estrogen in post-menopausal women, and the inhibition of aromatase represents a key approach to the treatment of hormone-receptor positive breast cancer. The aromatase inhibitor class of

drugs is widely used and effective for this indication, but their use is compromised by side effects that result in non-compliance and poor quality of life of breast cancer patients. It follows that it is important to develop more tolerable aromatase inhibitors with improved therapeutic index. At present, most post-menopausal women at high risk are treated either with tamoxifen or raloxifene, both of which are indicated in the prevention of breast cancer (Chlebowski et al. 1999). However, it has recently become clear that many patients eligible for preventive therapy with tamoxifen either refuse to take it, or are non-adherent (McCowan et al. 2008). Aromatase inhibitors are also under study for this indication and a recent report showed that therapy with one of the available AIs, exemestane, was associated with a 65% relative reduction in the annual incidence of invasive breast cancer in postmenopausal women who were at moderately increased risk for breast cancer (Goss et al. 2011). Unfortunately, musculoskeletal pain compromises adherence to therapy with available aromatase inhibitors (Henry et al. 2008). Alternative aromatase inhibitors may allow greater compliance by bringing about fewer of the side effects. It is possible that novel aromatase inhibitors that allow greater compliance may therefore be of value in the prevention setting. For these reasons, and as a first step in obtaining better understanding of drug interactions with aromatase, I set out to study the effects of xenobiotics on aromatase activity.

Since my prior work has showed that aromatase is able to metabolize methadone (Chapters Two and Three, this dissertation), I hypothesized that this enzyme may interact with a small group of drugs and/or their metabolites that I have selected based on the following criteria: 1) drugs that are cleared by metabolism via N- or O-demethylation, which are metabolic reactions similar to those that aromatase can carry out; 2) drugs that

are commonly prescribed to patients with breast cancer. Since understanding interactions between aromatase and xenobiotics may be important for the prediction and prevention of adverse drug interactions associated with the use of aromatase inhibitors, and since there is a need for developing more tolerable aromatase inhibitors with improved therapeutic window, I studied these selected xenobiotics for their ability to inhibit aromatase.

Results and discussion

Using carefully recorded medication data from trials of tamoxifen (Jin et al. 2005) and aromatase inhibitor (Henry et al. 2008) conducted by Dr. Flockhart and his collaborators in the Indiana University Cancer Center, we determined that selective estrogen receptor modulators (SERMs), antidepressants, non-steroidal anti-inflammatory drugs (NSAIDs) and opiates for pain control are commonly co-prescribed drugs. Drugs that satisfy both criteria include the SERMs, toremifene (Berthou et al. 1994) and tamoxifen (Desta et al. 2004); antidepressants, fluoxetine (Liu et al. 2001) and venlafaxine (Eap et al. 2003); the NSAIDs, naproxen (Miners et al. 1996) and ibuprofen (Hamman, Thompson, and Hall 1997); and the opiates, codeine (Yue et al. 1997), tramadol (Paar et al. 1997) and methadone (Sullivan and Due 1973; Chapters Two and Three, this dissertation). In addition, there are existing interests in understanding the effects of natural compounds that cause endocrine disruption by changing aromatase activity (Cheshenko et al. 2008; Sanderson 2006). Since the most clearly characterized and clinically important interaction between natural compounds and the cytochrome P450 system so far is the reduction of CYP3A activity brought about by grapefruit juice (Guengerich and Kim 1990), it seems important to understand the effects of grapefruit

juice components on aromatase activity. Naringenin is an active component within grapefruit juice and therefore was also included in the selected compounds to be tested for their ability to inhibit aromatase.

Each selected compound was tested using a fluorescent aromatase activity assay with microsomal incubations. Two of the current aromatase inhibitors: letrozole, a competitive inhibitor, and exemestane, a mechanism-based inhibitor, were used as positive controls. Since an important exemestane metabolite, 17-hydroxy exemestane, may contribute to the clinical effect of exemestane via a similar mechanism, its ability to inhibit aromatase was also tested in addition to the select group of compounds. The screening results are shown in Figure 4.1.

A

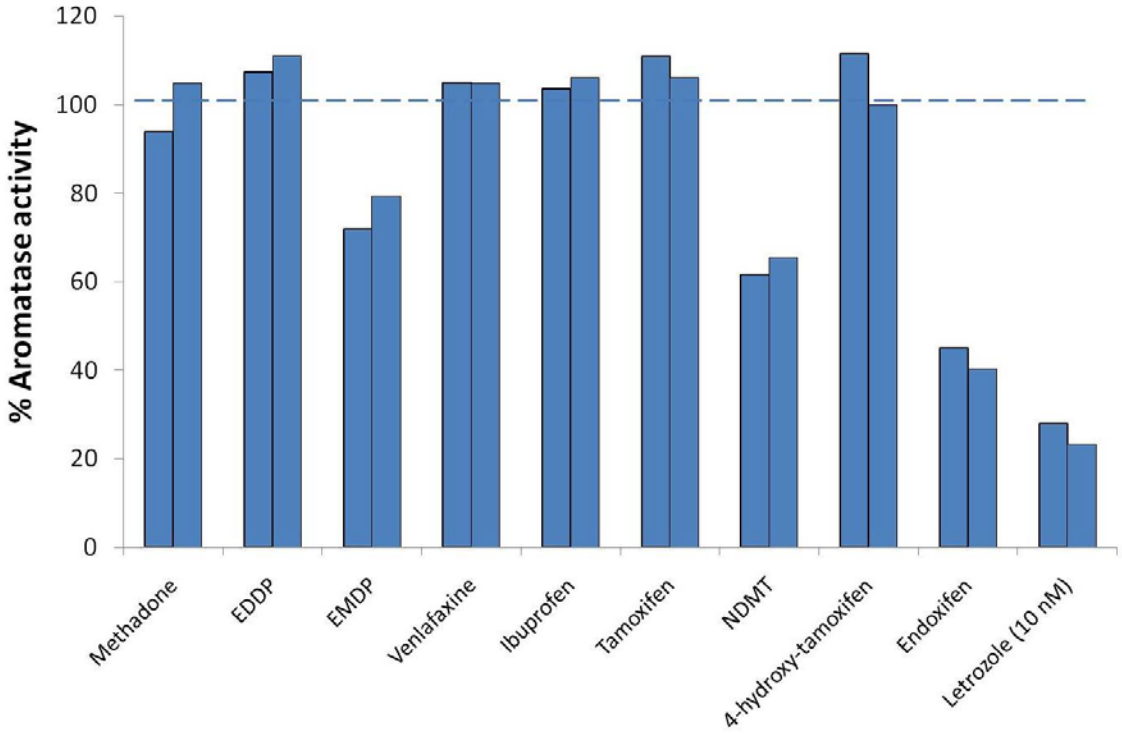
% Aromatase activity
120
100
80
60
40
20
0
Methadone
EDDP
EMDP
Venlafaxine
Ibuprofen
Tamoxifen
NDMT
4-hydroxy-tamoxifen
Endoxifen
Letrozole (10 nM)

B

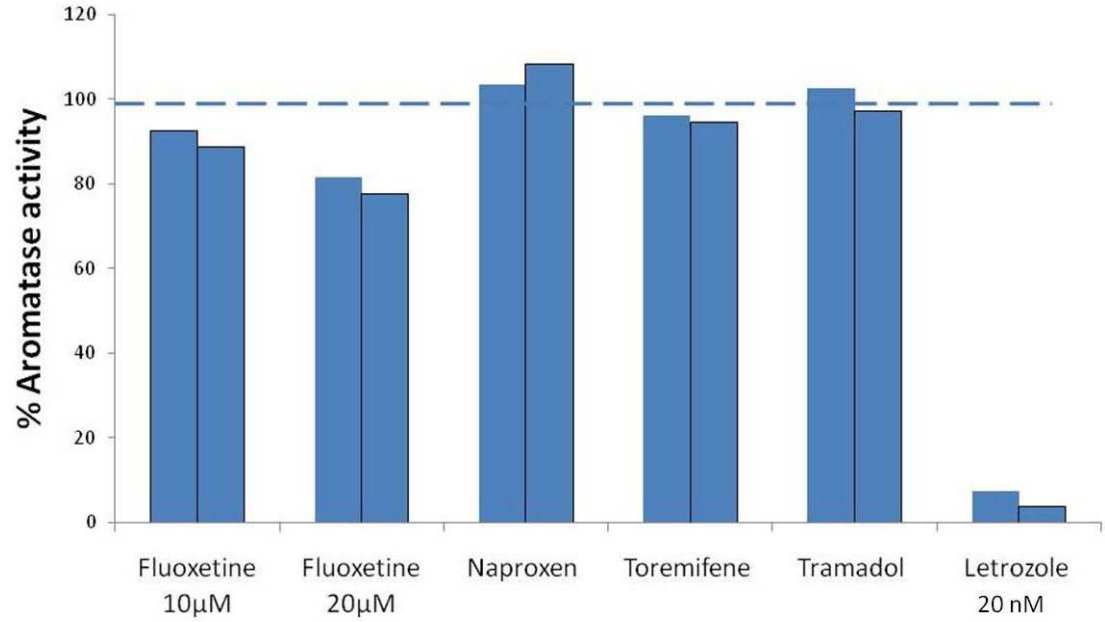
% Aromatase activity
120
100
80
60
40
20
0
Fluoxetine 10µM
Fluoxetine 20µM
Naproxen
Toremifene
Tramadol
Letrozole 20 nM

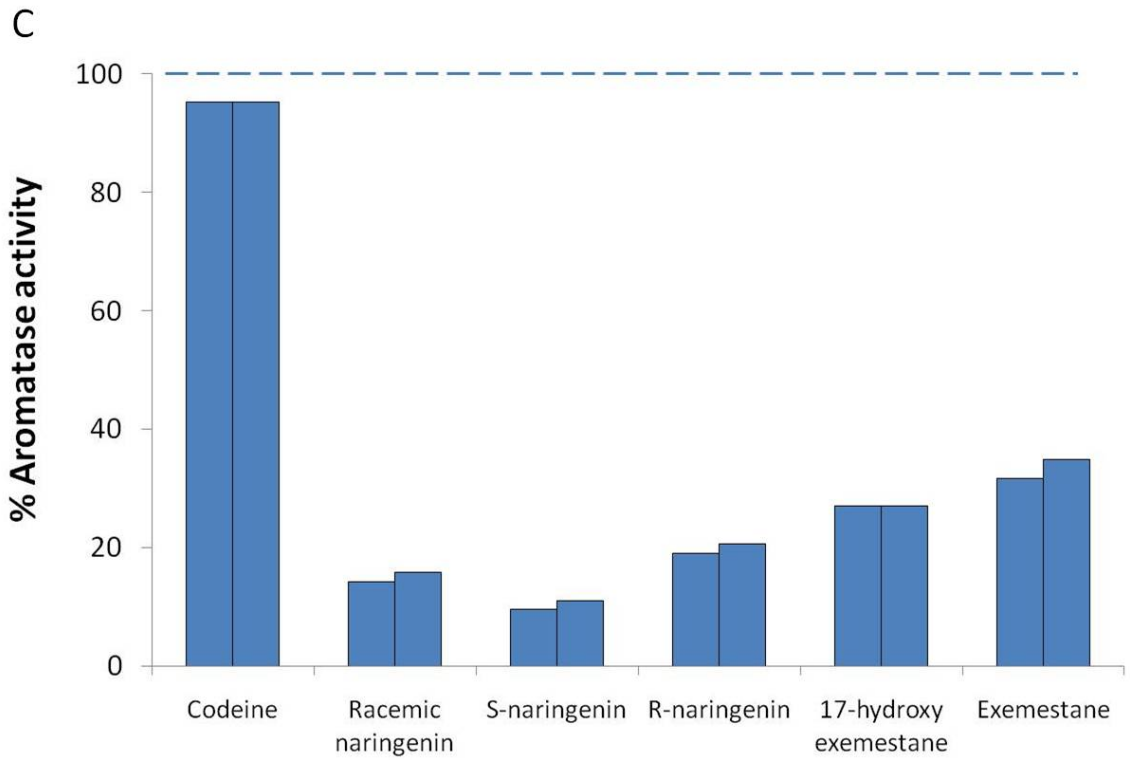

Figure 4.1. Screening selected compounds for their ability to inhibit aromatase. Data represent duplicate incubations for each tested compound. (A) The concentration of each tested inhibitor was 10 µM. Letrozole at 10 nM was used as a positive control. (B) The concentration of tested inhibitor was 10 µM, except that fluoxetine was tested at both 10 and 20 µM. Letrozole at 20 nM was used as a positive control. (C) The concentration of tested inhibitor was 10 µM, except that naringenin was tested at 20 µM. The mechanism-based inhibitor exemestane at 10 µM was used as a positive control.

The effects of tested inhibitor on aromatase activity were measured with inhibitor concentrations set at 10 or 20 µM, and were presented as percent enzyme activity remaining compared to vehicle controls. Data showed that methadone metabolite EMDP, tamoxifen metabolites N-desmethyl-tamoxifen (NDMT) and endoxifen, fluoxetine,

naringenin and 17-hydroxy-exemestane were able to reduce aromatase activity at the concentration tested, while methadone and its metabolite EDDP, venlafaxine, ibuprofen, tamoxifen and its metabolite 4-hydroxy-tamoxifen, naproxen, toremifene, tramadol and codeine did not inhibit aromatase at the concentration of 10 μM.

In order to better predict aromatase inhibitory effects of these drugs in breast cancer patients who are taking them, and to identify potential aromatase inhibitors within the current pharmaceutical armamentarium, I selected a few candidates for further studies to characterize their detailed inhibitory mechanisms. (1) Among the compounds that appeared to be active aromatase inhibitors, fluoxetine is a relatively weak inhibitor at 10 and 20 μM, and therefore is not likely to bring about clinically meaningful aromatase inhibition via a reversible mechanism. However, whether or not aromatase interacts with fluoxetine via demethylation merits further studies. (2) The exemestane metabolite, 17-hydroxy exemestane, is a steroid analogue like its parent drug exemestane. It is likely that 17-hydroxy-exemestane inhibits aromatase via mechanism-based inhibition similar to the action of exemestane, and so it was not included for further characterization because aromatase inhibition is already expected when exemestane is given to patients, and the efficacy and toxicity profile of 17-hydroxy-exemestane may be close to that of exemestane due to their structure and mechanistic similarity. (3) The methadone metabolite EMDP is a secondary metabolite and present at relatively very low concentrations in patients taking methadone (Lu, Zhou et al. 2011). Since it only inhibited aromatase activity by ~ 25% at 10 μM, it is not likely that EMDP itself has substantial inhibitory effect on aromatase in vivo. With that said, since aromatase is able to metabolize methadone, it is clear that the enzyme interacts with methadone in humans,

and the possibility of either competitive inhibition or irreversible mechanism-based inhibition by methadone at a higher concentration cannot be ruled out and merits future studies. (4) Naringenin substantially reduced aromatase activity at 20 μM. The enantiomers of naringenin, (R)- and (S)-naringenin appeared to have different potency as aromatase inhibitors and were selected for further investigation, especially for their stereoselectivity on aromatase. (5) Most interestingly, NDMT and endoxifen inhibited aromatase activity by ~ 37% and ~ 57% respectively. Tamoxifen is an effective therapy in the treatment of breast cancer, but the aromatase inhibitory effects brought about by tamoxifen metabolites were not known before. Since these effects may contribute to the beneficial effects of tamoxifen in breast cancer patients, the ability of tamoxifen metabolites to inhibit aromatase deserve detailed studies.

In summary, these data demonstrate that several xenobiotics interact with aromatase in vitro and this fact suggests potential clinical significance. Methadone and tamoxifen are common medications taken by breast cancer patients and these drugs, if they exert adequate aromatase inhibition in humans, might have beneficial effects that could prevent tumor growth and cancer recurrence. Naringenin is often ingested via fruit products such as grapefruit juice and therefore might also be protective for people with high breast cancer risk. These findings suggest that methadone, naringenin and tamoxifen metabolites are important candidates for further mechanistic studies. Moreover, these compounds are all structurally different from the known aromatase inhibitors. They might employ different kinetic actions on the target enzyme and/or have simultaneous actions on other receptors that result in improved risk/benefit profile as a therapy for breast cancer patients. Methadone, naringenin and tamoxifen metabolites require further study

to allow us to fully exploit their potential to serve as better aromatase inhibitors. For this reason, studies aimed to address these questions were designed and conducted as described in detail in the next three chapters.

Methods

Fluorescent assay for inhibition of aromatase in vitro

The activity of aromatase was determined by measuring the conversion rate of a fluorometric substrate, 7-methoxy-4-trifluoromethylcoumarin (MFC), to its fluorescent metabolite, 7-hydroxytrifluoromethylcoumarin (HFC) as described in "Chapter Ten: General Methods / Fluorescent assay for inhibition of aromatase in vitro".

CHAPTER FIVE

Mechanism-based Inhibition of Aromatase by Methadone

Introduction

Aromatase is able to metabolize methadone both in vitro and in vivo (Chapters Two and Three, this dissertation). However, the effects of methadone itself on aromatase have not been carefully studied and the effects of methadone on the metabolism of endogenous androgens have not been described or tested for. Although when tested at 10 μM, methadone did not act as a competitive aromatase inhibitor in vitro (Chapter Four, this dissertation), it remains possible that methadone has inhibitory effect on aromatase at higher tissue concentrations in humans or act as a mechanism–based inhibitor when it is metabolized by aromatase.

Auto-inhibition of methadone metabolism over time seen in some patients has been a concern in methadone use. Auto-inhibition during chronic methadone therapy might lead to unanticipated accumulation of methadone in patients with resultant potentially lethal consequences. A poor understanding of the effects of methadone on its own clearance over time also impedes our ability to dose accurately, to anticipate and manage withdrawal in clinical settings. Screening results described in the last chapter suggest that at least one methadone metabolite, EMDP, may have inhibitory effect on aromatase activity. Since it is clear that aromatase catalyzes metabolism of methadone, and since aromatase also interacts with methadone metabolites, it is possible that the aggregated effect of these interactions reduces the activity of aromatase in humans. In addition, this influence on aromatase activity might be in part responsible for methadone

action. Some side effects associated with methadone, such as bone loss, are reminiscent of estrogen withdrawal (Senay 1985; Backstrom 1995). It follows that the involvement of aromatase inhibition and the subsequent alterations in the downstream signaling pathways involving androgens and estrogens may help explain these side effects of methadone. Lastly, since there is a potential role of aromatase in the disposition of xenobiotic medications, methadone, an aromatase substrate, might have an effect on the pharmacokinetics of other exogenous substrates of aromatase.

For these reasons, and as a first step in obtaining a more complete understanding of methadone's interactions with aromatase, I tested the ability of methadone to inhibit aromatase under conditions in which either reversible or mechanism-based inhibition of the conversion of testosterone to estradiol by aromatase could be quantified.

Results

Testosterone metabolism by recombinant aromatase

To measure the activity of aromatase, the rate of aromatization of testosterone to 17-β-estradiol was used as a marker of enzyme activity. Aromatase was able to catalyze the generation of estradiol from testosterone with a V_{max} of 9.1 pmol/min/pmol P450 and K_m of 4.0 μM (pilot data not shown). Under the same incubation conditions, a concentration of testosterone at the K_m was chosen to test for reversible, competitive inhibition of aromatase by methadone. At 50 μM testosterone, the rate of estradiol formation was at V_{max}. This concentration was therefore chosen for experiments to test the mechanism-based inhibition of aromatase by methadone. The rate of estradiol formation was used as a measure of CYP activity.

No reversible inhibition of aromatase by methadone

To test for reversible inhibition, racemic methadone was incubated for 30 min with testosterone at the K_m (4 µM). Figure 5.1 shows the rate of estradiol formation from 4 µM testosterone in the presence of a range of methadone concentrations from 0 to 2 mM. No direct effect of methadone on the rate of metabolism of this probe for aromatase was observed under these conditions, even at the highest concentration of methadone used. The selective aromatase inhibitor letrozole (1 µM) used as positive control, on the other hand, was able was to completely block the formation of estradiol.

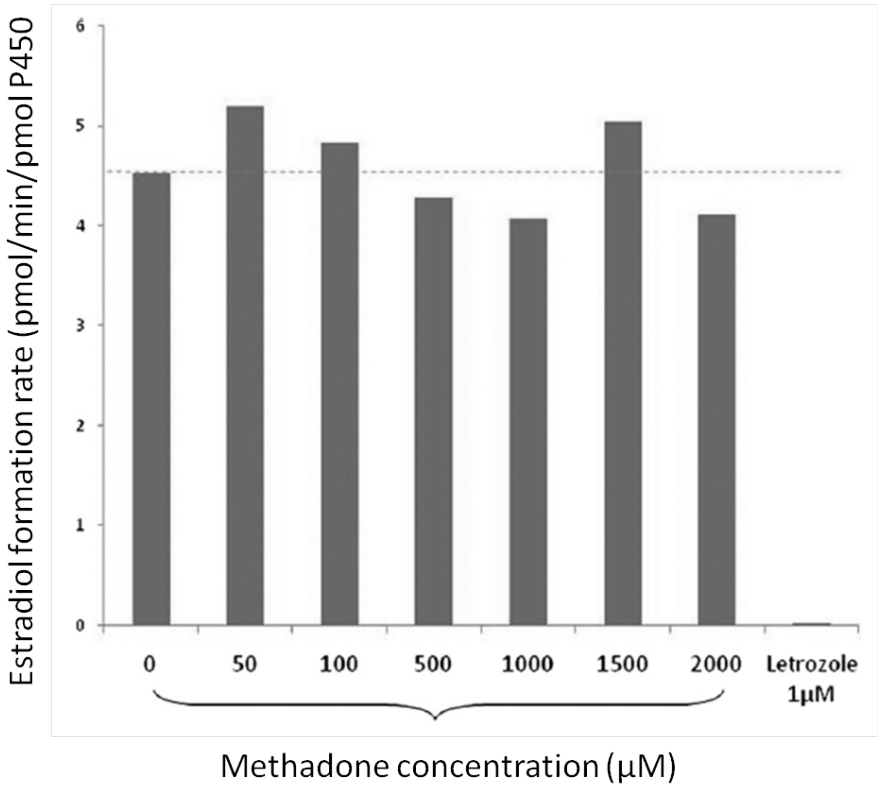

Figure 5.1. Methadone is not a reversible inhibitor of recombinant human aromatase.

Testosterone (4 μM) was incubated with a range of racemic methadone concentrations and recombinant human aromatase for 10 min, and aromatase activity was determined by measuring the generation of estradiol from testosterone in three experiments. Bars represent the average rate of estradiol formation in duplicate samples at increasing concentrations of methadone or in the presence of 1μM letrozole (positive control). The dotted line indicates the average rate obtained in the absence of methadone.

Mechanism-based inhibition of aromatase by methadone

Since methadone metabolism to EDDP could be catalyzed by aromatase, pilot experiments were conducted to test the ability of methadone to inactivate aromatase

activity in a time dependent manner. When aromatase was pre-incubated in the presence of 1 mM methadone and then incubated with a V_{max} concentration of testosterone (50 µM), a log linear time-dependent loss of aromatase activity occurred (pilot data not shown). If enzyme was pre-incubated under the same conditions without methadone, no decrease in enzyme activity was observed and the V_{max} activity of estradiol formation was maintained. This inactivation was also dependent on methadone concentration. When 0 - 500 µM racemic methadone was pre-incubated for 25 min, inhibition of 50% of activity was seen at approximately 50 µM methadone, while 30% inhibition was brought about by the presence of 10 µM methadone (pilot data not shown). When the individual enantiomers (0 - 500 µM, over 5 - 20 min) were separately tested under the same conditions, no stereoselectivity was observed (data not shown).

To estimate the kinetics of the interaction between methadone and aromatase during preincubation, a range of methadone concentrations and preincubation times were tested. Figure 5.2.A depicts the preincubation time and concentration dependence of the effect of methadone on aromatase activity. Control incubations were carried out in the presence of NADPH but without methadone. The rates of metabolism at zero preincubation time for each concentration were consistent with the V_{max} activity of aromatase under these conditions. It was therefore possible to normalize the data at each concentration to the activity seen at 0 min of preincubation. Kinetic analyses of the rates of enzyme inactivation in the presence of methadone were carried out using NONMEM®, and predicted time curves for inactivation at each methadone concentration were obtained (Figure 5.2.A). The K_I, and k_{inact} values were calculated to be 40.6 ± 2.8µM, and 0.061 ± 0.001min^{-1} respectively. A close correlation between observed and

predicted rates of aromatase was observed (Figure 5.2.B), indicating that the data are reliably represented by the model.

A

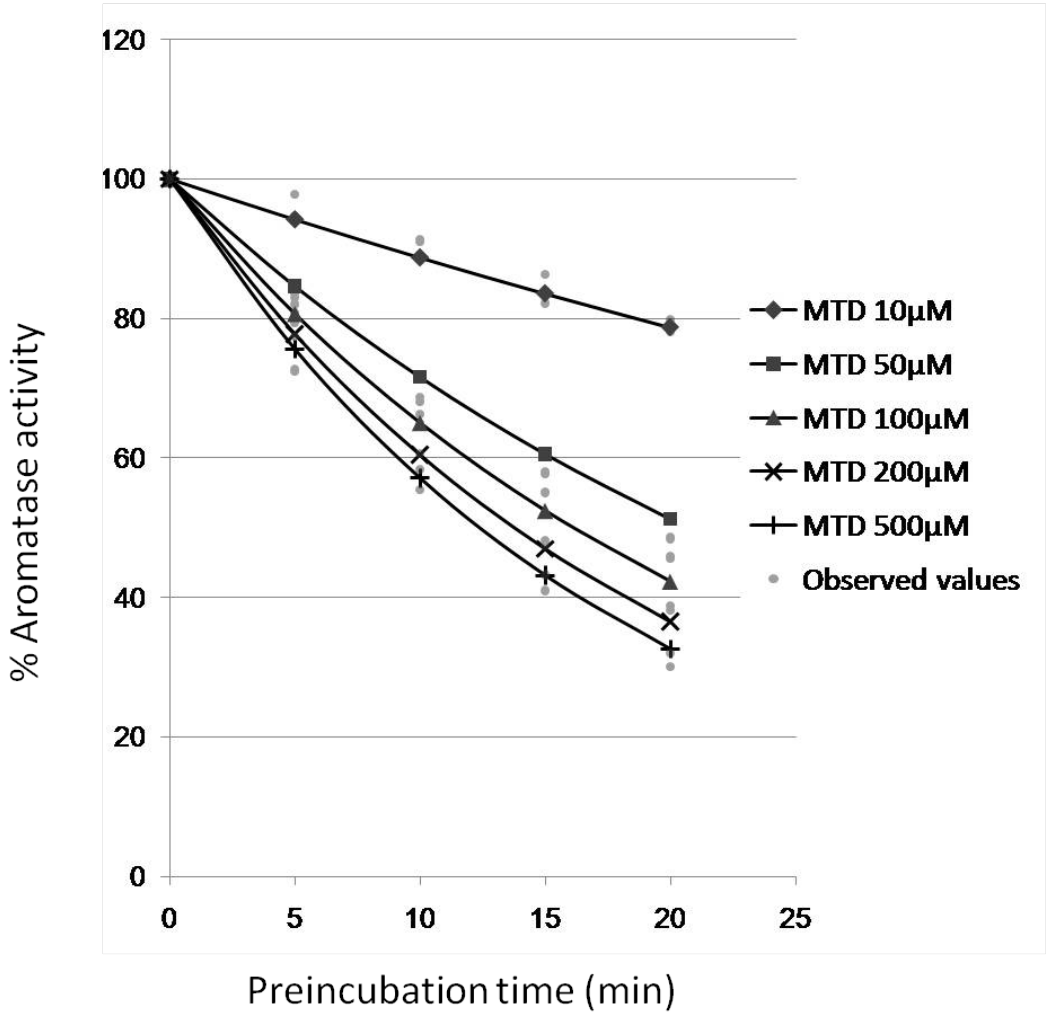

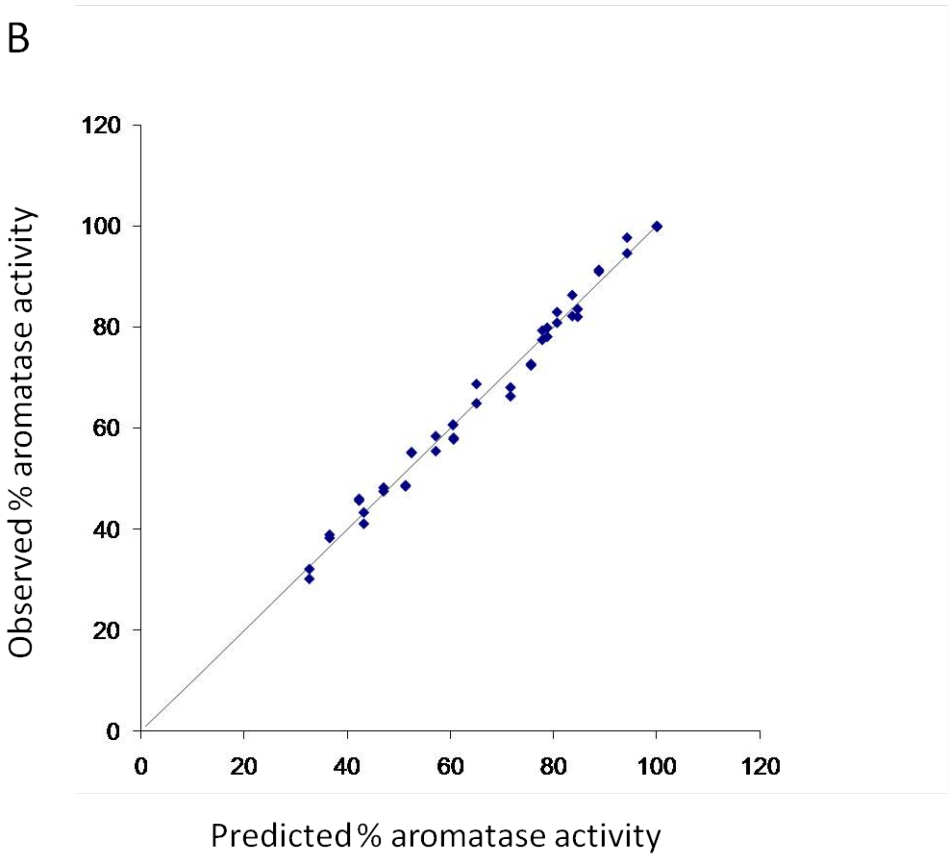

Figure 5.2. Kinetic analysis of mechanism-based inhibition of aromatase by racemic methadone.

(A) Time- and concentration-dependent inactivation. Methadone (MTD 10, 50, 100, 200, 500 µM) was pre-incubated with human recombinant aromatase (0.1 µM) for 0, 5, 10, 15, or 20 min, and then activity of aromatase (0.01 µM) was assessed in incubations carried out in duplicate (n = 2). Individual data points (grey dot) were plotted as the percent of aromatase activity observed at 0 min of preincubation. The curve of each plot represents the line of best fit for the inactivation reaction at the concentration indicated using NONMEM®. (B) Correlation between observed and NONMEM® predicted values of percent aromatase activity remaining**.** The solid line represents the line of equality. A correlation coefficient (R^2) of 0.99 was obtained.

Since methadone is metabolized by aromatase, I tested the possibility that inhibition of aromatase by methadone might be due to the metabolites formed. We directly tested its major metabolite, EDDP, in both reversible and irreversible experimental designs in the same way as described for methadone itself. Similar to the results for methadone, no competitive inhibition was observed when EDDP were tested at concentrations up to 100 μM (data not shown). When irreversible inhibition was tested, inactivation of aromatase was observed by both the primary metabolite, EDDP, and the secondary metabolite, EMDP, at concentrations as low as 10 μM (pilot data not shown). Figure 5.3 shows that the rate of inactivation by EDDP (100 μM) appeared equipotent as that by racemic methadone (100 μM), and the rate of inactivation by EMDP (100 μM) was relatively slower.

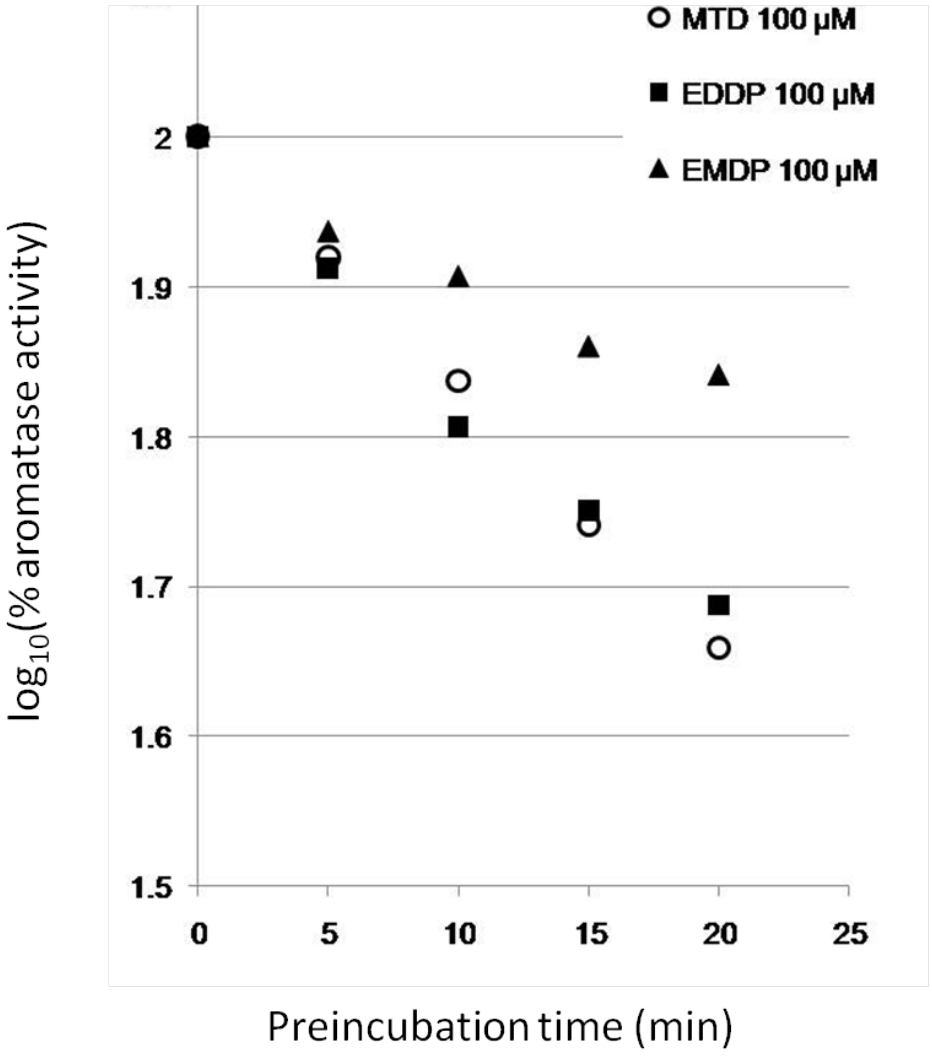

Figure 5.3. Mechanism-based inhibition of aromatase by racemic methadone, EDDP and EMDP.

Methadone, EDDP and EMDP (100 µM) were pre-incubated with recombinant human aromatase (0.1 µM) for 0, 5, 10, 15, or 20 min, and then activity of aromatase (0.01 µM) was assessed in incubations carried out in duplicate (n = 2). Representative data were plotted as the value of $\log_{10}$ (% aromatase activity observed), when normalized to control at 0 min of preincubation.

Discussion

Our data show that methadone is able to bring about time- and concentration-dependent inhibition of aromatase. Since a 10-fold dilution after preincubation of aromatase with methadone could not recover the loss of aromatase activity during the subsequent incubation of aromatase with testosterone, and since our data also show that methadone does not inhibit aromatase in a competitive setting (Figure 5.2), the time- and concentration-dependent inhibition of aromatase by methadone we observed is consistent with the action of an irreversible inhibitor. Since methadone is also metabolized by aromatase (Chapters Two and Three, this dissertation), our data meet established criteria (Silverman 1988) for the involvement of methadone as a mechanism-based or "suicide" inhibitor of aromatase. Such inhibitory activity is dependent on the catalytic mechanism and activity of the enzyme itself, which must first bind the drug and then catalytically activate it (Jones et al. 1999). The activated moiety irreversibly alters the enzyme and removes it permanently from the pool of active enzyme.

Because methadone can be metabolized by aromatase, it is possible that during preincubation, a portion of methadone is metabolized to its downstream metabolites by aromatase. My prior work has shown that the K_m value of the conversion of methadone to EDDP by aromatase in our recombinant system in vitro is relatively high (314 μM, Chapter Two, this dissertation) and the amount of EDDP formation would be very low given the preincubation conditions. Since my data also show that the primary metabolite EDDP does not have reversible inhibitory activity on aromatase at concentrations up to 100 μM, and secondary metabolite EMDP only inhibited aromatase activity by ~ 25% at 10 μM (Chapter Four Figure 4.1.A), it is unlikely that the decreased aromatase activity

during incubation with testosterone was due to inhibition by the methadone metabolites formed via a reversible mechanism. However, it is possible that EDDP and EMDP generated from methadone can inhibit aromatase via an irreversible mechanism during preincubation and therefore contribute to the decreased aromatase activity observed when methadone was tested. In fact, when EDDP and EMDP were separately tested for their ability to irreversibly inhibit aromatase, both metabolites showed time-dependent inactivation of aromatase (Figure 5.3). With that said, the potency of these metabolites are similar to or lower than that for methadone, and the concentrations of these metabolites present in preincubation mixture should be much lower than methadone concentrations. As a result, the contribution of methadone metabolism to the observed inactivation of aromatase would be minimal.

Our data indicate that methadone appeared to be a mechanism-based inhibitor of aromatase with an inactivation constant K_I of ~ 40 μM. Mechanism-based inhibition can result from bioactivation of a reactive intermediate that interacts with the heme prosthetic group of a cytochrome P450, or that covalently modifies the apoprotein (Hollenberg, Kent, and Bumpus 2008; Kalgutkar, Obach, and Maurer 2007), and can involve the subsequent formation of a metabolite intermediate complex that inactivates the enzyme and takes it out of the active pool (Jones et al. 1999). Such inhibition brought about by the formation of a metabolite intermediate complex has been demonstrated for a number of N-demethylated drugs including diltiazem (Jones et al. 1999) and erythromycin (Ortiz de Montellano et al. 1981). Although my work presented here does not address the detailed biochemical interactions underlying the mechanism-based inhibition of

aromatase by methadone, it is clear that methadone can irreversibly inactivate aromatase in vitro.

This irreversible inhibition by methadone might be important. Compared to reversible inhibition, irreversible inhibition more frequently results in unfavorable drug-drug interactions as the inactivated P450 enzyme has to be replaced by newly synthesized protein (Kalgutkar, Obach, and Maurer 2007), and severe clinical consequences may result (Wilkinson 2005). However, the clinical relevance of our data is difficult to extrapolate from in vitro data for the following reasons: The concentration of aromatase used in our experiments was relatively high. A K_m of 4 µM for the conversion of testosterone to estradiol was observed when 0.01 µM recombinant aromatase was used, while the K_m previously reported for this reaction in human placental microsomes was 0.2 µM (Zharikova et al. 2006). Furthermore, the K_I (40 µM) observed here was obtained with an aromatase concentration of 0.1 µM, even ten times higher than that mentioned above. This relatively high enzyme concentration for preincubation was a limit of our studies, but it was chosen to insure accurate quantification of estrogen generation in the diluted incubation mixture. Therefore, although the observed K_I was higher than the plasma concentrations of methadone seen in patients, it may be anticipated that a lower K_I would be obtained if methadone acts as a mechanism-based inhibitor in the human placenta or other tissues due to the lower enzyme concentrations likely to be present in tissues in vivo. In addition, while (R)-methadone therapeutic concentrations observed in plasma at steady state are in the 0.5 - 1 µM range (Eap, Buclin, and Baumann 2002), the concentration of this highly hydrophobic drug in tissues and at the aromatase active site may be substantially higher (Levine et al. 1995). It remains possible that methadone

reduces local aromatase activity in human tissues where aromatase concentration is much lower than that was used in our studies. Thus, future investigation is required in order to address whether or not methadone inhibits aromatase in vivo.

In addition, EDDP appeared to be as potent an irreversible inhibitor of aromatase as methadone itself, while EMDP appeared weaker, suggesting that methadone metabolites might be able to inhibit aromatase in vivo. However, this is not likely in patients taking methadone because these metabolites are present at much lower concentrations than methadone (Lu, Zhou et al. 2011; Kharasch et al. 2008). Of note, the conversion of EDDP to EMDP is a demethylation reaction. Whether or not aromatase is able to carry out this reaction has not been tested, but this possibility remains.

A few clinical observations are consistent with inhibition of aromatase by methadone. Deceased aromatase activity leads to altered metabolism and disposition of endogenous testosterone and androstenedione. Lower concentrations of estradiol and of follicle-stimulating hormone have been documented in men taking methadone (Hallinan et al. 2009), and low bone mineral density that may be due to low estrogen concentrations has been documented in 83% of patients in a methadone maintenance treatment program (Kim et al. 2006). Conceivably, other side effects of methadone that include flushing, muscle pain and symptoms consistent with estrogen withdrawal (Senay 1985; Backstrom 1995) may be explained in part by the drug's action on aromatase. In addition, unexpected methadone accumulation over time occurs in some patients, and multiple factors may underlie the variability observed in methadone pharmacokinetics including auto-inhibition (Morton 2007). The inhibitory effects of methadone on its own

metabolism by aromatase may be a contributor to the auto-inhibition of methadone clearance.

Overall, these studies have shown that methadone and its metabolites are irreversible inhibitors of aromatase in vitro. Since methadone itself is metabolized by aromatase, these interactions improve our understanding of possible mechanisms underlying variability in methadone clearance. While the clinical relevance of the inhibition of aromatase by methadone or its metabolites is not clear, the ability of these compounds to inhibit aromatase improves our understanding of aromatase. The irreversible mechanisms employed by these compounds could be further exploited for new ways to regulate aromatase activity for therapeutic purposes.

Methods

Testosterone metabolism in vitro by recombinant aromatase

All incubations were carried out under the incubation conditions described in "Chapter Ten: General Methods / Testosterone and methadone metabolism in vitro by recombinant aromatase".

Quantification of estradiol formation

High performance liquid chromatography (HPLC) assays with ultraviolet (UV) detection were developed for the quantification of testosterone conversion to estradiol as described in "Chapter Ten: General Methods / HPLC-UV assays for the quantifications of estradiol and EDDP formation".

Reversible inhibition of recombinant aromatase

Solutions of testosterone and tested inhibitor were mixed, and methanol was removed by drying in speed vacuum before the incubation. Incubations were then carried out in the same way as described in "Chapter Ten: General Methods / Testosterone and methadone metabolism in vitro by recombinant aromatase" except that the final testosterone and aromatase concentrations were 4 μM and 0.01μM, respectively. The inhibition of aromatase by methadone or letrozole was determined by measuring the conversion rate of testosterone to estradiol.

Mechanism-based inhibition of recombinant aromatase

Irreversible inhibition of recombinant aromatase was tested by preincubating aromatase with various concentrations of tested inhibitor as described in "Chapter Ten: General Methods / Mechanism-based inhibition of aromatase in vitro". The extent of inactivation of aromatase was determined by measuring the conversion rate of testosterone to estradiol during incubation.

Kinetic analyses

Formation rates of estradiol at different testosterone concentrations were fit to one site Michaelis-Menten kinetic models using Prism version 5.01 for Windows (GraphPad Software Inc., San Diego, CA).

The rates of metabolite formation from substrate probes in the presence of the test inhibitors were compared with those for control in which the inhibitor was replaced with vehicle. The inhibition data were fit to different models of enzyme inhibition

(competitive, non-competitive, and uncompetitive). The equations for kinetic and inhibition analyses of the data were constructed using NONMEM V v1.1 ® (ICON, Hanover MD and UCSF), utilizing the nonlinear regression functionality. The appropriateness of the fit was determined by visual inspection and by using the objective function, residual patterns, residual sums of squares, and precision of the parameter estimates. The correlation coefficient and its corresponding statistical significance were determined by conventional methods.

Determination of k_{inact} and K_I

K_I and k_{inact} values were estimated using an approach that involves a simultaneous fit of all the data. Data from experiments documenting the time course of inactivation were used for the calculation of inhibition kinetic parameters. Estradiol formation was expressed as pmol/min/pmol aromatase and the percentage of remaining activity was calculated as shown in the following equation:

$$\%\ \text{of remaining enzyme activity} = \frac{E_t}{E_0} * 100$$

where E_t is the enzyme activity expressed as estradiol formation at time t, and E_0 is the average estradiol formation at preincubation time zero (100%). The extent of inhibition was expressed as: 1 – % of remaining enzyme activity.

The pseudo first-order rate constant for enzyme inactivation, λ, was estimated from the aggregation of all the data using equation:

$$E_{(t)} = E_0 * e^{-\lambda t}$$

The relationship between λ and inhibitor concentration was fit to the following equation:

$$\lambda = k_{inact} * [I]/(K_I + [I])$$

where k_{inact} is the rate constant for inactivation, [I] is inhibitor or inactivator concentration, and K_I is the inactivator concentration that produced half the maximal rate of inactivation, analogous to a K_m. This equation assumes there was negligible change of [I] during the incubation period and that loss of enzyme was due to inactivation. As indicated above, all the data were fitted for each inhibitor concentration to obtain a single estimate for k_{inact} and a single estimate for K_I using these equations.

Note: Equations are quoted from (Jones et al. 1999).

Note: The work described in this chapter has been published (Lu et al. 2010).

CHAPTER SIX

Stereoselective Inhibition of Aromatase by Naringenin

Introduction

There is existing interest in the effects of dietary factors on the cytochrome P450 system in order to better understand food-drug interactions. Interactions between food and aromatase (CYP19) are also of interest due to potential influence on estrogen synthesis. Xenoestrogens are industrial or dietary compounds that can affect steroidogenesis and cause endocrine disruption by changing aromatase activity. Our preliminary results (Chapter Four, this dissertation) suggest that naringenin may be one of these xenoestrogens that can inhibit aromatase in vivo. Naringenin (Figure 6.1, Structure 1) is a chiral flavanone belonging to the flavonoid class. It is contained in some citrus species, in particular grapefruit, that contain large amounts of its 7-O-neohesperidoside, naringin (Figure 6.1, Structure 2). Upon ingestion, naringin undergoes cleavage of the sugar moiety, leaving the free aglycone, naringenin in the gastrointestinal tract (Yanez and Davies 2005). Naringenin is known to reduce CYP3A activity in humans, but its effects on aromatase has not been carefully studied. My prior screening results (Chapter Four, this dissertation) indicate that naringenin substantially reduced aromatase activity at 20 μM and the enantiomers of naringenin, (R)- and (S)-naringenin, appeared to have different potency as aromatase inhibitors. These data suggest that fruit products containing naringenin might affect aromatase activity in vivo.

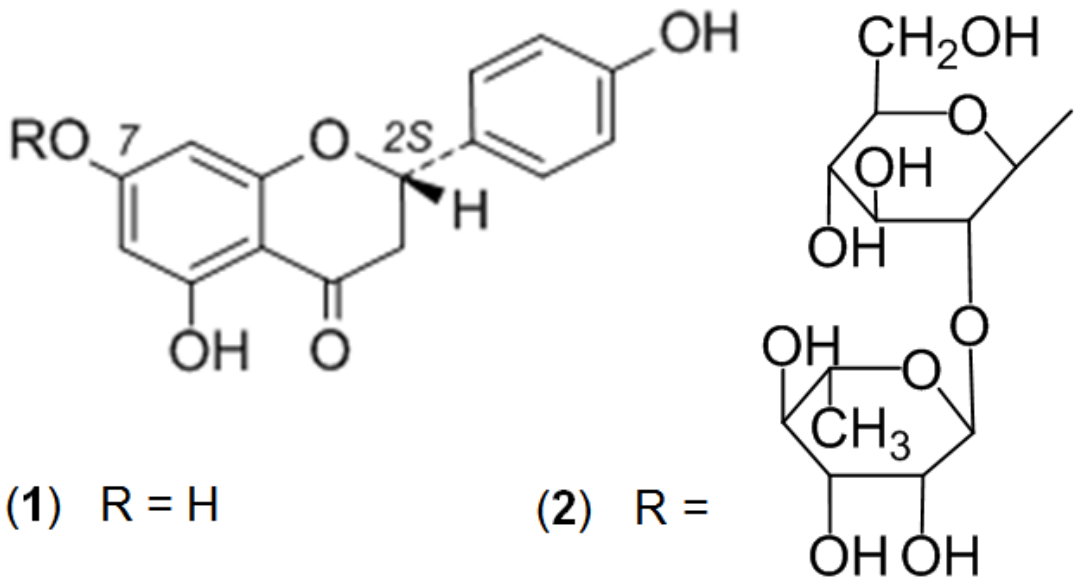

Figure 6.1. Structures of naringenin and naringin.

Compound structure represents naringenin when R = H (1) or naringin when R = neohesperidosyl (2). Source: modified from structure figures provided by our collaborator Dr. Salvatore Caccamese at Università di Catania, Catania, Italy.

The inhibition of CYP enzymes by flavonoids like naringenin may be of medical importance. Since the demonstration that grapefruit juice can inhibit the metabolism of the CYP3A substrate felodipine (Bailey et al. 1993), it has become widely appreciated that the ingestion of a number of fruit juices can slow drug metabolism (Bailey et al. 2004), and thereby increase the concentrations of important medications such as cyclosporine (Lee et al. 2001) and methadone (Benmebarek et al. 2004). The biochemical basis for these interactions involves the interaction of flavonoids with specific CYP isoforms. In order to be aware of any potential clinically relevant interactions between naringenin and both endogenous and exogenous substrates of aromatase, it is therefore important to study interactions of naringenin with aromatase.

Naringenin has been reported to have a number of potential health related properties. In a previous study, naringenin was found to inhibit the CYP3A4-mediated oxidation of two dihydropyridine cardiodepressive drugs, more markedly than naringin (Guengerich and Kim 1990). Later, naringenin was found inter alia to inhibit the activity of CYP isoforms that activate the potent environmental carcinogen, nicotine-derived nitrosamine ketone (Bear and Teel 2000). Naringenin also inhibited quinine 3-hydroxylation mediated by CYP3A4 (Ho, Saville, and Wanwimolruk 2001). It may also act as a potent immunomodulator in mice with pulmonary fibrosis (Du et al. 2009), and the antioxidant properties of naringenin and other polyphenols have been well studied (Manthey, Grohmann, and Guthrie 2001).

Despite a volume of research over many years, the relevance of stereochemistry at the C-2 stereogenic centre of naringenin has not been carefully evaluated. It is well known that interactions between an enzyme system and a substrate are frequently stereospecific (Crossley 1992), and often influence the potency of, and the response to a single enantiomer (Hutt 2006). For example, quinidine is a clinically relevant and potent inhibitor of CYP2D6, while its diastereomer quinine is not (Muralidharan et al. 1991), (S)-lansoprazole is a more potent inhibitor of CYP2C9, CYP2C19, CYP2D6, CYP2E1 and CYP3A4-mediated hydroxylation than (R)-lansoprazole (Liu et al. 2005) and many other chiral drugs have been well documented to exhibit enantioselective inhibition of P450-mediated metabolism (Carabaza et al. 1997; Shin, Kane, and Flockhart 2001; Dilmaghanian et al. 2004). Difficulties in separating enantiomers and the resulting absence of readily available pure enantiomers have limited research in this area until now.

In this study, we obtained purified (R)- and (S)- naringenin preparations together with the racemate, rac-naringenin, and tested for their ability to inhibit aromatase, with a focus on the enantioselectivity of the interaction. In addition, in order to obtain a better understanding of naringenin action on the CYP system, the effects of the (R)-, (S)- and rac-naringenin on other important human drug-metabolizing CYP isoforms, including CYP2B6, 2C9, 2C19, 2D6 and 3A, and their corresponding enantioselectivity were also tested.

Results

Dose-dependent inhibition of recombinant human aromatase by naringenin was demonstrated (Figure 6.2). When the enantiomers of naringenin were tested, stereoselective inhibition was shown. Specifically, the (S)-naringenin inhibited aromatase with an IC_{50} value of 1.4 (1.1, 1.7) μM, and was approximately 2-fold more potent than the (R)-naringenin, which had an IC_{50} value of 2.8 (2.4, 3.4) μM. The IC_{50} value for rac-naringenin was 2.0 (1.7, 2.4) μM, between that for the (R)-enantiomer and that for the (S)-enantiomer (Figure 6.2).

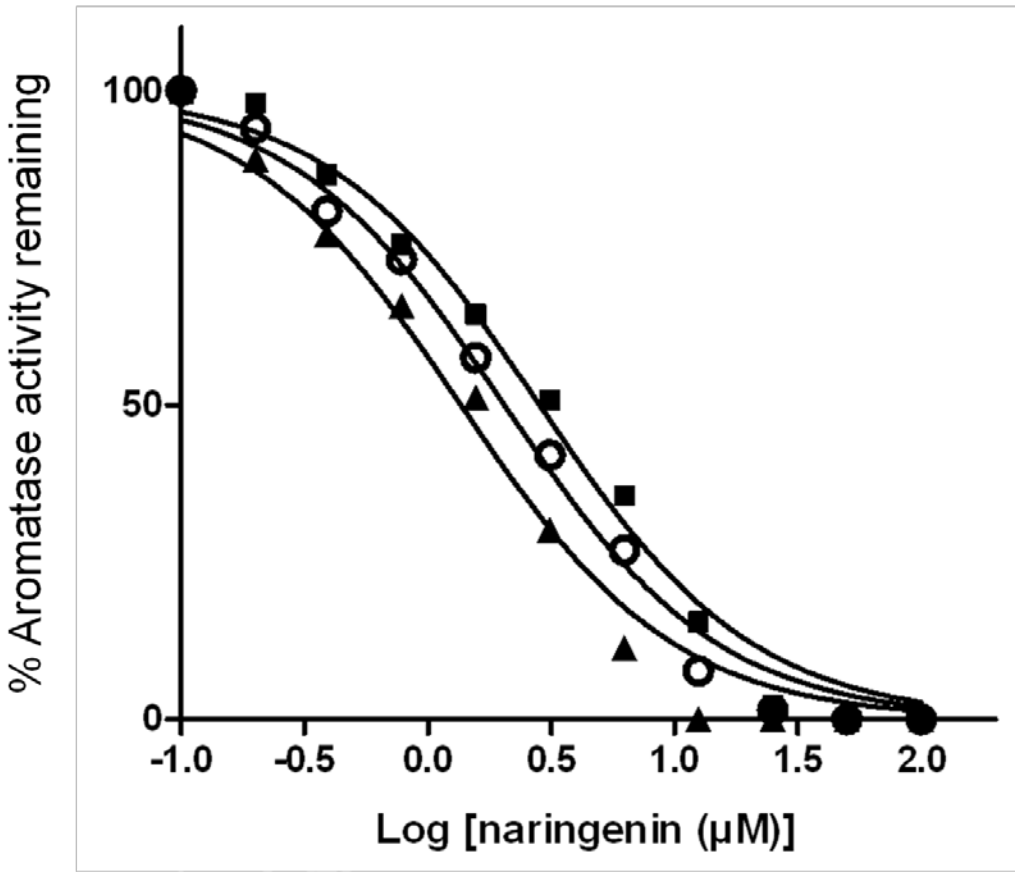

Figure 6.2. Enantioselective inhibition of human aromatase by naringenin.

A range of concentrations of rac-naringenin (open circle), (R)-naringenin (dark square), or (S)-naringenin (dark triangle) was incubated with recombinant human aromatase (7.5 nM) and substrate MFC at 37 °C for 30 min and enzyme activity was determined in three independent experiments. Individual points represent the mean of duplicate incubations.

Naringenin was also tested for its ability to inhibit a number of other important drug-metabolizing CYP isoforms. Data indicate that naringenin inhibited CYP2C9, CYP2C19, and CYP3A in an enantioselective way (Figures 6.3 - 6.5). While the (S)-enantiomer was approximately 2-fold more potent than the (R)-enantiomer as an inhibitor of CYP2C19, the (R)-enantiomer was about 2-fold more potent as an inhibitor of

CYP2C9 and CYP3A (Table 6.1). In each case, the IC_{50} value for rac-naringenin was between that for the (R)-enantiomer and that for the (S)-enantiomer. No appreciable inhibition of CYP2B6 or CYP2D6 was observed at concentrations up to 10 μM (data not shown).

Note: Experiments using human liver CYP3A were performed by my colleague Cong Xu in the Department of Pharmacology and Toxicology here at Indiana University.

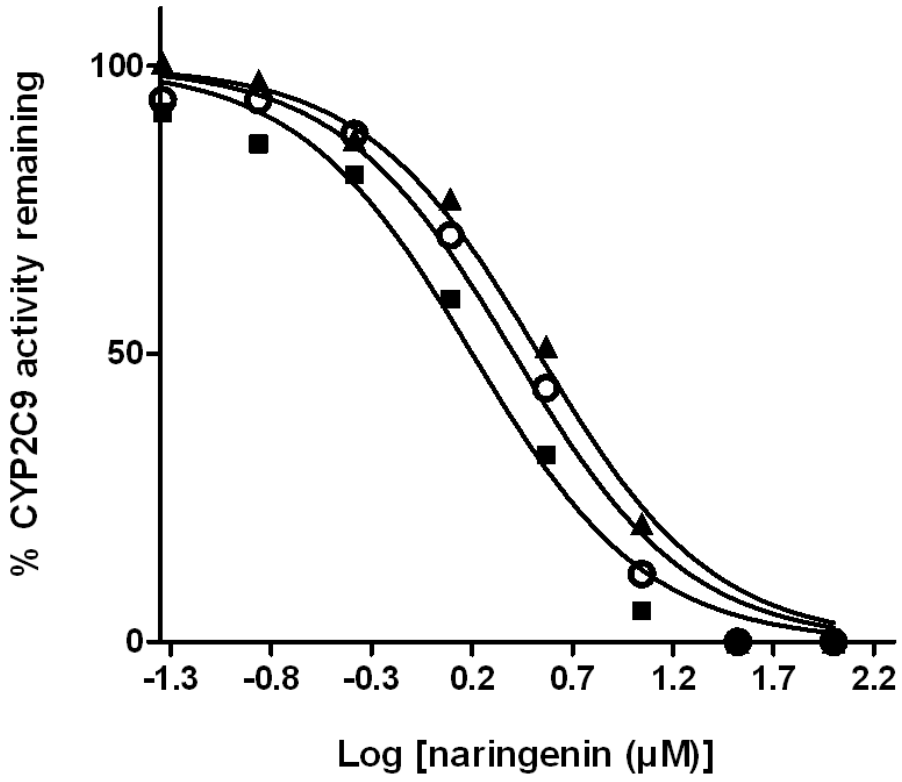

Figure 6.3. Enantioselective inhibition of human CYP2C9 by naringenin.

A range of concentrations of rac-naringenin (open circle), (R)-naringenin (dark square), or (S)-naringenin (dark triangle) was incubated with recombinant human CYP2C9 (15 nM) and substrate MFC at 37 °C for 45 min and enzyme activity was determined in three independent experiments. Individual points represent the mean of duplicate incubations.

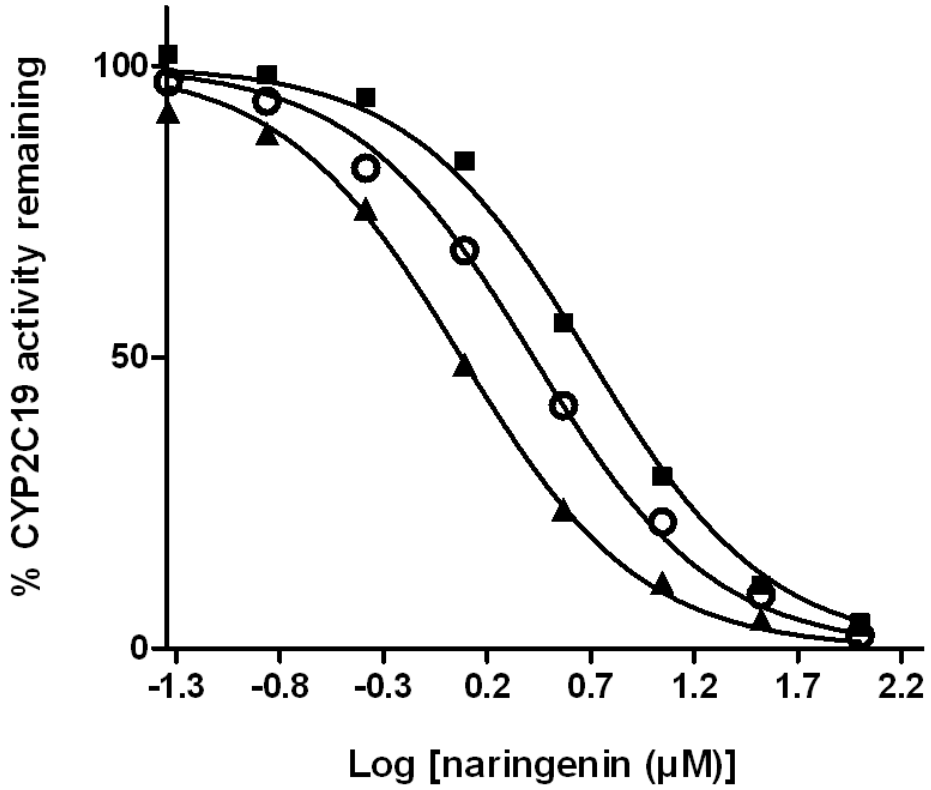

Figure 6.4. Enantioselective inhibition of human CYP2C19 by naringenin.

A range of concentrations of rac-naringenin (open circle), (R)-naringenin (dark square), or (S)-naringenin (dark triangle) was incubated with recombinant human CYP2C19 (7.5 nM) and substrate CEC at 37 °C for 30 min and enzyme activity was determined in three independent experiments. Individual points represent the mean of duplicate incubations.

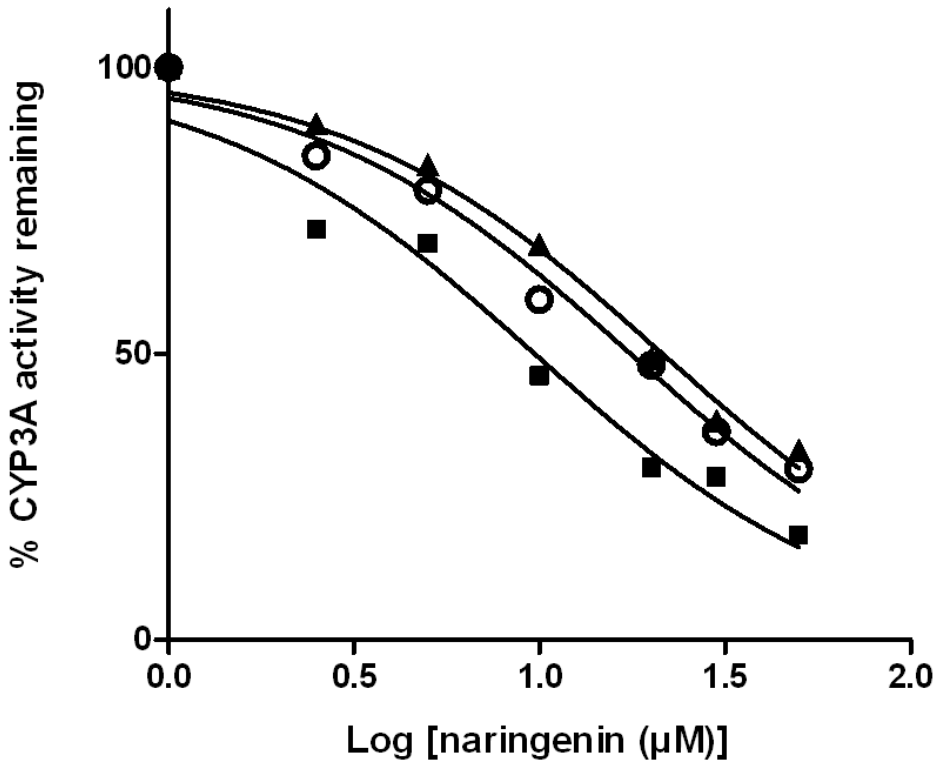

Figure 6.5. Enantioselective inhibition of human CYP3A by naringenin.

A range of concentrations of rac-naringenin (open circle), (R)-naringenin (dark square), or (S)-naringenin (dark triangle) was incubated with pooled human liver microsomes (protein concentration 0.25 mg/ml) and probe substrate testosterone at 37 °C for 15 min and enzyme activity was determined in two independent experiments. Individual points represent the mean of duplicate incubations. Source: These experiments using human liver CYP3A were performed by my colleague Cong Xu. The study design and data analysis were carried out by me.

Table 6.1. IC_{50} values for enantioselective inhibition of multiple human CYP isoforms by naringenin.

μM	CYP19	CYP2C9	CYP2C19	CYP3A
rac-naringenin	2.0 (1.7, 2.4)	2.6 (2.0, 3.4)	2.6 (2.4, 2.9)	17.6 (14.8, 20.8)
(R)-naringenin	2.8 (2.4, 3.4)	1.6 (1.2, 2.1)	4.9 (4.4, 5.5)	9.7 (7.3, 12.8)
(S)-naringenin	1.4 (1.1, 1.7)	3.4 (2.6, 4.5)	1.2 (1.1, 1.4)	21.4 (18.5, 24.7)

Note: IC_{50} values are expressed as mean (95% confidence interval). Source: Data on CYP19, 2C9 and 2C19 were from me, and data on CYP3A were generated in collaboration with my colleague Cong Xu.

Discussion

Many naturally occurring flavonoids and isoflavanoids exist as stereoisometric mixtures, in which one enantiomer predominates. These studies demonstrate the ability of naringenin to inhibit aromatase and several other CYP isoforms in vitro. Previous studies have shown that maximal plasma concentrations of naringenin after ingestion of grapefruit juice are ~ 6 μM (Erlund et al. 2001). The IC_{50} values of naringenin we observed all fall in the low micromolar range (Table 6.1). These data suggest that naringenin may have effects in vivo on the activity of multiple enzymes, including aromatase, CYP2C9, CYP2C19 and CYP3A. Such inhibitory effects might contribute to the clinically observed food-drug interactions brought about by grapefruit juice and other fruit products (Dresser and Bailey 2003). Our data are consistent with those reported on inhibition of CYP3A by grapefruit and other juices in humans (Bailey, Dresser, and Bend

2003; Bailey et al. 2004). However, fruit juices contain other components that might also inhibit CYP3A in vivo. The quantitative contribution of naringenin to the overall clinical effect is currently unclear. Whether or not interactions between naringenin and other CYP isoforms, including aromatase, carry similar clinical relevance must await further research.

While a large literature exists on the effects of grapefruit and other juices on CYP3A, few attempts have been made to study their effects on other isoforms. Our studies have characterized for the first time the different pharmacologic properties of the enantiomers of naringenin on multiple enzymes. Studies with purified (R)- and (S)-naringenin showed that the individual enantiomers had different affinities for every enzyme tested, indicating that naringenin is a pleiotropic and stereoselective inhibitor in vitro. While this stereoselective inhibition is clear, the potency difference between enantiomers was about two fold in every case. Whether or not this stereoselectivity represents clinical significance is unknown. Since the predominant enantiomer of naringenin in natural fruits is also unknown, the vulnerability of specific enzymes in vivo cannot be estimated yet. Nevertheless, our findings identify interactions between specific CYP isoform and naringenin that deserve further study in order to more precisely predict the potential risks for food-drug interactions. Such future studies are potentially important because interactions between naringenin and drugs that are substrates of CYP2C9 such as (S)-warfarin (Rettie et al. 1992), of CYP2C19, such as clopidogrel (Kreutz et al. 2010), and of aromatase, such as methadone (Chapters Two and Three, this dissertation) may exist.

Our data also shed light on the stereoselective preferences of specific CYP isoforms. Since other chiral flavonoids contained in fruits may also possess similar stereoselective pharmacologic and biological effects, this work improves our understanding of the susceptibility of individual CYP isoforms to inhibition by dietary factors. In particular, inhibition of aromatase by natural products might be therapeutically useful for breast cancer patients, and might be protective for people who are at risk. Although our in vitro results indicate that naringenin itself is not likely to serve as a selective candidate for this purpose because it inhibits several CYPs, the development of novel aromatase inhibitors from natural compounds that are more selective still represents a potentially important direction for future research. Of note, naringin, the natural precursor of naringenin, is present as (2S)- and (2R)-diastereomers in grapefruit, sour orange and pummelo with the (2S)-naringin being predominant, and the ratio (2S) / (2R) of the concentrations of the diastereomers markedly decreases during maturation (Caccamese, Manna, and Scivoli 2003; Caccamese, Bianca, and Santo 2007; Caccamese and Chillemi 2010). Since our data show that the inhibitory effect of natural compounds such as naringenin on aromatase can be stereoselective, the effects of fruit juices on aromatase may be affected by the degree of maturation of the fruits.

Although the clinical relevance of these findings warrant further research, inhibition of aromatase by naringenin observed in vitro may be exploited to understand pharmacokinetic changes seen in vivo. The stereoselective properties exhibited by naringenin here could provide insight into the use of naringenin and other flavonoids as novel, selective therapeutic agents.

Methods

Fluorescent assay for inhibition of aromatase in vitro

The activity of aromatase was determined by measuring the conversion rate of a fluorometric substrate, 7-methoxy-4-trifluoromethylcoumarin (MFC), to its fluorescent metabolite, 7-hydroxytrifluoromethylcoumarin (HFC) as described in "Chapter Ten: General Methods / Fluorescent assay for inhibition of aromatase in vitro".

Inhibition of recombinant human CYP isoforms

The activity of each recombinant human CYP isoform was determined by measuring the conversion rate of a fluorometric substrate to its fluorescent metabolite as described in "Chapter Ten: General Methods / Inhibition of recombinant human CYP isoforms".

Kinetic analyses

The rates of metabolite formation from substrate probes in the presence of the test inhibitors were compared with those for control in which the inhibitor was replaced with vehicle. The extent of CYP inhibition was expressed as percent enzyme activity remaining compared to control. IC_{50} values were determined as the inhibitor concentration that brought about a 50% reduction in enzyme activity by fitting all the data to a one-site competition equation using Prism version 5.01 for Windows (GraphPad Software Inc., San Diego, CA).

Note: The work described in this chapter has been published (Lu, Ferlito et al. 2011).

CHAPTER SEVEN

Competitive and Non-competitive Inhibition of Aromatase by Tamoxifen Metabolites

Introduction

Prior screening results (Chapter Four, this dissertation) indicate that at least two tamoxifen metabolites can decrease aromatase activity when tested at 10 μM in vitro. Tamoxifen is a selective estrogen receptor modulator also used in the treatment of estrogen-sensitive breast cancer. The biochemical mechanism of action of tamoxifen in the treatment of breast cancer is widely understood to involve two active metabolites, 4-hydroxy-N-desmethyl-tamoxifen (endoxifen) and (Z)-4-hydroxy-tamoxifen (4HT). The anti-estrogenic effects of tamoxifen were thought to be exclusively mediated via these active metabolites that bind to estrogen receptor and thereby modulate estrogen signaling. These metabolites are approximately 100 times more potent, relative to the parent drug, as antagonists of estrogen binding to the estrogen receptor and as inhibitors of estrogen-stimulated growth in sensitive breast cancer cell lines (Furr and Jordan 1984; Kisanga et al. 2004; Jin et al. 2005). The discovery that the principal active metabolite, endoxifen is produced via metabolism from N-desmethyl-tamoxifen (NDMT), by a genetically polymorphic enzyme, CYP2D6 (Jin et al. 2005; Stearns et al. 2003), has led many clinical investigators to test the possibility that CYP2D6 genotype might be a useful biomarker of tamoxifen efficacy. These efforts have produced mixed results (Goetz et al. 2005; Wegman et al. 2007; Higgins and Stearns 2010). While some investigators have shown a association between CYP2D6 poor metabolizer genotype and increased

recurrence of breast cancer in some settings (Goetz et al. 2005), other investigators, using different trial designs and alternative study approaches have either failed to show any association (Nowell et al. 2005), or have shown an association in the opposite direction (Wegman et al. 2007). As a result, the clinical utility of a CYP2D6 genotype guided approach to predicting response to tamoxifen has not been clearly demonstrated (Higgins et al. 2009). The closely related concept that endoxifen or 4HT concentrations in the blood might predict the outcome of tamoxifen therapy in individual patients has also not been validated in any clinical study. Similarly, predicting which patients are at risk for side effects of tamoxifen is also difficult. Many patients experience hot flashes (Mortimer et al. 2008; Henry et al. 2009), muscle aches (Fisher et al. 2005) and other symptoms that limit their compliance with treatment, and clearly result in increased rates of breast cancer recurrence (Thompson et al. 2010). Although it has been suspected that these side effects are caused by estrogen receptor antagonism, no relationship between the concentrations of the estrogen receptor modulating metabolites of tamoxifen and the incidence or severity of side effects has been reported. Furthermore, although CYP2D6 genotype is clearly associated with the concentrations of these active metabolites (Jin et al. 2005), it has not been consistently shown to predict hot flashes experienced by patients taking tamoxifen (Goetz et al. 2005; Henry et al. 2009).

One possible explanation for this lack of association may be the involvement of mechanisms discrete from the 2D6-dependent estrogen receptor antagonism. Tamoxifen has a complex metabolic profile involving many active and inactive metabolites (Desta et al. 2004). The estrogen receptor binding characteristics of a large number of these metabolites have been extensively documented in the search for novel SERMs

(Katzenellenbogen et al. 2000; Lim et al. 2005). In fact, a key, potent metabolite, endoxifen is under active clinical development (Ahmad, Ali et al. 2010; Ahmad, Shahabuddin et al. 2010). In contrast, the ability of many tamoxifen metabolites to exert anti-estrogenic effects via alternative mechanisms has not been studied. Among alternative mechanisms for tamoxifen action, the inhibition of aromatase seems possible because the aromatase inhibitor class of drugs bring about hot flashes and musculoskeletal pains similar to those experienced by patients taking tamoxifen (Howell et al. 2005; Zivian and Salgado 2008). The commonality of these side effects may reflect a shared biochemical mechanism. Consistent with a reduction in aromatase activity, tamoxifen significantly lowers estrogen in post-menopausal women (Lonning et al. 1995).

Tamoxifen and the AI class of drugs are both effective endocrine therapies for breast cancer, and they bring about some common side effects, but the effect of tamoxifen therapy on aromatase has not been studied until now. Since tamoxifen is metabolized via several pathways to various downstream molecules in humans, and since anti-estrogenic effects may be brought about not only by estrogen antagonism, but also by reduced estrogen synthesis. For these reasons, I hypothesize that the clinical effects of tamoxifen may be mediated in part by actions of tamoxifen or its metabolites as aromatase inhibitors. To investigate this possibility, I tested the ability of tamoxifen, its three major human metabolites and a number of its minor metabolites to inhibit the activity of aromatase in vitro.

Results

Non-competitive inhibition of aromatase by endoxifen and NDMT

Inhibition of aromatase by tamoxifen and its three major metabolites, 4HT, NDMT and endoxifen, was separately tested by measuring their effects on the rate of generation of a fluorescent metabolite from a fluorometric substrate, MFC, during incubation with aromatase. As shown in Figure 7.1, endoxifen and NDMT inhibited aromatase with higher potency than tamoxifen or 4HT. When substrate concentration was set at 25 μM, endoxifen and NDMT exhibited IC_{50} values of 6.1 μM and 20.7 μM, respectively, while tamoxifen and 4HT were estimated to have IC_{50}s of 986 μM and 531 μM, respectively (Table 7.1). Under the same conditions, letrozole was used as a positive control and had an IC_{50} of 5.3 nM. When the endogenous substrate of aromatase, testosterone, was included as a competing substrate, an IC_{50} of 0.33 μM was observed.

Table 7.1. IC_{50} values of inhibitors of recombinant human aromatase.

Inhibitor	Endoxifen	NDMT	4HT	Tamoxifen	Letrozole	Testosterone
IC_{50} (μM)	6.1	20.7	531	986	0.0053	0.33

Note: IC_{50} values were determined when substrate MFC and aromatase concentrations were set at 25 μM and 7.5 nM respectively as describe in the “Methods” section.

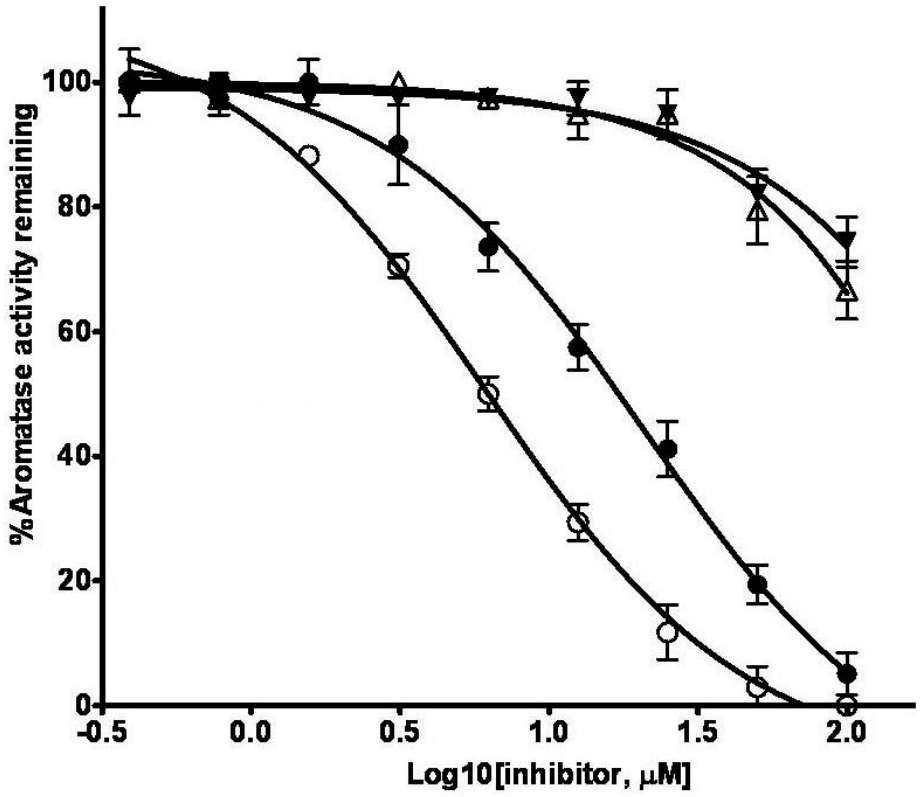

Figure 7.1. Inhibition of aromatase by tamoxifen and its metabolites.

Curves represent percent aromatase activity remaining in the presence of a range of concentrations of endoxifen (open circle), tamoxifen (dark triangle), NDMT (dark circle) and 4HT (open triangle). Individual points represent the mean of four independent incubations.

To further explore the mechanism of the inhibition by endoxifen and NDMT, I tested inhibition by these metabolites across a range of fluorometric substrate concentrations. The data were plotted as Dixon and Eadie-Hofstee plots (Figures 8.2 and 8.3). The profile of the lines on the resulting Dixon plots: straight lines intersecting at a common point on the x-axis, is consistent with non-competitive inhibition by endoxifen and NDMT (Figures 7.2.A and 8.3.A). The parallel relationship of the lines in the Eadie-

Hofstee plots is consistent with decreasing maximum enzyme activity V_{maxi} and unchanged substrate equilibrium dissociation constant K_{Sapp} as inhibitor concentration was increased (Figures 7.2.B and 8.3.B), observations that were also consistent with a non-competitive mechanism. The data indicate a K_i for endoxifen of 4.0 µM, and a K_i for NDMT of 15.9 µM.

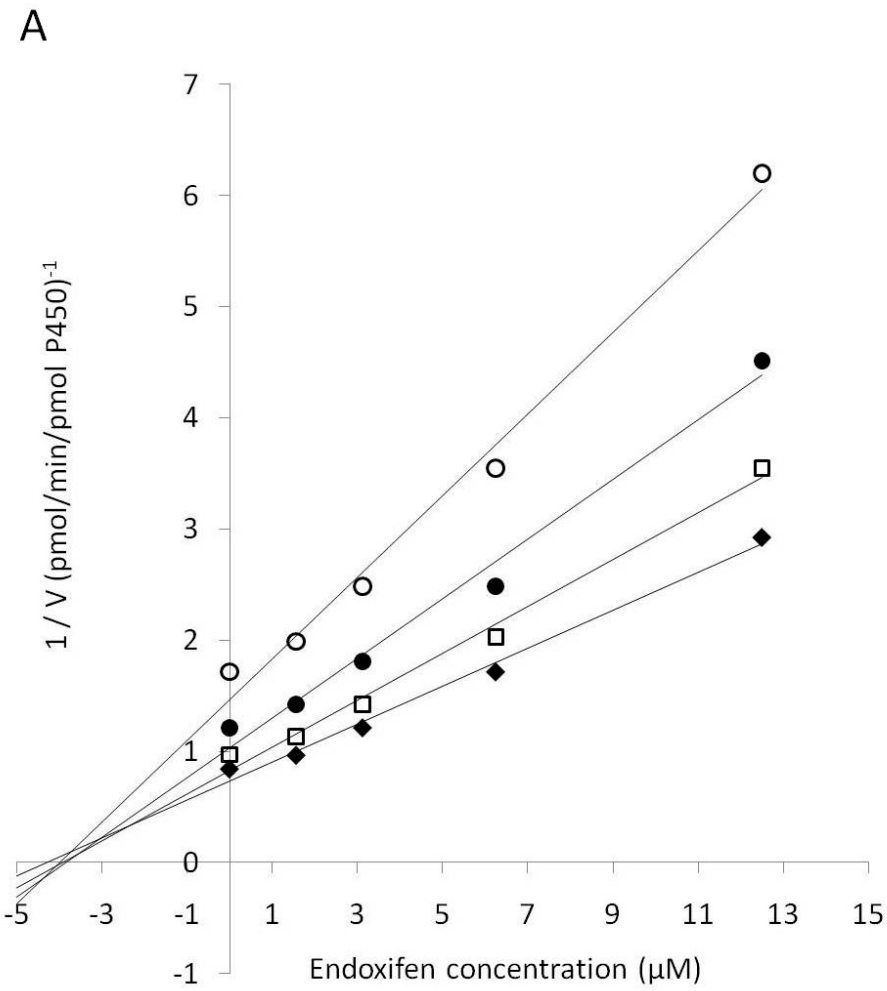

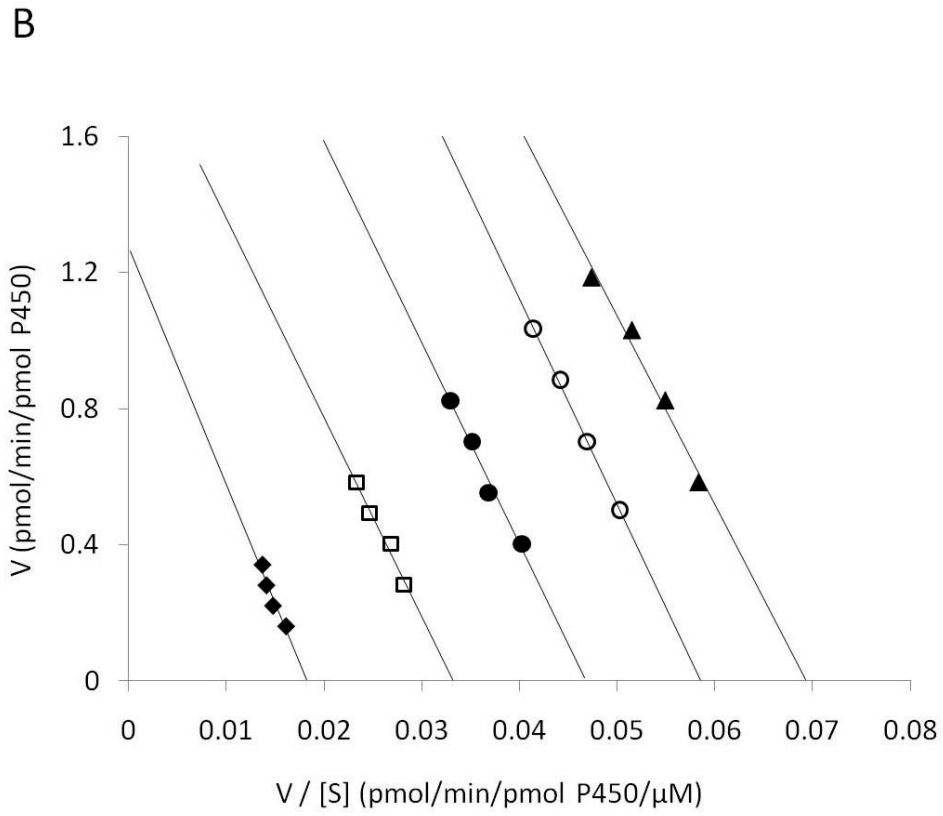

Figure 7.2. Non-competitive inhibition of MFC metabolism by endoxifen.

(A) Dixon plot of inhibition of aromatase by endoxifen with MFC concentrations set at 10 (open circle), 15 (dark circle), 20 (open square) and 25 (dark diamond) µM. (B) Eadie-Hofstee plot of inhibition of aromatase by endoxifen with increasing inhibitor concentrations: 0 (dark triangle), 1.56 (open circle), 3.13 (dark circle), 6.25 (open square) and 12.5 (dark diamond) µM. A range of MFC concentrations was incubated with 7.5 nM recombinant human aromatase for 30 min in the absence and presence of 1.56, 3.13, 6.25 or 12.5 µM endoxifen. Individual points represent the mean of duplicate incubations.

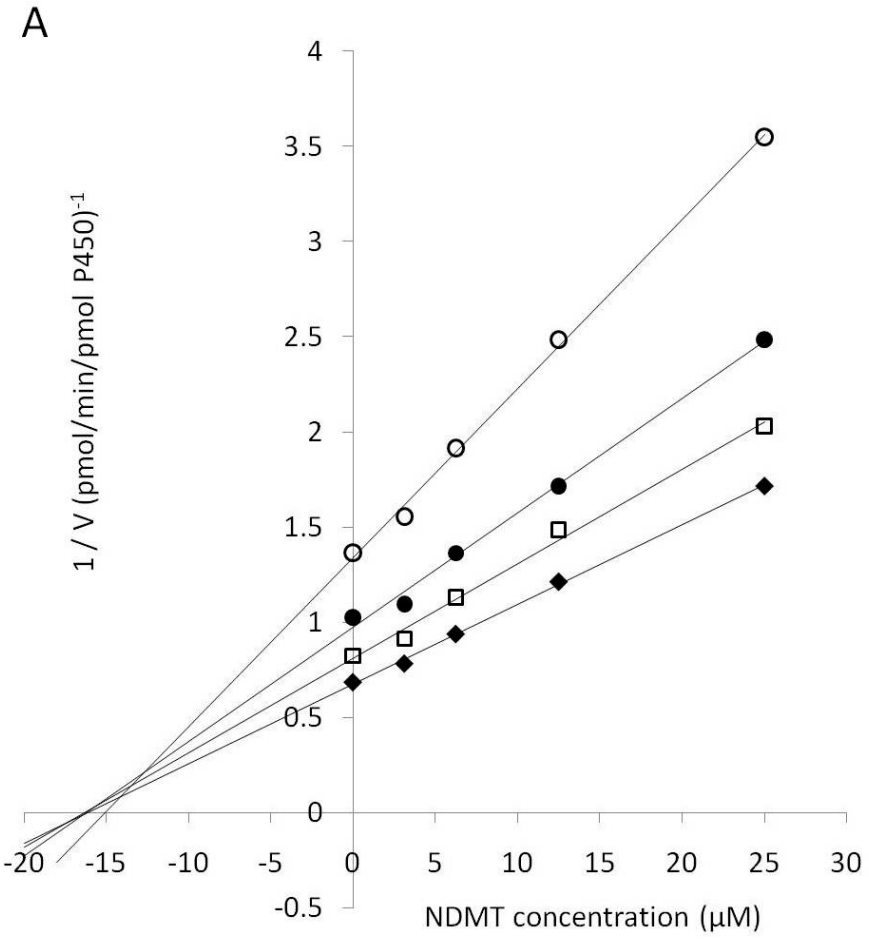
A
4
3.5
3
2.5
2
1.5
1
0.5
0
-0.5
-20
-15
-10
-5
0
5
10
15
20
25
30
1 / V (pmol/min/pmol P450)-1
NDMT concentration (µM)

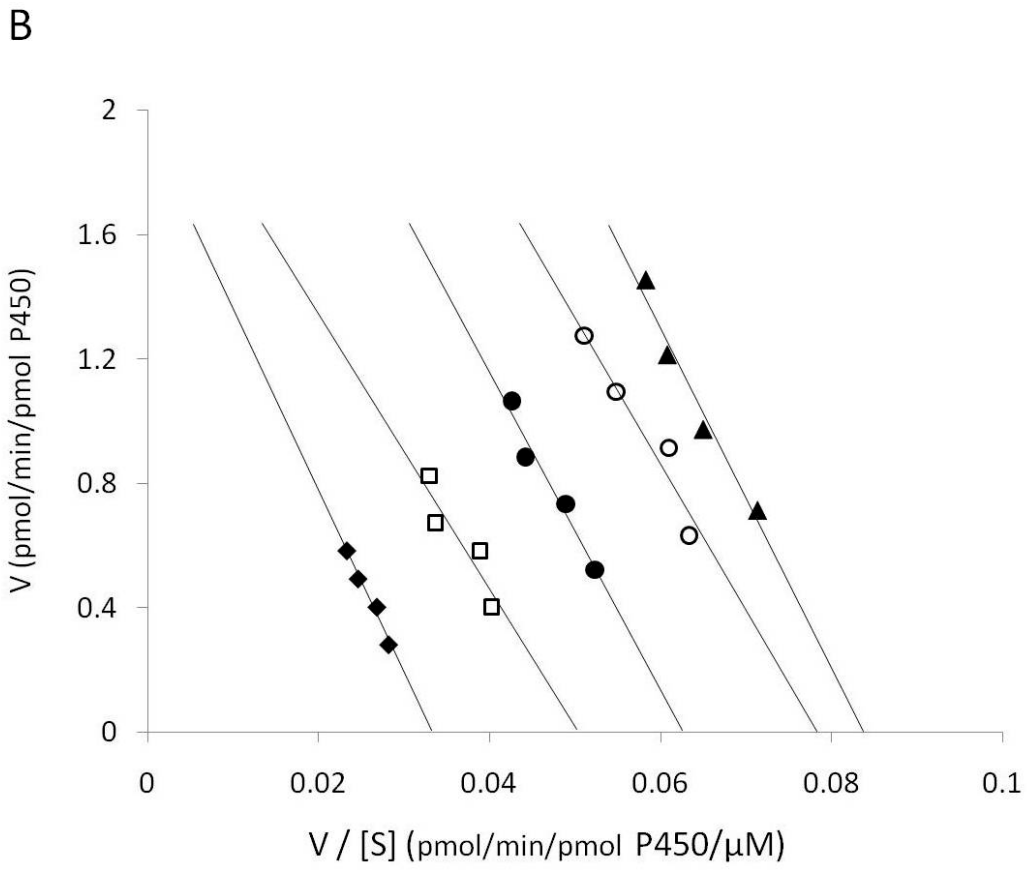

Figure 7.3. Non-competitive inhibition of MFC metabolism by NDMT.

(A) Dixon plot of inhibition of aromatase by NDMT with MFC concentrations set at 10 (open circle), 15 (dark circle), 20 (open square) and 25 (dark diamond) µM. (B) Eadie-Hofstee plot of inhibition of aromatase by NDMT with increasing inhibitor concentrations: 0 (dark triangle), 3.13 (open circle), 6.25 (dark circle), 12.5 (open square) and 25 (dark diamond) µM. A range of MFC concentrations was incubated with 7.5 nM recombinant human aromatase for 30 min in the absence and presence of 3.13, 6.25, 12.5 or 25 µM NDMT. Individual points represent the mean of duplicate incubations.

To study the inhibitory mechanism using an alternative approach, the same data were plotted using Lineweaver-Burke plots. The data obtained also indicate that both

endoxifen and NDMT decreased the apparent V_{max} (V_{maxi}), while leaving the apparent K_m (K_{Sapp}) unchanged (Table 7.2), once more consistent with non-competitive inhibition.

Table 7.2. Effect of endoxifen and NDMT on K_{Sapp} and V_{maxi} of recombinant human aromatase.

Inhibitor (μM)	K_{Sapp} (μM)	V_{maxi} (pmol/min/pmol P450)
Endoxifen		
0	58.5	4.05
1.56	60.8	3.56
3.13	57.8	2.72
6.25	61.9	2.03
12.5	66.2	1.22
NDMT		
0	52.4	4.43
3.13	54.2	4.09
6.25	51.9	3.23
12.5	52.4	2.53
25	61.8	2.03

Note: K_{Sapp} and V_{maxi} values were determined using Lineweaver-Burke plot as described in the "Methods" section.

Furthermore, I tested the ability of the metabolites that inhibited MFC metabolism by aromatase to inhibit testosterone metabolism to estrogen. In order to confidently detect the generation of estrogen, I incubated a higher concentration of aromatase (50 nM) with multiple testosterone concentrations chosen to be within the linear range around the K_m (4 μM). When a range of concentrations of endoxifen were incubated with testosterone and aromatase under these conditions, endoxifen inhibited the generation of estrogen with

a K_i of 178 µM, with kinetics examined using Dixon and Eadie-Hofstee plots that again indicate non-competitive inhibition (Figure 7.4). Equivalent experiments with NDMT indicated that NDMT was a weaker inhibitor than endoxifen (data not shown), but experiments for K_i determination could not be carried out due to its relative insolubility at higher concentrations which were desired.

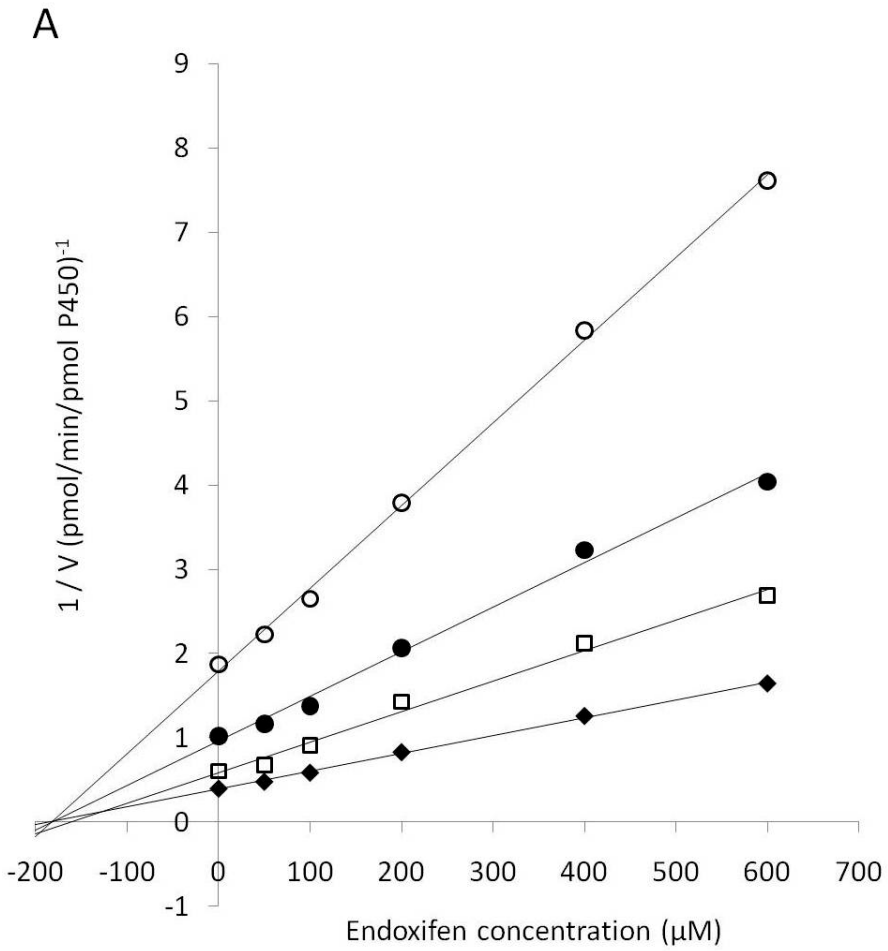

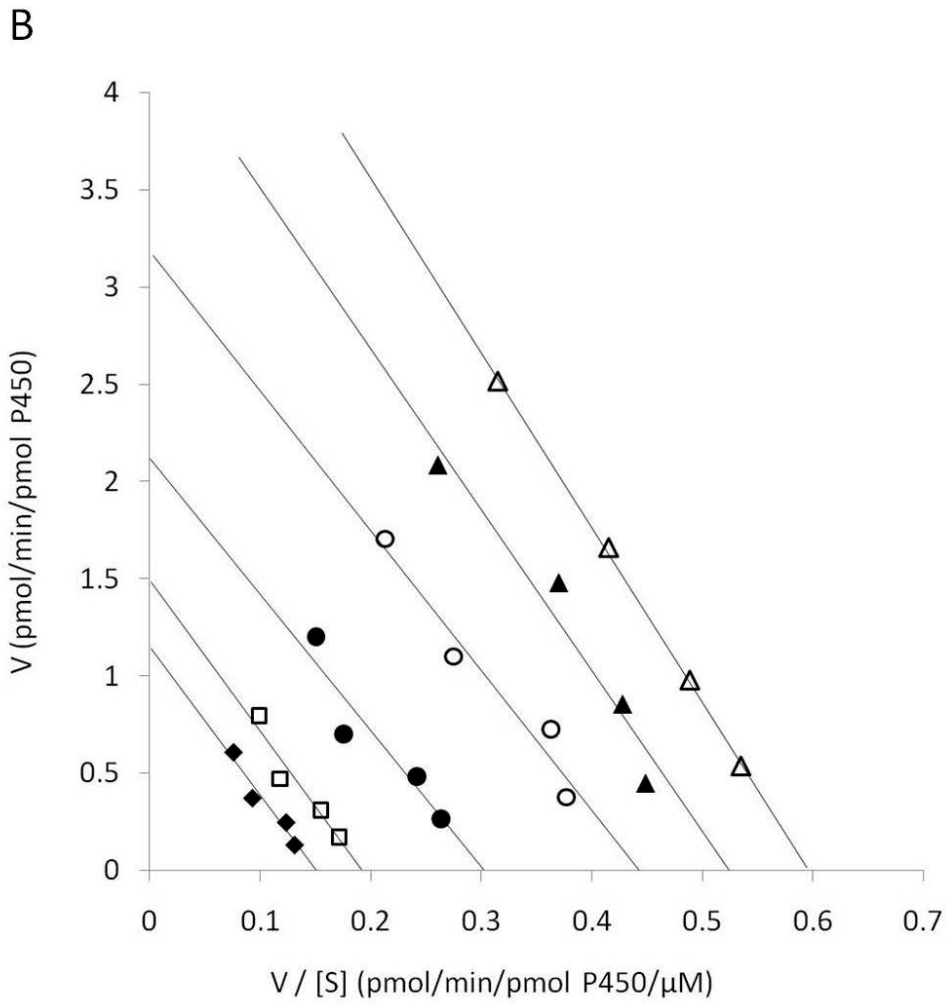

Figure 7.4. Non-competitive inhibition of testosterone metabolism by endoxifen.

(A) Dixon plot of inhibition of aromatase by endoxifen with testosterone concentrations set at 1 (open circle), 2 (dark circle), 4 (open square) and 8 (dark diamond) µM. (B) Eadie-Hofstee plot of inhibition of aromatase by endoxifen with increasing inhibitor concentrations: 0 (open triangle), 50 (dark triangle), 100 (open circle), 200 (dark circle), 400 (open square) and 600 (dark diamond) µM. A range of testosterone concentrations was incubated with 50 nM recombinant human aromatase for 10 min in the absence and presence of 0, 50, 100, 200, 400 or 600 µM endoxifen. Individual points represent the mean of duplicate incubations.

In order to further test whether these observations applied in a more physiologically relevant system, I tested the ability of tamoxifen, 4HT, endoxifen and letrozole to inhibit the conversion of MFC to HFC by human placental aromatase. Under the same conditions as used in MFC incubations with recombinant enzyme, and with the substrate concentration set at 25 µM, the selective inhibitor letrozole (20 nM) completely inhibited aromatase activity. Endoxifen was able to inhibit placental aromatase with an IC_{50} of 5 µM. Consistent with our previous data, NDMT inhibited placental aromatase with a weaker potency while tamoxifen and 4HT did not inhibit at concentrations up to 50 µM (data not shown).

Since the K_i for endoxifen determined at this higher enzyme concentration (50 nM) using testosterone as substrate, was notably higher than that obtained at 7.5 nM of aromatase using MFC as substrate, I tested whether the experimental conditions used in the testosterone incubations, including in particular the increased enzyme concentration would result in an increase in the observed IC_{50} of endoxifen. Under the same conditions as those when an enzyme concentration of 50 nM was used, an IC_{50} of 95 µM for endoxifen was observed in inhibition of MFC metabolism (data not shown), which was 15 to 16 fold higher in comparison to 6.1 nM as shown in Table 7.1.

When tamoxifen, 4HT, NDMT or endoxifen was pre-incubated with aromatase for 5, 10, 15 and 20 min to test the possibility of irreversible inhibition, no decrease in MFC metabolism to HFC or testosterone metabolism to estradiol relative to control was observed (data not shown). These data suggest that the inhibition of aromatase observed with endoxifen and NDMT is a reversible process.

Competitive inhibition of aromatase by norendoxifen

Pilot studies suggested that among a number of minor tamoxifen metabolites, a tertiary metabolite, N,N-didesmethyl-4-hydroxytamoxifen, might have the most potent inhibitory effects on aromatase activity (Chapter Eight Figure 8.1). Since N,N-didesmethyl-4-hydroxytamoxifen is the demethylated product from endoxifen, we have named it norendoxifen. The effects of norendoxifen on aromatase activity were tested across a range of fluorometric substrate concentrations. The data were plotted as Dixon and Lineweaver-Burke plots. The lines on the resulting Dixon plot intersecting at a common point indicated a K_i of 35 nM (Figure 7.5.A). The profile of the lines on the resulting Lineweaver-Burke plot: straight lines intersecting at a common point on the y-axis was consistent with a competitive mechanism of inhibition by norendoxifen (Figure 7.5.B). In order to explore the stereoselectivity of norendoxifen, the potency of the purified (E)-enantiomer of norendoxifen was tested. Under the same experimental conditions, the IC_{50} values for (E)-norendoxifen and the unseparated mixture were both approximately 30 nM (data not shown). No obvious stereoselectivity was observed.

A number of other minor tamoxifen metabolites were also found to be relatively weak aromatase inhibitors in vitro. The activities of these metabolites are described in the next chapter.

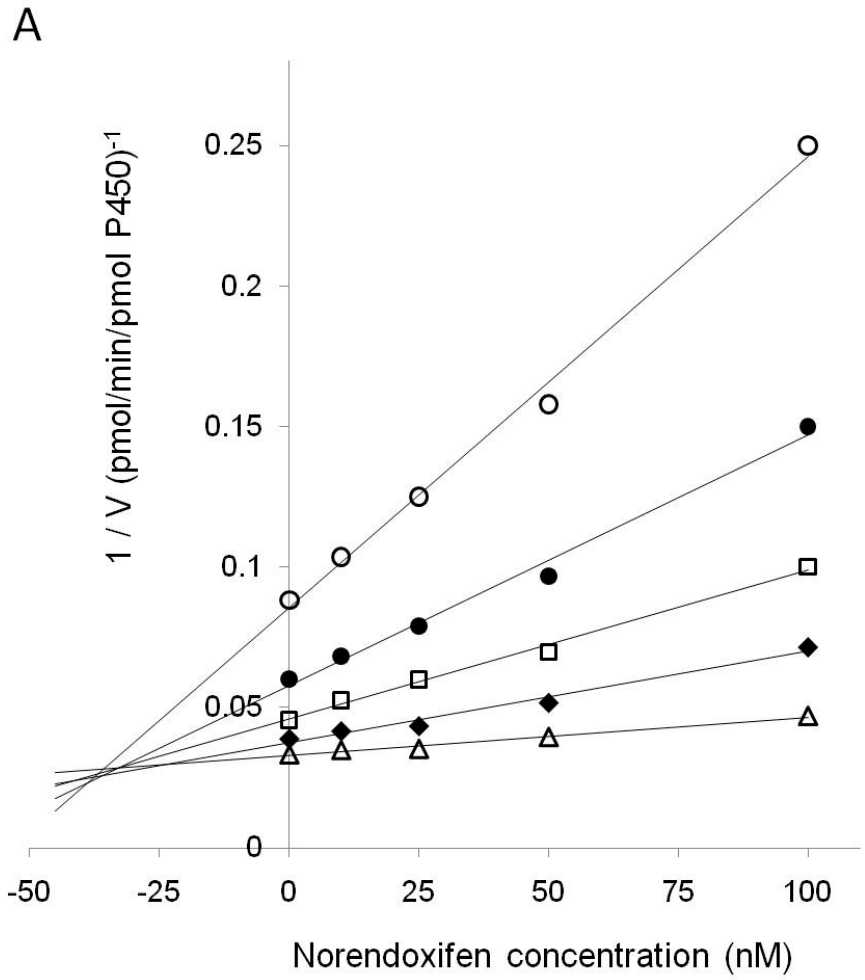
A
1 / V (pmol/min/pmol P450)-1
0.25
0.2
0.15
0.1
0.05
0
-50
-25
0
25
50
75
100
Norendoxifen concentration (nM)

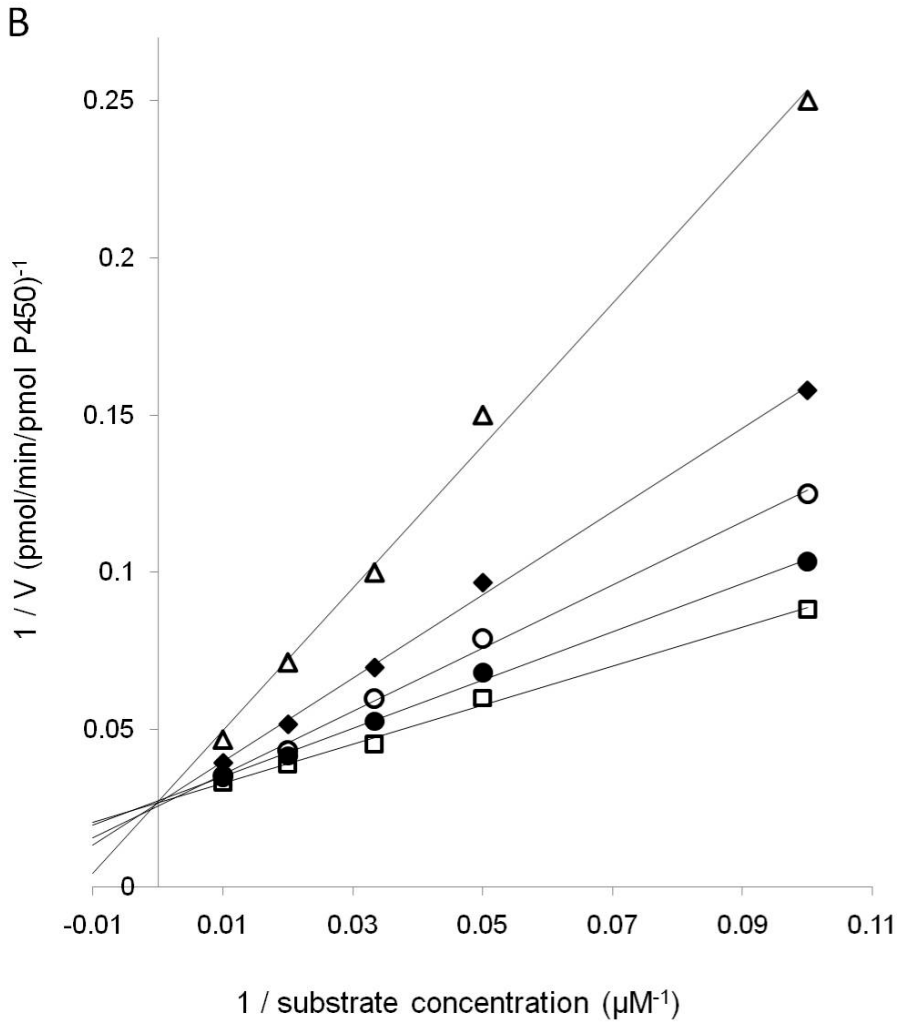

Figure 7.5. Competitive inhibition of aromatase by norendoxifen.

A range of substrate (MFC) concentrations was incubated with 7.5 nM recombinant human aromatase for 30 min in the absence and presence of norendoxifen. (A) Dixon plot of inhibition of aromatase by norendoxifen with substrate (MFC) concentrations set at 10 (open circle), 20 (dark circle), 30 (open square), 50 (dark diamond) and 100 (open triangle) µM. (B) Lineweaver-Burke plot of inhibition of aromatase with increasing norendoxifen concentrations: 0 (open square), 10 (dark circle), 25 (open circle), 50 (dark diamond) and 100 (open triangle) nM. Individual points represent the mean of duplicate incubations.

In order to test whether the inhibitory effect of norendoxifen on aromatase extends to other CYP enzymes, the ability of this compound to inhibit other important drug-metabolizing CYP enzymes was tested, including CYP2B6, CYP2C9, CYP2C19, CYP2D6 and CYP3A. When CYP2B6 and CYP2D6 were tested, no substantial inhibition by norendoxifen was observed at concentrations up to 1 μM. Three experimental systems were used to test inhibition of aromatase, CYP2C9, CYP2C19 and CYP3A by norendoxifen: drug incubations with recombinant CYP isoforms, pooled placental microsomes or pooled human liver microsomes. Initially, when recombinant CYP isoforms were used, norendoxifen inhibited aromatase, CYP2C9 and CYP2C19 with IC_{50} values of 30, 95 and 61 nM respectively. These data did not suggest obvious CYP isoform selectivity. Since the enzyme concentrations and configurations present in recombinant systems may not represent the dynamic multi-enzyme system present in vivo, CYP3A was not tested in this system. Instead, the selectivity of norendoxifen was further characterized using pooled placental and pooled human liver microsomes under more physiologic conditions and with similar total protein concentrations. Norendoxifen inhibited placental aromatase with an IC_{50} value of 90 nM, while it inhibited human liver CYP2C9 and CYP3A with IC_{50} values of 990 and 908 nM respectively (Figure 7.6). Inhibition of human liver CYP2C19 by norendoxifen appeared even weaker, with less than 25% inhibition observed at concentrations up to 5 μM (Figure 7.6).

Note: Experiments using human liver microsomes were performed by my colleagues Zifan Pei (CYP2C9) and Cong Xu (CYP2C19 and CYP3A) in the Department of Pharmacology and Toxicology here at Indiana University.

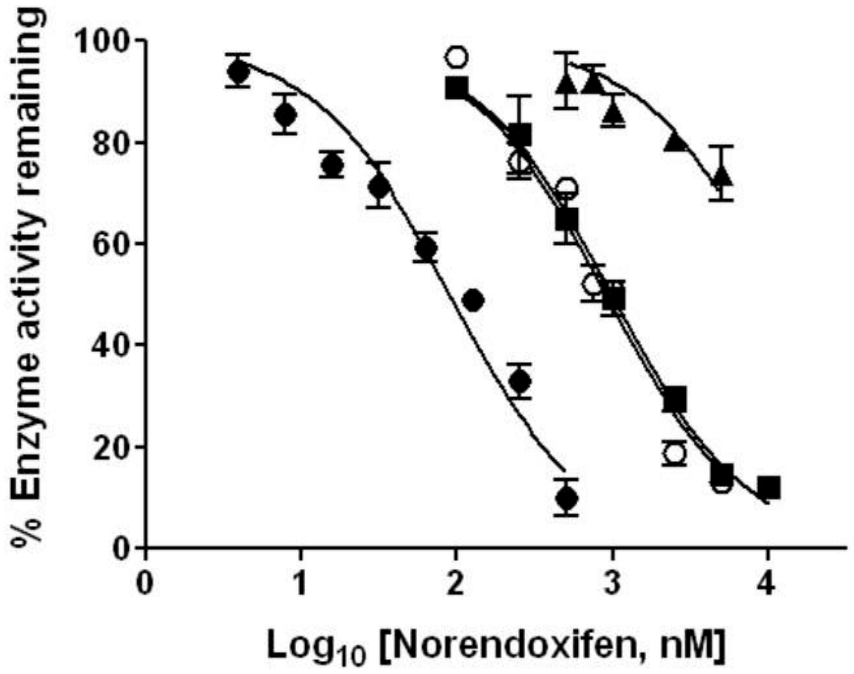

Figure 7.6. Selective inhibition of CYP isoforms by norendoxifen.

In the presence of a range of norendoxifen concentrations, the remaining activity of human placental aromatase (dark circle), human liver CYP3A (open circle), human liver CYP2C9 (dark square) and human liver CYP2C19 (dark triangle) were determined by measuring the formation rates of metabolites from specific probe drugs and were expressed as percentage of control. Individual points represent the mean of three to four independent incubations. Source: Experiments using human liver microsomes were performed by my colleagues Zifan Pei (CYP2C9) and Cong Xu (CYP2C19 and CYP3A). The study design, experiments using placental aromatase and all data analysis were carried out by me.

Discussion

These studies characterized inhibition of human aromatase in vitro by three tamoxifen metabolites: endoxifen, NDMT and norendoxifen. These findings have a number of implications. While the serum concentrations of endoxifen in humans are in the 10 - 150 nM range (Borges et al. 2006; Jin et al. 2005), tissue concentrations of endoxifen are higher, especially in breast tumors, where they appear to be 10 to 100 times more, i.e. about 1 - 15 μM (Lien et al. 1991). The inhibitory concentrations for endoxifen we observed in vitro (K_i of 4.0 μM) fall in the same range. Furthermore, in rats the ratio of endoxifen concentrations in uterus to those in serum has been reported to be at least 20:1, and to be at least 500 : 1 between lung and serum (Lien, Solheim, and Ueland 1991). NDMT concentration in human treated with tamoxifen is more than 10 times higher than that for endoxifen (Jin et al. 2005). These high tissue concentrations are consistent with the large apparent distribution volume for tamoxifen, the parent drug, which is about 50 to 60 L/kg in humans (Lien et al. 1989), indicating that most of the drug (99.9%) is present in peripheral compartments, and suggesting extensive tissue accumulation. This wide tissue distribution (Lien, Solheim, and Ueland 1991), and the relatively long apparent half lives of NDMT and endoxifen (~ 14 and 44 days respectively) (Jordan 1982; Johnson et al. 2004; Ahmad, Shahabuddin et al. 2010) in humans treated with tamoxifen are consistent with an extended period of tissue exposure. Sustained aromatase inhibition in vivo by these metabolites would therefore seem a possibility.

Since the initial observations were carried out using an artificial, fluorometric substrate for aromatase, I examined the physiologic relevance of these data by testing the

ability of endoxifen to inhibit metabolism of the endogenous substrate of aromatase, testosterone. The inhibition of testosterone metabolism to estradiol was studied under conditions involving higher aromatase concentrations so that the generation of estradiol could be quantitatively monitored. A K_i of 178 μM for endoxifen was observed under incubation conditions that included a 6.7 fold higher enzyme concentration (50 nM). It is possible that endoxifen is less potent as an inhibitor of testosterone metabolism. An alternative explanation would be that this observed higher K_i is an artificial result of different experimental conditions. When I tested the latter possibility, two observations suggest that in conditions involving lower aromatase concentrations, testosterone metabolism may be inhibited by lower concentrations of endoxifen: (1) In the two experimental conditions tested, the IC_{50} of endoxifen for the same substrate, MFC, differed by 15 - 16 fold (6.1 μM at 7.5 nM aromatase, compared to 95 μM at 50 nM aromatase), suggesting a lower K_i at lower enzyme concentrations. (2) The K_m for testosterone metabolism observed in this system was 4 μM, significantly higher than that (0.2 μM) reported in placental microsomes (Zharikova et al. 2006). It follows that under physiologic conditions, where the concentrations of aromatase and of testosterone in vivo are lower than those used in vitro, inhibition is likely to occur at relatively low inhibitor concentrations.

Aromatase inhibition by endoxifen and NDMT was observed to be through a non-competitive mechanism. This mechanism explains why it was possible for endoxifen to effectively inhibit testosterone metabolism, although the observed IC_{50} value for inhibition of MFC metabolism by testosterone was 19-fold lower than that of endoxifen (Table 7.1). A non-competitive mechanism means that there might be allosteric

interactions with aromatase. It is possible that endoxifen brings about non-competitive inhibition via a site remote from the substrate-binding site of aromatase, or that it could occur via interaction of two compounds that bind differently within the same catalytic site. The structure of the catalytic site of aromatase has been well studied through interactions between testosterone and this active site (Ghosh et al. 2010). Allosteric drug binding sites or regulatory regions of aromatase have not been considered until now. Of note, mutation of a site distant from the substrate-binding site has been shown to increase enzyme activity and reduce the susceptibility to inhibition of aromatase by aminoglutethimide (Payne et al. 2009). These observations raise the possibility that an allosteric mechanism might contribute to the pharmacologic regulation of aromatase and could be exploited to modulate aromatase activity for therapeutic benefit.

Our studies also demonstrate that norendoxifen is a relatively potent and selective inhibitor of human aromatase with a K_i value in the nanomolar range, close to the potency of letrozole, which is the most potent aromatase inhibitor that is available for clinical use. Although norendoxifen is a known metabolite of tamoxifen in humans (Lien et al. 1991; Jin et al. 2005), little is known about its tissue concentrations or its contribution to tamoxifen effects. It is a minor metabolite of tamoxifen that exists at notably lower concentrations than the parent drug or its major metabolites, but our data make clear that it is a much more potent inhibitor of aromatase than the well-known metabolites, endoxifen and NDMT. In as much as these two major metabolites may contribute to tamoxifen action via aromatase inhibition, it is equally possible that norendoxifen contributes significantly to the clinical effects of tamoxifen. In addition, endoxifen itself is being developed as a drug (Ahmad, Ali et al. 2010; Ahmad,

Shahabuddin et al. 2010), and so the role of norendoxifen, the primary demethylated metabolite of endoxifen, in endoxifen action may be important for this reason.

In this context it is important to note that endoxifen is a widely recognized and potent estrogen receptor modulator (Jin et al. 2005; Johnson et al. 2004; Jordan 2007). It follows that its demethylated metabolite, norendoxifen, may also act as an estrogen receptor ligand. However, the binding affinity of norendoxifen for estrogen receptors and the activity of norendoxifen at estrogen receptors, whether it is estrogenic or anti-estrogenic, merit future studies. Tamoxifen therapy is known to have tissue-specific estrogen receptor modulation activities in humans. Such activities effectively limit estrogen signalling at breast tumors but preserve some estrogenic effects at other sites including the musculoskeletal and cardiovascular systems. Therefore, tamoxifen metabolites or their derivatives may therefore be valuable as alternative aromatase inhibitors that are able to mitigate the debilitating musculoskeletal toxicities experienced by breast cancer patients via tissue specific mechanisms. This possibility deserves further investigation.

The metabolism of tamoxifen is complex (Johnson et al. 2004) and so its ultimate effects reflect the aggregation of the actions of multiple metabolites on the estrogen receptors, on aromatase and also possibly via other mechanisms that have been reported (Tian et al. 2009; da Rocha et al. 1999). The interpretation of these studies is limited by the difficulty of inferring drug concentrations at the effect site in vivo, given the acknowledged gradient between serum and tissue concentrations (Lien, Solheim, and Ueland 1991). As a result, the aggregated effect on aromatase activity in vivo and the

relative contributions of endoxifen, NDMT and norendoxifen to aromatase inhibition remain unclear.

Our findings presented here could help explain a number of currently unexplained observations. (1) Inhibition of aromatase by tamoxifen metabolites in vitro is consistent with the observation that estrogen concentrations decreased on average in post-menopausal women being treated with tamoxifen (Lonning et al. 1995). An alternative reason for such decrease would be effects downstream of estrogen receptor modulation by tamoxifen metabolites. (2) Inhibition of aromatase by tamoxifen metabolites might help explain why tamoxifen causes musculoskeletal pain, similar to that commonly experienced by patients taking aromatase inhibitors in some patients (Howell et al. 2005; Zivian and Salgado 2008). This side effect of tamoxifen appears debilitating and prominent in Asian women (Love et al. 1999). It is possible that, in the sub-population of post-menopausal women in whom musculoskeletal pain is a severe side effect of tamoxifen, aromatase inhibition by its metabolites is more prominent. Since musculoskeletal toxicities are less frequent in patients taking tamoxifen compared to AI therapies, aromatase inhibition by tamoxifen metabolites may not occur in every patient. (3) Aromatase inhibition by NDMT may help explain the inconsistency in observed associations between CYP2D6 genotype and outcomes in patients with breast cancer (Goetz et al. 2005; Wegman et al. 2007; Nowell et al. 2005). If aromatase inhibition contributes to the action of tamoxifen, then it is possible that this inhibition may confound simple associations between endoxifen concentrations and clinical outcomes. (4) Mechanistic studies that employ only 4HT, an estrogen receptor modulator that is not an aromatase inhibitor, may inadequately represent tamoxifen action in vivo.

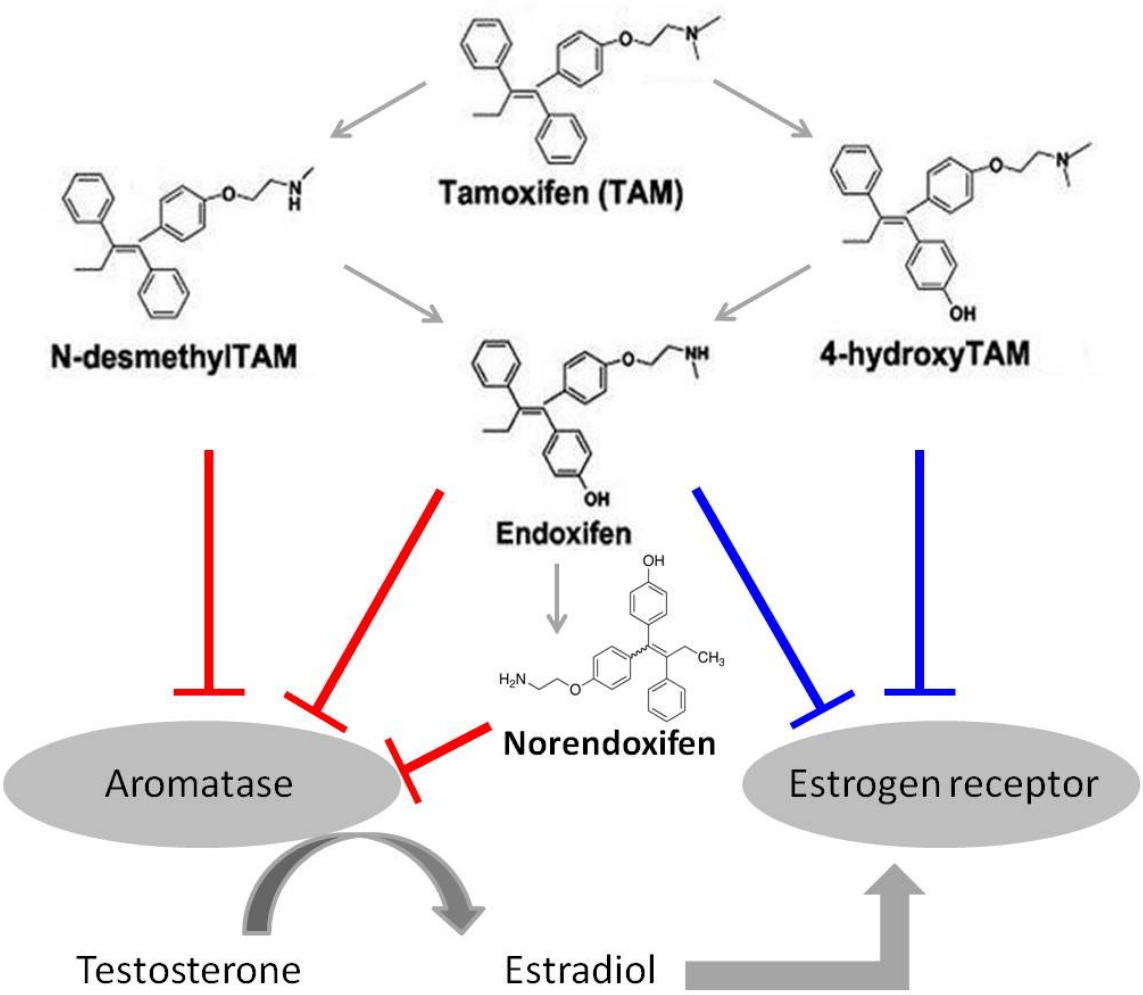

Figure 7.7. Diagram of possible mechanisms underlying anti-estrogenic effects of tamoxifen and its metabolites based on in vitro data.

NDMT, endoxifen and norendoxifen are able to act as aromatase inhibitors, while 4HT and endoxifen are the most potent antagonists at the estrogen receptor.

Overall, our data identify a novel mechanism of tamoxifen action that may contribute to its efficacy in the treatment of breast cancer, and may help explain its side effects. Although the overall contribution of aromatase inhibition to tamoxifen action is

unclear at this point, the data emphasize that tamoxifen and endoxifen may have multiple pharmacologic effects that are mediated by their active metabolites. Most notably, a previously unrecognized active metabolite, norendoxifen, is a relatively potent and selective aromatase inhibitor. The balance between tamoxifen's effects as an estrogen receptor modulator and as an aromatase inhibitor (Figure 7.7) may vary between individuals and across populations. This balance may contribute to the clinical effects of tamoxifen on serum and tissue estrogen concentrations, and may explain in part the variability in bone density, hot flashes, serum lipid concentration, severity of musculoskeletal pain and breast cancer recurrence observed in patients taking tamoxifen. Relationships between tamoxifen metabolite concentrations and clinical outcomes may be complex, and should be interpreted and studied with an open mind.

Methods

Fluorescent assay for inhibition of aromatase in vitro

The activity of both recombinant and placental human aromatase was determined as described in "Chapter Ten: General Methods / Fluorescent assay for inhibition of aromatase in vitro".

Inhibition of testosterone metabolism by aromatase in vitro

The activity of aromatase was determined by measuring the rate of conversion of testosterone to estradiol as described in "Chapter Ten: General Methods / Inhibition of testosterone metabolism by aromatase in vitro".

Quantifications of estradiol formation

High performance liquid chromatography (HPLC) assays with ultraviolet (UV) detection were developed for the quantification of testosterone conversion to estradiol as described in “Chapter Ten: General Methods / HPLC-UV assays for the quantifications of estradiol and EDDP formation”, with the modification that 25 μl of 25 μM letrozole was added to each sample as an internal standard.

Inhibition of recombinant human CYP isoforms

The activities of recombinant human CYP2C9, CYP2C19 and CYP2D6 were determined by measuring the conversion rates of their fluorometric substrates to the corresponding fluorescent metabolites as described in “Chapter Ten: General Methods / Inhibition of recombinant human CYP isoforms”.

Inhibition of specific CYP isoforms using pooled HLMs

Inhibition of CYP2B6, CYP2C9, CYP2C19 and CYP3A using pooled HLMs was determined by measuring the conversion rates of specific probe drugs to their metabolites as described in “Chapter Ten: General Methods / Inhibition of specific CYP isoforms using pooled HLMs”. The formation rates of 4-hydroxybupropion from bupropion, of 4-hydroxytolbutamide from tolbutamide, of 5′-hydroxyomeprazole from omeprazole and of 6-β hydroxytestosterone from testosterone served as markers of CYP2B6, CYP2C9, CYP2C19 and CYP3A activity respectively.

Kinetic analyses

The rates of metabolite formation from substrate probes in the presence of the test inhibitors were compared with those for control in which the inhibitor was replaced with vehicle. The extent of aromatase inhibition was expressed as percent enzyme activity remaining compared to control. The percent of aromatase activity remaining at different inhibitor concentrations was used to estimate IC_{50} values when the substrate concentration was set at 25 µM. IC_{50} values were determined as the inhibitor concentration which brought about a 50% reduction in enzyme activity by fitting all the data to a one-site competition equation using Prism version 5.01 for Windows (GraphPad Software Inc., San Diego, CA).

In order to estimate inhibition constants, formation rates of metabolite at different substrate concentrations were plotted as Dixon plots according to the following equation:

$$\frac{1}{v} = \frac{\left(1 + \frac{K_m}{[S]}\right)}{V_{max} K_i} [I] + \frac{1}{V_{max}} \left(1 + \frac{K_m}{[S]}\right)$$

where v is the velocity of reaction, [S] is the substrate concentration, [I] is the inhibitor concentration, K_m is the Michaelis constant, and V_{max} is the maximum reaction rate. The equilibrium dissociation constant of the inhibitor K_i was determined by estimating the corresponding value on the X-axis of the common intercept using linear regression.

To further characterize the mechanism of inhibition, the same data were plotted as Eadie-Hofstee plots according to the following equation:

$$v = -K_{S_{app}} \frac{v}{[S]} + V_{max_i}$$

where K_{Sapp} is the apparent Michaelis constant and V_{maxi} is the apparent maximum reaction rate in the presence of the inhibitor. The relationships between the slopes of

these lines generated by linear regression were used to determine the inhibitory mechanisms involved (Segel 1993).

For non-competitive inhibition, in order to estimate K_{Sapp} and V_{maxi} at different inhibitor concentrations, the same data were plotted as Lineweaver–Burk plots according to the following equation:

$$\frac{1}{v} = \frac{K_m}{V_{max}}\left(1 + \frac{[I]}{K_i}\right)\frac{1}{[S]} + \frac{1}{V_{max}}\left(1 + \frac{[I]}{K_i}\right)$$

Using linear regression, the intercepts on the X-axis were used to determine K_{Sapp} values and intercepts on the Y-axis were used to determine V_{maxi} values.

For competitive inhibition, all data on the formation rates of metabolite at different substrate concentrations were plotted as Lineweaver–Burk plots according to the following equation:

$$\frac{1}{v} = \frac{K_m}{V_{max}}\left(1 + \frac{[I]}{K_i}\right)\frac{1}{[S]} + \frac{1}{V_{max}}$$

Note: Equations are quoted from (Segel 1993).

Note: The work described in this chapter has been published (Lu, Desta, and Flockhart 2011; Lu, Xu et al. 2011).

CHAPTER EIGHT

A New Conceptual Framework for Aromatase Inhibition

Introduction

To improve the treatment of breast cancer, there is a need to develop novel aromatase inhibitors (AIs) that have improved therapeutic window than those currently available. Improved AIs may bring about adequate aromatase inhibition, while limiting side effects. Since some of the tamoxifen metabolites can inhibit the activity of aromatase (Chapter Seven, this dissertation), these compounds represent important candidate structures in the search for novel and clinically useful AIs for three reasons. First, their structures are markedly different from any previously reported AIs, suggesting alternative biochemical mechanisms of action and also the possibility of improved benefit and toxicity profiles. Second, some of these compounds are able to bind to estrogen receptors. These metabolites may be able effectively reduce estrogen synthesis and at the same time modulate estrogen signaling by binding to estrogen receptors in a tissue-specific manner. Therefore, these structures or their derivatives may be valuable as alternative AIs that are able to mitigate the debilitating toxicities associated with estrogen depletion via tissue-specific mechanisms. Third, these compounds are metabolites of a widely used drug, and many patients have already been exposed to them. To explore the ability of a range of structurally related tamoxifen metabolites to act as AIs, I tested and compared the activity of these compounds using recombinant human aromatase. Since these tamoxifen metabolites are structurally different from any known aromatase inhibitors, it would be important to understand the mechanism of action employed by these compounds. Thus, I

analyzed the structure-activity relationships of these compounds and estimated structure-dependent interactions between these compounds and aromatase as a first step towards the development of lead candidates for novel inhibitors.

Furthermore, in order to establish a lead optimization strategy, I collaborated with the laboratory of Professor Mark Cushman at Purdue University, and they used computerized molecular docking with the X-ray crystallographic structure of aromatase to describe possible biochemical interactions employed by tamoxifen metabolites, and also to explore other potential derivatives of the most potent inhibitor we identified as potential candidate structures.

Results and discussion

The ability of tamoxifen and its nine metabolites to inhibit recombinant human aromatase at an inhibitor concentration of 10 μM was tested and their activities were compared. While tamoxifen itself was not able to inhibit aromatase, many tamoxifen metabolites were capable of doing so. Figure 8.1 shows the relative potency of tamoxifen and its available metabolites as AIs. Among the primary metabolites, N-desmethyl-tamoxifen, 4'-hydroxy-tamoxifen and tamoxifen-N-oxide were all relatively weak inhibitors. Among the secondary metabolites of tamoxifen, endoxifen and 4,4'-dihydroxy-tamoxifen were more potent inhibitors than the primary metabolites. Interestingly, a tertiary metabolite, norendoxifen, was the most potent of all the inhibitors tested, and the only metabolite that completely inhibited enzyme activity at 10 μM.

The inhibitory potency order of the tested compounds was as follows: norendoxifen >> 4,4'-dihydroxy-tamoxifen > endoxifen > N-desmethyl-tamoxifen, N-

desmethyl-4'-hydroxy-tamoxifen, tamoxifen-N-oxide, 4'-hydroxy-tamoxifen, N-desmethyl-droloxifene > 4–hydroxy-tamoxifen, tamoxifen. Consideration of the structure-activity relationships generated by these data makes clear that a number of consistent relationships exist. As methyl groups are progressively removed, inhibitory potency of a compound increases substantially, while the addition of a single hydroxyl group also increases potency (Figures 8.1 and 8.2).

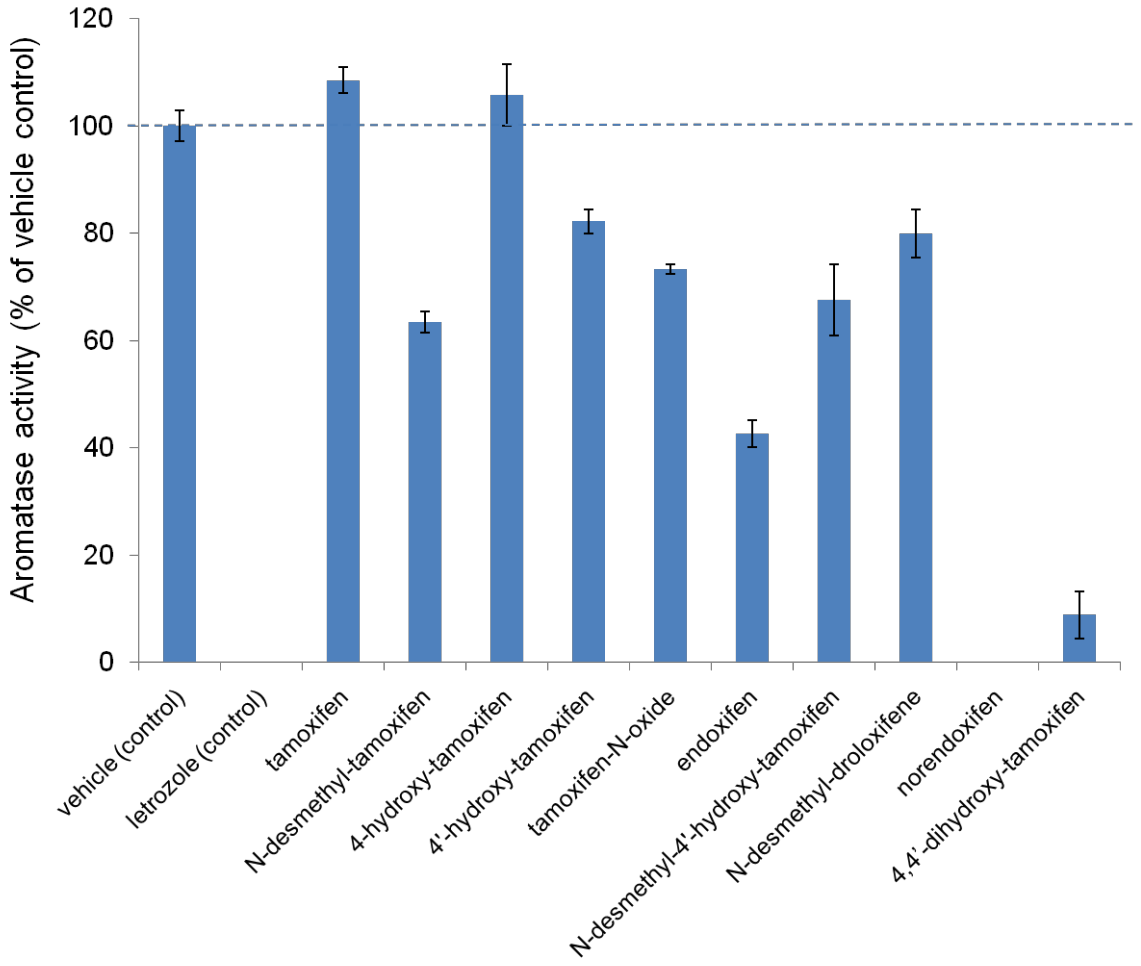

Figure 8.1. Relative potency of tamoxifen and its primary, secondary and tertiary metabolites in the inhibition of aromatase.

Test compounds (10 µM) were incubated with 7.5 nM recombinant human aromatase at 37 °C for 30 min. Letrozole (0.1 µM) and vehicle (acetonitrile) were used as positive and negative controls respectively. Data are plotted as means of triplicate incubations with standard deviations. The dotted line represents 100 percent activity that was observed with the vehicle control.

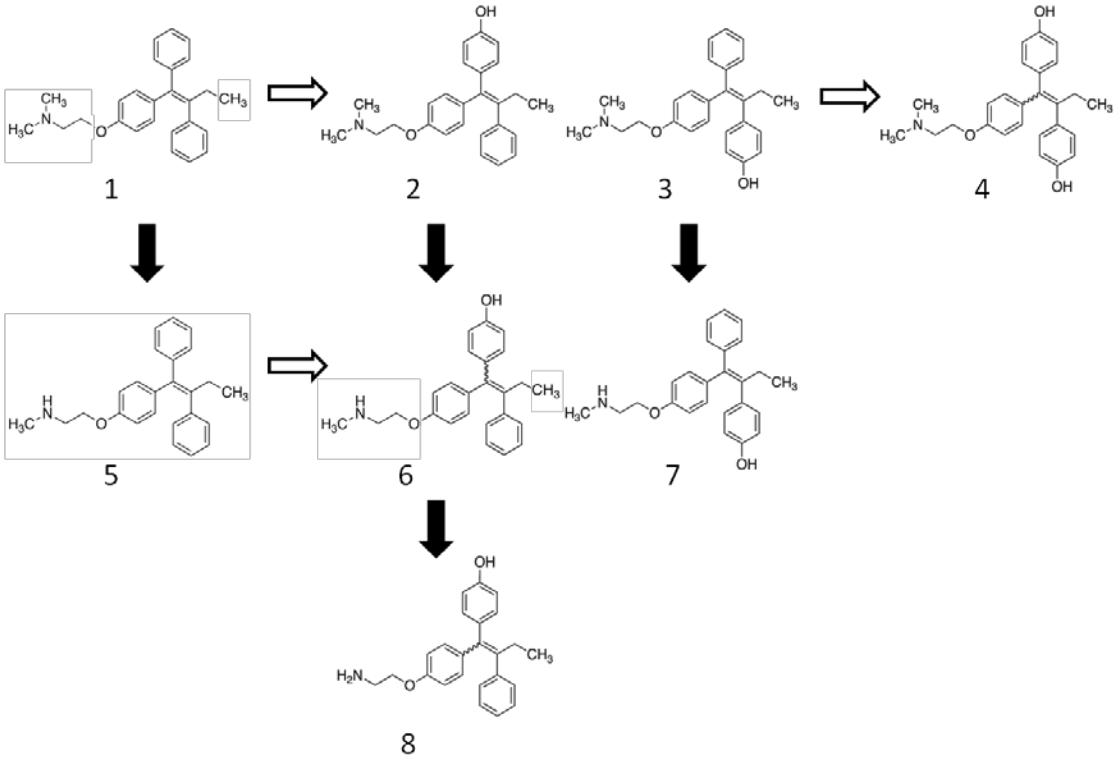

Figure 8.2. Structure-function relationships: stepwise hydroxylation and demethylation of tamoxifen progressively increase the potency of aromatase inhibition.

The horizontal open arrows represent the addition of a hydroxyl group. The vertical dark arrows represent the removal of a methyl group. Available compounds tested were: (1) tamoxifen; (2) 4-hydroxy-tamoxifen; (3) 4'-hydroxy-tamoxifen; (4) 4,4'-dihydroxy-tamoxifen; (5) N-desmethyl-tamoxifen; (6) N-desmethyl-4-hydroxy-tamoxifen or endoxifen, (7) N-desmethyl-4'-hydroxy-tamoxifen; (8) N,N-didesmethyl-4-hydroxy-tamoxifen or norendoxifen

Table 8.1. Calculated binding free energy for most stable docking poses (MM-BPSA) and the experimental IC_{50} values of compounds.

Compound	Calculated Binding Free Energy (Kcal/mol)	Experimental IC_{50}
(Z)-norendoxifen	-65.2	30 nM*
(E)- norendoxifen	-58.9	
(Z)-endoxifen	-61.0	6 μM*
(E)-endoxifen	-60.1	
N-desmethyl-tamoxifen	-59.6	20 μM
(Z)-4-hydroxy-tamoxifen	-50.5	530 μM
Tamoxifen	-50.6	985 μM

Note: *****, IC_{50} values were determined when mixtures of unseparated (E) and (Z) isomers were tested. The data on experimental IC_{50} values were generated by me and the data on calculated binding free energy were from the Cushman Lab at Purdue University.

Based on the structure-function relationships that I proposed, a series of molecular modeling studies were performed in collaboration with the Cushman Lab at Purdue University to study the biochemical mechanisms by which tamoxifen metabolites inhibit aromatase. These investigators docked proposed compounds into the active site of aromatase (PDB ID 3eqm) (Ghosh et al. 2010) using GOLD software (Verdonk et al. 2003) and the energies of the complexes were minimized using the Amber force field and Amber charges. The binding free energies calculated by them are summarized together with my experimental aromatase IC_{50} values in Table 8.1. These estimated free energies appeared positively associated with the relative inhibitory potencies observed. They also

validated this docking and energy minimization procedure by reproducing the published crystal structure of aromatase-androstenedione complex by extracting the ligand structure and then docking it back into the aromatase active site, merging the highest-scored binding pose with the protein, and then minimizing the complex energy following the same protocol used with other tamoxifen metabolites. The root mean standard deviation between the structure of the newly generated complex derived from molecular modeling and the original crystal structure (PDB ID 3eqm) was 1.73 Å.

In order to further characterize the activity of the most potent inhibitor--one that might represent a lead compound to guide future rational drug design--we studied the hypothetical binding modes of the norendoxifen isomers using computerized molecular docking models produced by our collaborators at Purdue University. Both isomers have similar binding modes, with the phenolic hydroxyl groups of both isomers bind to the carbonyl group of Met374 (Figures 8.3 and 8.4). The other oxygen atoms of both forms are calculated to exist near the iron atom; however, the ether oxygen atom of the E isomer was calculated to be 0.8 Å closer to the iron atom with better directionality for binding than the Z form. A hydrogen bond is apparent between the terminal aliphatic amino group in the E form and the carbonyl group of Ala306. A similar interaction is not predicted for the Z form, in which the terminal aliphatic amino nitrogen atom was calculated to at least 5 Å away from the closest atom that it could hydrogen bond to.

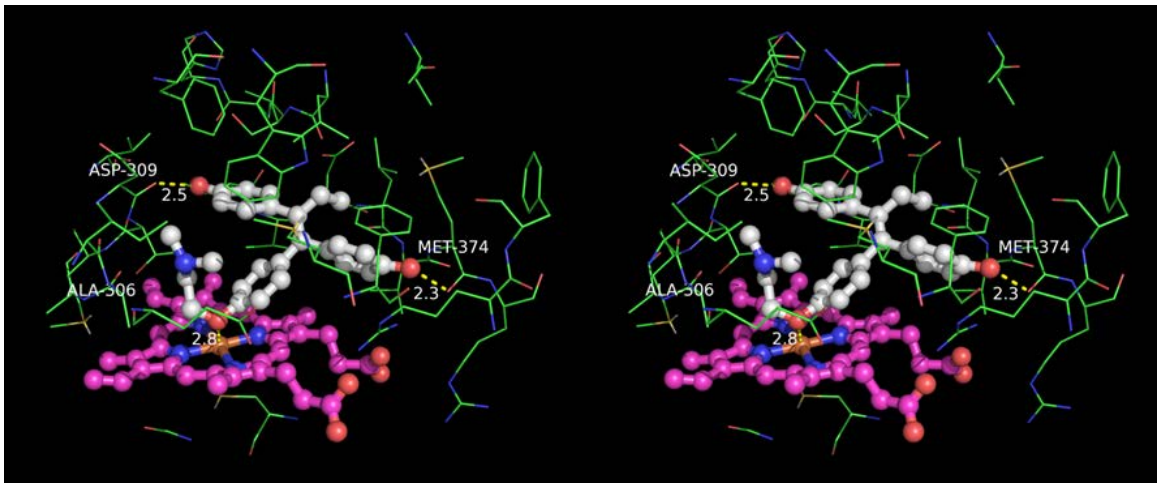

Figure 8.3. Hypothetical binding mode of (E)-norendoxifen in the human aromatase active site (PDB ID 3eqm).

The ligands are gray, with oxygen depicted in red and nitrogen in blue. The protein is colored green, and the heme is colored magenta. Yellow dashed lines represent the distances between hydrogen bond donors and acceptors. The stereoview is programmed for wall-eyed (relaxed) viewing. Source: from the Cushman Lab at Purdue University.

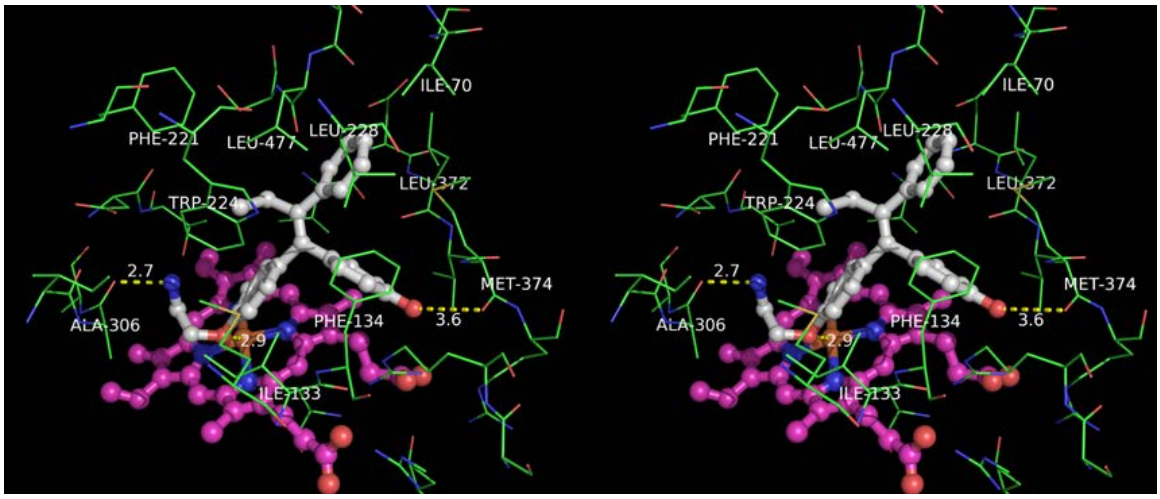

Figure 8.4. Hypothetical binding mode of (Z)-norendoxifen in the human aromatase active site (PDB ID 3eqm).

The ligands are gray, with oxygen depicted in red and nitrogen in blue. The protein is colored green, and the heme is colored magenta. Yellow dashed lines represent the distances between hydrogen bond donors and acceptors. The stereoview is programmed for wall-eyed (relaxed) viewing. Source: from the Cushman Lab at Purdue University.

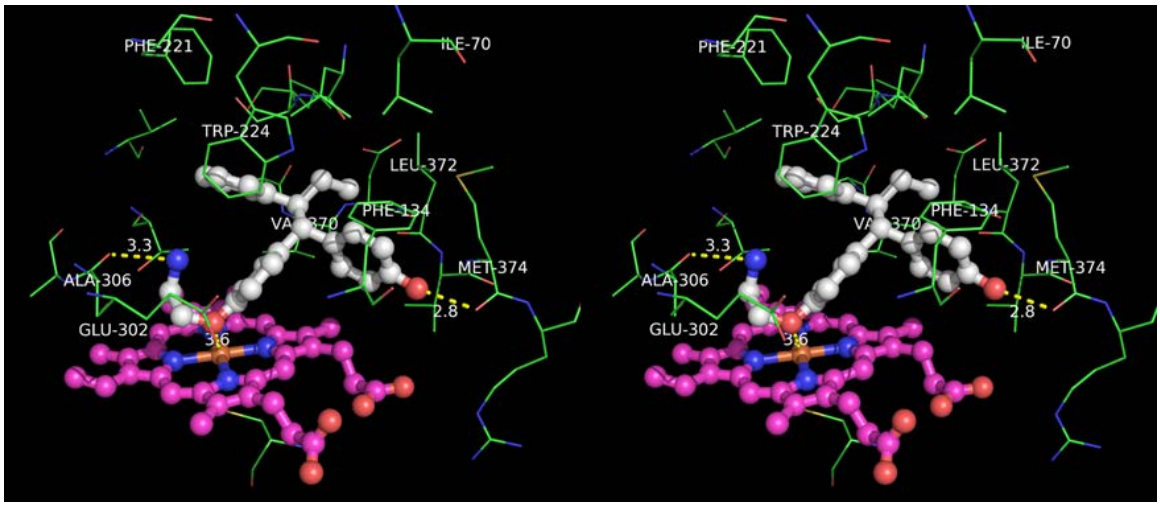

Figure 8.5. Hypothetical binding mode of 4,4'-dihydroxy-tamoxifen in the human aromatase active site (PDB ID 3eqm).

The ligands are gray, with oxygen depicted in red and nitrogen in blue. The protein is colored green, and the heme is colored magenta. Yellow dashed lines represent the distances between hydrogen bond donors and acceptors. The stereoview is programmed for wall-eyed (relaxed) viewing. Source: from the Cushman Lab at Purdue University.

On the other hand, the unsubstituted phenyl ring and the ethyl moiety in both E and Z forms are surrounded by hydrophobic residues including Phe221, Leu477, Val370, Ile70, and the benzene ring of Trp224. In addition, the phenyl ring that contains the hydroxyl group is calculated to from a possible side-to-face stacking interaction with Phe134 in both isomeric forms. A comparison of the two complexes reveals that the ethyl and phenyl groups switch locations, but the two remaining phenyl rings that contain hydrogen bonding substituents maintain their positions.

In this study, a number of tamoxifen metabolites were shown to have activity as AIs with a wide range of potencies. Although these studies are limited to the commercially available tamoxifen metabolites, they are sufficient to allow the exploration of relationships between the structures of the compounds we tested and their function. The data indicate that stepwise hydroxylation and demethylation of tamoxifen both resulted in progressive increases in inhibitory potency (Figures 8.1 and 8.2). This is consistent with the collaborative data from Mark Cushman's Lab: The activities of 4-hydroxy-tamoxifen (Figure 8.2 Structure 2, IC_{50} 530 µM), endoxifen (Structure 6, IC_{50} 6 µM), and norendoxifen (Structure 8, IC_{50} 30 nM) show that sequential N-demethylation results in a very significant increase in aromatase inhibitory potency. The molecular models (Figures 8.3 - 8.5) document limited space available in the ligand binding site surrounding the amine, and the decrease in activity observed with the presence of more methyl groups can be attributed to steric factors. The models displayed in Figures 8.3 and 8.4 indicate that the amino groups of both isomers are hydrogen bonded to the carbonyl oxygen atom of Ala306. This suggests that the loss of activity seen with the methylation of the amine may also result from a decrease in its capacity to act as a hydrogen bond donor toward the Ala306 carbonyl oxygen. The models displayed in Figures 8.3 and 8.4 also indicate that the unsubstituted phenyl rings and ethyl groups of the double bond isomers of norendoxifen are buried in hydrophobic cavities. In the in vitro experimental data, the E and Z/E mixture of norendoxifen appeared to have the same enzyme inhibitory activities suggesting that the activities of the Z and E isomers are equal. The similar activities of the two isomers and the perspective offered by the molecular models, suggest that the locations of the phenyl and ethyl groups can be switched with no change

in activity. Of note, it is suggested by Dr. Mark Cushman that the ethyl and unsubstituted phenyl groups therefore appear to contribute to enzyme affinity through the presence of general hydrophobic and dispersion (van der Waals) interactions, as opposed to being due to specific interactions with particular amino acid side chains of the enzyme. Overall, the data suggest that the double bond stereochemistry in this series of AIs may not have a large impact on biological activity, although smaller effects remain possible, since in silico, the molecular models did indicate a greater calculated binding free energy for the Z isomer (Table 8.1). More research is needed in order to determine the precise enantioselectivity of this compound.

Comparison of the activities of N-desmethyl-tamoxifen (Figure 8.2 Structure 5, IC_{50} 20 μM) and endoxifen (Structure 6, IC_{50} 6 μM) documents a positive contribution made by the 4-hydroxyl group. The molecular models suggest that this may reflect hydrogen bonding of the phenol with the carbonyl of Met374. Furthermore, comparison of the activities of 4-hydroxytamoxifen (Structure 2) and 4,4'-dihydroxy-tamoxifen (Structure 4) represented in Figure 8.1 indicates that the 4'-hydroxyl group makes a large positive contribution to the activity. The hypothetical model of the complex of human aromatase with 4,4'-dihydroxy-tamoxifen (Structure 4) suggests that the 4'-hydroxyl groups contribute to the affinity of the ligand through hydrogen bonding with the carbonyl oxygen of Asp309 (Figure 8.5).

These results lead us to postulate that modifications to the basic triphenylalkene structure of tamoxifen (Figure 8.6) that preserve hydrogen bonding to the Ala306, Met374 and Asp309 residues might be a valuable approach in the development of the next generation of AIs. Of note, the specific interactions described here with Ala306 and

Met374 were also noted as being key to favorable interactions between aromatase and a series of other ligands (Punetha, Shanmugam, and Sundar 2011). In this context, since norendoxifen is a potent and selective inhibitor in vitro (Chapter Seven Figures 7.5 and 7.6), it merits further investigation as a clinical AI, and may be able to serve as a lead compound for the rational design of new therapeutic agents for breast cancer.

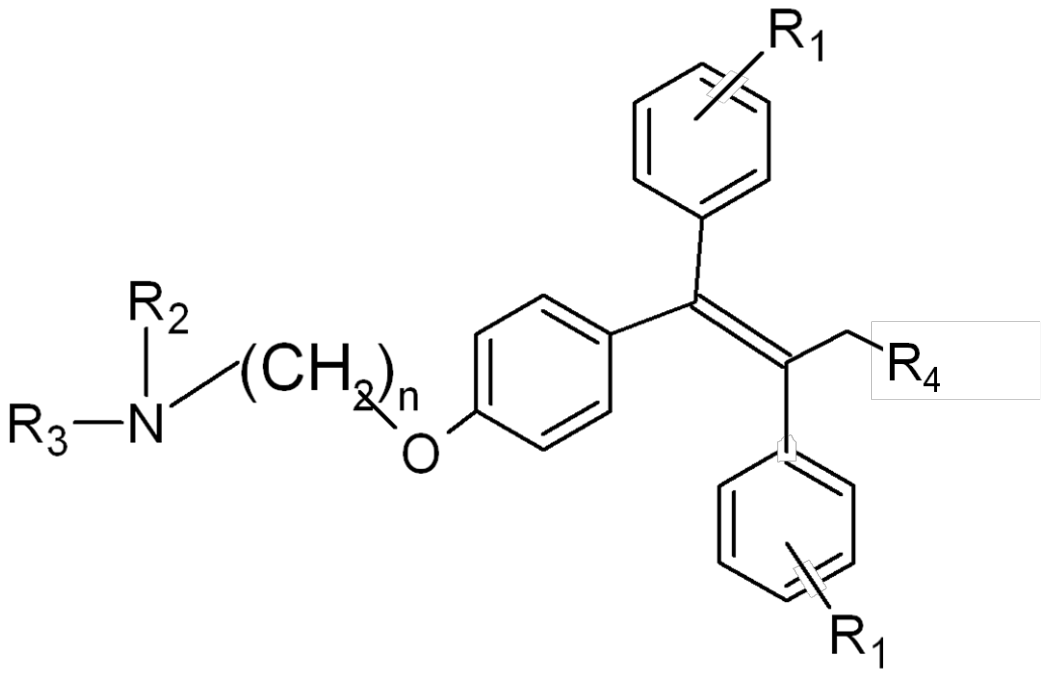

Figure 8.6. The new structural basis for the development of improved aromatase inhibitors.

This basic triphenylalkene structure was developed based on the structures of tamoxifen metabolites. The oxyalkylamine side chain on the phenyl group may have structural variants including: length in $-(CH_2)_n-$, n = 1, 2, 3, 4 or 5, such as CH_2-CH_2-, CH_2-CH_2-CH_2-, CH_2-CH_2-CH_2- CH_2-and CH_2-CH_2-CH_2-CH_2- CH_2-, position on the phenyl group; position of oxygen in relation to $-(CH_2)_n-$ chain; and oxyalkene composition of the side chain; R_1 may be independently selected from the group consisting of H, CH_3 and OH; R_2 and R_3 are independently selected from the group consisting of H, CH_3-, CH_3-CH_2-, CH_3-CH_2-CH_2-; R_4 is selected from the group consisting of: H, CH_3-, CH_3-$(CH_2)_n$-, hydroxy, methoxy, ethoxy; and n = 1, 2, 3, 4 or 5.

In summary, the range of structures tested in this study and their pharmacologic potencies provide a reasonable pharmacophore upon which to build novel aromatase inhibitors. Based on these findings, a series of compounds that have triphenylalkene structure with side chain(s) on the phenyl group(s) that are oxyalkanes or oxyalkenes and that terminate in an unsubstituted or mono-substituted amine (Figure 8.6) can be exploited as new inhibitors for aromatase. These structures may have the potential to provide benefit to patients who are treated with AIs for breast cancer and other conditions by expanding their treatment options with the goal of enhancing treatment efficacy and reducing toxicity. Most of all, norendoxifen may be able to serve as a potent and selective lead compound in the rational design of improved AIs.

Methods

Fluorescent assay for inhibition of aromatase in vitro

The activity of aromatase was determined by measuring the conversion rate of a fluorometric substrate to its fluorescent metabolite as described in "Chapter Ten: General Methods / Fluorescent assay for inhibition of aromatase in vitro".

Computerized molecular modeling

Computerized molecular docking with the X-ray crystallographic structure of aromatase was performed in collaboration with Mark Cushman Lab at Purdue University as described in "Chapter Ten: General Methods / Computerized molecular modeling".

Note: The work described in this chapter has been published (Lu, Xu et al. 2011).

CHAPTER NINE

Conclusions and Future Directions

Aromatase as a drug-metabolizing enzyme in humans

The studies presented here are the first to directly test the effects of aromatase inhibition on drug disposition in humans and demonstrate that aromatase may be in part responsible for the metabolism of methadone. The data indicate that, on average, aromatase seems to account for ~ 22% of the clearance of a single dose of methadone (2 mg) in a group of post-menopausal women (Chapter Three, this dissertation). The discovery of this new metabolic route for methadone improves our understanding of methadone clearance, and emphasizes that aromatase can serve as a drug-metabolizing enzyme, beyond its important role in catalyzing endogenous steroid synthesis.

Our data also indicate that the decrease in methadone clearance brought about by aromatase inhibition is variable in the group of people studied, suggesting that there might be variability in the relative contribution of aromatase to overall methadone clearance in individual people. The balance between aromatase and other enzymes in contribution to methadone metabolism may be different among people. Mechanisms underlying the large variability in methadone pharmacokinetics may be complex and might involve factors that influence aromatase activity.

The studies presented in this work also suggest a broader clinical role for aromatase in the disposition of xenobiotics. A quantitatively important role for aromatase in drug metabolism raises the possibility of clinically meaningful pharmacokinetic drug-drug interactions with aromatase inhibitors that would not otherwise have been

anticipated, especially in patients taking aromatase inhibitors for a range of indications including breast cancer, the treatment of infertility and other off-label uses.

A novel structural basis for the development of improved aromatase inhibitors

There is a need for alternative aromatase inhibitors that bring about adequate enzyme activity inhibition, while limiting treatment side effects. By testing a carefully selected group of xenobiotics for their ability to inhibit aromatase, this work demonstrates that, in contrary to conventional wisdom, which holds that aromatase has strict ligand requirements, aromatase interacts with a structurally wide range of compounds other than the known endogenous substrates or the current inhibitors. These compounds include methadone and its metabolites EDDP and EMDP, tamoxifen and a number of its metabolites, fluoxetine, naringenin and 17-hydroxy exemestane. Among these compounds, a number of novel aromatase inhibitors that employ diverse kinetic mechanisms have been identified and characterized. Data indicate that methadone (K_I of 40.6 ± 2.8 μM; k_{inact} of 0.061 ± 0.001 min^{-1}) and its major metabolites are mechanism-based inhibitors (Chapter Five Figure 5.2), naringenin (IC_{50}s of 2.8 μM for (R)-naringenin and 1.4 μM for (S)-naringenin) is a stereoselective inhibitor (Chapter Six Figure 6.2), endoxifen (K_i of 4.0 μM) and N-desmethyl-tamoxifen (K_i of 15.9 μM) are two non-competitive inhibitors (Chapter Seven Figures 7.2 and 7.3), and norendoxifen (K_i of 35 nM) is a relatively potent, selective, and competitive inhibitor (Chapter Seven Figures 7.5 and 7.6). These findings illuminate the biochemistry and pharmacology of aromatase. Of note, the biochemical mechanism of inhibition by some of these metabolites is allosteric, suggesting that there might be an alternative site that could be

exploited in the search for new therapies to modulate aromatase activity. The range of structures tested in this work and their different pharmacological properties provide a reasonable pharmacophore upon which to build improved aromatase inhibitors.

In the search for better aromatase inhibitors, my work demonstrates that tamoxifen metabolites represent important candidate structures. They are a series of compounds that have triphenylalkene structure with side chain(s) on the phenyl group(s) that are oxyalkanes or oxyalkenes and that terminate in an unsubstituted or mono-substituted amine (Chapter Eight Figure 8.6). Based on the observed various potencies of these compounds, several consistent structure-function relationships exist: stepwise demethylation and hydroxylation of tamoxifen both progressively increase the potency of the compound as an aromatase inhibitor (Chapter Eight Figures 8.1 and 8.2). My work also shows that the most potent inhibitor identified, norendoxifen, is a relatively selective aromatase inhibitor, when its inhibitory effects on clinically important cytochrome P450 enzymes were tested and compared (Chapter Seven Figure 7.6). In addition, collaborative data generated using molecular modeling improve our understanding of possible biochemical mechanisms employed by norendoxifen to interact with the active site of aromatase. These findings, together with the structure-function relationships identified, suggest that modification to the basic triphenylalkene structure of tamoxifen that preserves hydrogen bonding to the Ala306, Met374 and Asp309 residues of the active site might be a valuable approach in the rational design of new and effective aromatase inhibitors that work by a similar mechanism. In this context, norendoxifen may be able to serve as a lead compound for the development of drugs with improved therapeutic index.

Clinical implications

This work has a number of potentially important clinical implications. The new roles for aromatase in drug disposition and pharmacokinetic drug-drug interactions described herein may help optimize therapy and prevent toxicity.

First, improved understanding of interactions between methadone and aromatase may help explain a few clinical observations. Methadone dosing is difficult to manage and unanticipated accumulation of methadone in patients can lead to high methadone concentrations with resultant potentially lethal consequences. Since methadone is both a substrate and a mechanism-based inhibitor of aromatase (Chapters Two and Five, this dissertation), methadone accumulation over time due to auto-inhibition of its own metabolism seen in some patients (Morton 2007) may be a result of the irreversible inhibition of aromatase by itself. Consistent with inhibition of aromatase by methadone, lower concentrations of estradiol and of follicle-stimulating hormone have been documented in men taking methadone (Hallinan et al. 2009), and low bone mineral density that may be due to low estrogen concentrations has been documented in 83% of patients in a methadone maintenance treatment program (Kim et al. 2006). This improved understanding of interactions between aromatase and methadone may help us develop new and rational strategies to prevent methadone overexposure. On the other hand, aromatase activity has large interindividual variability, and so the identification of a metabolic route for methadone via this enzyme may help to anticipate and manage withdrawal in multiple clinical settings where current predictive ability is low. These include the withdrawal that neonates of methadone-treated mothers' experience (Serane

and Kurian 2008), methadone withdrawal that often occurs during pregnancy (Pond et al. 1985), and that occurs in routine use of methadone to treat pain or heroin addiction.

Second, tamoxifen is an important treatment for breast cancer, whose activity is known to be mediated via active metabolites, primarily by endoxifen which blocks estrogen binding to estrogen receptors. Our work demonstrates that some tamoxifen metabolites also act as aromatase inhibitors (Chapters Seven and Eight, this dissertation), suggesting that blockade of estrogen production may also contribute to the clinical effects of tamoxifen. This effect may explain the changes in serum and tissue estrogen concentrations seen in patients taking tamoxifen (Lonning et al. 1995). These data also improve our understanding of possible relationships between concentrations of active tamoxifen metabolites and clinical outcomes of tamoxifen therapy. For example, if aromatase inhibition contributes to the action of tamoxifen, then it is possible that this effect confounds a simple association between endoxifen concentration and clinical outcome. Aromatase inhibition mediated by multiple active tamoxifen metabolites may help explain the inconsistency in observed associations between CYP2D6 genotype and treatment outcome in breast cancer patients taking tamoxifen (Goetz et al. 2005; Nowell et al. 2005; Wegman et al. 2007). There may be a variable balance among patients between the blockage of estrogen production and the antagonism at estrogen receptors. This balance may therefore explain in part the variability in bone density, serum lipid concentrations, experience with hot flashes, severity of musculoskeletal pain and breast cancer recurrence observed in patients taking tamoxifen.

Third, the novel aromatase inhibitors and their mechanisms of action identified here may contribute to the search for new approaches to breast cancer therapy both in the

treatment and prevention settings. For example, data suggest that medications, such as methadone and tamoxifen, are commonly taken by breast cancer patients, and may exert adequate aromatase inhibition beneficial in the prevention of tumor growth and cancer recurrence. Such effects may augment the treatment of breast cancer and may be therapeutically useful. Naringenin is often ingested via fruit products such as grapefruit juice and therefore might also be protective for people at risk for breast cancer.

Lastly, inhibition of aromatase by the inhibitors identified in this work might occur in vivo and therefore may alter the metabolism of endogenous testosterone and androstenedione. As a result, side effects of these drugs, such as flushing, muscle pain and symptoms reminiscent of estrogen withdrawal (Senay 1985; Backstrom 1995), may be explained in part by the drugs' action on aromatase.

Overall, our findings have the potential to improve the use of methadone, tamoxifen and current aromatase inhibitors, all of which are commonly co-prescribed with a wide range of other drugs. These findings also improve our understanding of the potential clinical effects of the studied xenobiotic medications and dietary compounds on aromatase activity. As a result, it may be possible to more consistently treat patients, particularly in breast cancer, with current medications in ways that maximize efficacy, minimize side effects, better anticipate drug interactions and therefore improve the quality of life of patients.

Future directions

Based on the findings of my work, it would be valuable to further evaluate the following in the future:

(1) To investigate the influence of genetic variants of aromatase on methadone metabolism in humans. The results of the current study indicate that methadone is metabolized by aromatase in humans but the effect of aromatase inhibition on systemic methadone clearance is highly variable (Chapter Three, this dissertation). The relative contribution of aromatase and other enzymes suggested to be important in the metabolism of methadone, including particularly CYP2B6 (Crettol et al. 2005; Wang et al. 2011), may be influenced by genetic variants of aromatase and those of CYP2B6. This balance may be an important factor in the under- or over-dosing often seen in methadone patients. Future genetic studies both in vitro and in vivo that address the relationships between enzyme genotype and its quantitative contribution to overall methadone clearance should be performed. In the case of aromatase, several variants that influence its activity have been reported. The most widely studied is a tetranucleotide (TTTA)n tandem repeat polymorphism located in intron 4 of the human *CYP19A1* gene, and it has been reported that the number of TTTA repeats is associated with estrogen levels (Somner et al. 2004), age at menarche (Xita et al. 2010), obesity (Hammoud et al. 2010), polycystic ovarian syndrome (Hao et al. 2010), risks for breast cancer (Ahsan et al. 2005; Kristensen et al. 2000) and osteoporosis (Gennari et al. 2004; Masi et al. 2001). There have also been a few reports of a very rare autosomal recessive disease, human aromatase deficiency, caused by loss-of-function mutations in the *CYP19A1* gene (Bulun 2000; Belgorosky et al. 2009; Rochira and Carani 2009). Interindividual variability in methadone dosage requirement has been shown to be polygenetic and cannot be explained by a single-gene effect (Hung et al. 2011). Demonstrating a clinically relevant relationship between

aromatase genotype and methadone clearance across multiple doses of the drug will help to achieve safer use of methadone.

(2) To investigate the involvement of aromatase in the clinical disposition of other drugs. This work has shown that aromatase is responsible for methadone metabolism in humans. Placental aromatase has also been implicated in the metabolism and specifically the demethylation of buprenorphine (Deshmukh, Nanovskaya, and Ahmed 2003) and cocaine (Osawa et al. 1997) in vitro, it is therefore reasonable to directly examine the role that this enzyme plays in the metabolism of these drugs in clinical settings. Since the biochemical mechanism by which aromatase catalyzes the metabolism of either endogenous substrates or exogenous drugs involves the removal of a methyl group, it follows that other medications that are similarly metabolized may also be aromatase substrates. In particular, the results generated from screening compounds for aromatase inhibitors indicate that fluoxetine interacts with aromatase in vitro (Chapter Four Figure 4.1.B). Fluoxetine is also a drug that primarily undergoes N-demethylation to norfluoxetine and aromatase might be involved in the biotransformation of this drug. This possibility deserves further study.

(3) To further investigate the potential of norendoxifen as a clinically useful aromatase inhibitor. First, the current study has characterized norendoxifen as a potent and selective inhibitor in vitro (Chapter Seven Figures 7.5 and 7.6). The next step is to assess whether or not this action of norendoxifen is likely to happen in vivo. Although norendoxifen is a known metabolite of tamoxifen in humans (Lien et al. 1991; Jin et al. 2005), little is known about its tissue concentrations or its contribution to tamoxifen effects. While norendoxifen is a tertiary metabolite of tamoxifen and its in vivo

concentration is probably at notably lower concentrations than the parent drug or its major metabolites, it is known that tamoxifen metabolites concentrate in tissue compartments. For example, the concentrations of endoxifen in breast tumors appear to be 10 to 100 times higher than its serum concentrations in humans (Lien et al. 1991). This serum-tissue gradient is more prominently shown by studies in rats. The ratio of endoxifen concentrations in tissue to those in serum can be as high as 500 : 1 (Lien, Solheim, and Ueland 1991). It follows that tissue accumulation of norendoxifen and thereby local aromatase inhibitions in vivo seem a possibility. In order to evaluate the contribution of norendoxifen to the therapeutic effects of its parent drug, tamoxifen or endoxifen, it is important to determine the serum and tumor concentrations of norendoxifen in people who undergo these therapies for breast cancer. The potency of this mechanism in vivo merits future studies. Second, it is important to note that norendoxifen is the metabolite of endoxifen and 4-hydroxy-tamoxifen, two widely recognized and potent estrogen receptor modulators (Jin et al. 2005; Johnson et al. 2004; Jordan 2007). It follows that norendoxifen may also act as an estrogen receptor ligand, that is able to modulate estrogen signaling. Studies should be carried out to determine the ability of norendoxifen to bind to estrogen receptors, and to assess its effects on estrogen signaling. The present studies demonstrate that norendoxifen is not only an aromatase inhibitor with potency close to letrozole, but that it also has the potential ability to mitigate the debilitating musculoskeletal toxicities experienced by breast cancer patients via tissue specific mechanisms involving estrogen receptor signaling. For example, a new aromatase inhibitor that is also an agonist at estrogen receptors in bone may prevent the high prevalence of vertebral fractures seen in breast cancer patients starting aromatase

inhibitor therapy (Bouvard et al. 2011). Norendoxifen and its derivatives may therefore be valuable candidates for a dual-mechanism therapy involving both aromatase inhibition and selective estrogen receptor modulation, which might be exploited in the development of alternative breast cancer therapies.

(4) To investigate the influence of genetic variants of aromatase on its susceptibility to inhibition by different inhibitors. Aromatase inhibition has become the standard of care for ER-positive (~ 70% of all) breast cancer (Taylor and Muss 2010; Howell and Dowsett 1997). Although this therapy remains the most clinically effective treatment in preventing breast tumor growth and cancer recurrence, about 50% of all patients taking aromatase inhibitors in the adjuvant setting still recur within 5 years after surgery (Howell et al. 2005). There is a large variability in patients' response to current aromatase inhibitors, both in efficacy and side effects. It is possible that genetic biomarkers such as aromatase genotype can help identify patients who benefit from this therapy and those who don't. The reason for this difference is likely to be the influence of genetic variants on the 3-D structure of aromatase and therefore on its susceptibility to inhibition. Therefore, the susceptibility of aromatase variants to different inhibitors may be different, and it is possible to develop stratification strategies to identify the optimal aromatase inhibitor for individual breast cancer patients based on their genetic information. With the ongoing search for new aromatase inhibitors, a large number of in vitro aromatase inhibitors have been identified. These findings provide a pool of candidate compounds for in vitro testing on various aromatase variants. In this work, endoxifen and NDMT have been characterized as aromatase inhibitors via a non-competitive mechanism, which is consistent with an allosteric interaction with aromatase

(Chapter Seven Figures 7.2 and 7.3). It is possible that this allosteric inhibition occurs via interactions at a site remote from the catalytic site of the enzyme, or that it occurs via interactions of two drugs that bind differently within the active site. Of note, mutation of a site distant from the substrate binding site of aromatase has been shown to increase enzyme activity and reduce the susceptibility to inhibition of aromatase by aminoglutethimide (Payne et al. 2009). These observations raise the possibility that allosteric mechanisms might contribute to the pharmacologic regulation of aromatase and could be exploited to modulate aromatase activity for therapeutic benefit. The knowledge of using selective aromatase inhibitors to overcome genetic influence will help develop diagnostic tests that could be used in a personalized approach to treat breast cancer.

(5) To identify new biomarkers that can distinguish breast cancer patients who are destined to experience debilitating toxicity or benefit from treatment with aromatase inhibitors. Not all patients respond favorably to aromatase inhibition. In the long term, biomarker-guided individualization of therapy for cancer holds great promise to improve treatment outcomes. Breast cancer mortality is increasing rapidly in Asia while decreasing in Western countries (Aihara et al. 2010; Deapen et al. 2002). Many effective therapies, developed exclusively in Caucasians, have not been optimized for Asian patients despite the fact that there are many ethnic differences in breast cancer. These include the prevalence of molecular subtypes of the disease, genetic polymorphisms in pathways involved in estrogen biosynthesis and metabolism, vulnerability to debilitating side effects of anti-estrogenic therapies, pharmacokinetic-pharmacodynamic relationships, and effects of demographic factors (Toi et al. 2010; Miyoshi and Noguchi 2003). As a result, personalized approaches guided by genomic and other biomarkers

seem particularly promising in improving breast cancer treatments, especially in Asian populations. It is well-known that in a subset of patients aromatase inhibition therapy is either ineffective or brings about musculoskeletal pain which results in poor quality of life and thereby non-compliance. In fact, 25 - 50% of women prescribed an aromatase inhibitor have been reported to stop taking the drug within 3 years (Ziller et al. 2009; Partridge et al. 2008; Hershman et al. 2010), and more than 50% of patients experience musculoskeletal pain, the principal reason for non-adherence (Zivian and Salgado 2008; Oberguggenberger et al. 2011; Aihara et al. 2010). In order to identify inherited pharmacogenetic variants that associate with treatment response, prospective and retrospective clinical studies can be designed and conducted using an informed genome-wide association (GWA) approach. Genetic variants to be tested should include those suggested by prior broad GWA studies (Ingle et al. 2010), as well as variants in candidate genes involved in estrogen biosynthesis, metabolism and signaling pathways (Mao et al. 2011). Clinical response can be assessed by measuring musculoskeletal toxicity using the Health Assessment Questionnaire (Thompson and Pegley 1991) and Visual Analogue Pain Rating Scale (Henry et al. 2010), and by analyzing data on cancer recurrence from patients' medical records. These studies will identify novel biomarkers that can be combined in diagnostic tests and that inform future stratification of breast cancer therapy.

Summary

Cytochrome P450s in humans are enzymes responsible for the metabolism and elimination of the majority of therapeutic xenobiotics. One member of this class of enzymes, aromatase (CYP19), is less known for its interactions with xenobiotics. Our

studies presented here demonstrate potentially important roles for aromatase in drug disposition and pharmacokinetic drug-drug interactions. Specifically, this work discovers an involvement of aromatase in the metabolic pathways of methadone and improves our understanding of the pharmacologic action of tamoxifen. In addition, aromatase represents a key target in the treatment of a number of estrogen-related conditions including breast cancer. This work provides a new mechanistic framework for targeting aromatase by characterizing novel aromatase inhibitors that employ diverse kinetic actions. As a result, the range of tested structures and their attendant pharmacologic potencies provides a reasonable pharmacophore upon which to build novel aromatase inhibitors.

CHAPTER TEN

General Methods

Chemicals and reagents

(R) / (–)-methadone and (S) / (+)-methadone were generously provided by the National Institute on Drug Abuse Drug Supply Program (Bethesda, MD). Methadone metabolites 2-ethylidene-1,5-dimethyl-3,3-diphenylpyrrolidine (EDDP) iodide and 2-ethyl-5-methyl-3,3-diphenylpyrroline (EMDP) hydrochloride were obtained from Alltech (Deerfield, IL). (R)-, (S)- and rac-naringenin were generously provided by Dr. Salvatore Caccamese at the Dipartimento di Scienze Chimiche, Università di Catania, Italy. Tamoxifen, all tamoxifen metabolites, bupropion, 4-hydroxybupropion, (R)-hydroxyomeprazole, (R)-lansoprazole, norgestrol, nevirapine and letrozole were obtained from Toronto Research Chemicals Inc. (North York, ON, Canada). Racemic methadone hydrochloride, desmethyldiazepam, 17-β-estradiol, testosterone, (R)-omeprazole, tolbutamide, 4-hydroxytolbutamide, chloropropamide, β-NADP, glucose-6-phosphate dehydrogenase, and glucose-6-phosphate were purchased from Sigma-Aldrich (St. Louis, MO). Monobasic and dibasic sodium phosphate, monobasic potassium phosphate, magnesium chloride, HPLC-grade methyl tert-butyl ether, acetonitrile and methanol were purchased from Fisher Scientific (Pittsburgh, PA). Glycine (electrophoresis purity reagent) was obtained from Bio-Rad Laboratories (Hercules, CA, USA). All drug solutions were prepared by dissolving each compound in methanol or acetonitrile, and were stored at − 20 °C. Tamoxifen and its metabolites were prepared under dim light and in brown tubes to minimize photodegradation.

Baculovirus-insect cell-expressed human aromatase (with oxidoreductase) microsomal preparations, pooled human liver microsomes (HLMs) and the cytochrome P450 inhibitor screening kits for aromatase (CYP19), 2C9, 2C19 and 2D6 were purchased from BD Biosciences (San Jose, CA). Placental microsomal preparations were a generous gift from Dr. Mahmoud S. Ahmed at the University of Texas Medical Branch, Galveston. All microsomal preparations were stored at – 80 °C until used.

Methadone for IV administration was obtained from Xanodyne (Newport, KY) as a 10 mg/ml solution. Volumes of methadone used for each administration were recorded as 0.6 ml (6 mg). This dose was diluted in 50 ml of normal saline for IV infusion. The same lot number was used for each administration of methadone, and was prepared by the Indiana University Hospital Pharmacy, Investigational Drug Services. Letrozole pills (Femara® 2.5 mg tablets) were obtained from Novartis (Basel, Switzerland).

Testosterone and methadone metabolism in vitro by recombinant aromatase

All incubations were carried out using incubation times and protein concentrations that were within the linear range for reaction velocity. Testosterone and methadone were dissolved in methanol and diluted with the same solvent to the required concentrations. Any methanol in the incubation tubes was removed by drying in speed vacuum before the incubation. All incubations contained recombinant human aromatase in 100 mM sodium phosphate buffer (pH = 7.4), with a NADPH-generating system (1.3 mM NADP, 3.3 mM glucose-6-phosphate, 3.3 mM $MgCl_2$, and 0.4 U/ml glucose 6-phosphate dehydrogenase) and various concentrations of aromatase substrate in a final volume of 250 µl. When inhibition of metabolism was tested, the tested inhibitor was

mixed with the substrate and was present at a range of concentrations during the incubation. The incubation mixture was prewarmed for 5 min at 37 °C, initiated by addition of the NADPH-generating system, and incubated at 37 °C. When testosterone was the substrate, final aromatase concentration used was 0.01 μM and the incubation time was 10 min. When methadone was the substrate, final aromatase concentration used was 0.05 μM and the incubation time was 30 min. All reactions were terminated by the addition of 20 μL of 60 % (w / v) perchloric acid, immediate vortex and then placing the tubes on ice.

HPLC-UV assays for the quantifications of estradiol and EDDP formation

All samples were extracted immediately after the incubation. First, 25 μL of 500 μM norgestrol was added to each sample as an internal standard. The incubation mixture was centrifuged at 14,000 rpm for 5 min at room temperature. The supernatant layer was made alkaline by adding 500 μL of 1M glycine-NaOH buffer (pH 11.3) and extracted by adding 6 mL of ethyl acetate. This mixture was vortex-mixed for 10 seconds and then centrifuged at 26,000 rpm for 15 min. The organic layer was transferred to 13 × 100-mm glass culture tubes and evaporated to dryness. The resulting residue was reconstituted with mobile phase (50% 10mM monobasic potassium phosphate, 40% acetonitrile and 10% methanol) and analyzed as described below immediately.

High performance liquid chromatography (HPLC) assays with ultraviolet (UV) detection were developed for the quantification of testosterone conversion to estradiol and of methadone conversion to EDDP. The HPLC-UV system was comprised of a Waters (Milford, MA) model 510 HPLC pump and a Waters model 717 plus

autosampler, coupled with a Waters 486 tunable absorbance detector. The separation system consisted of a Zorbax SB-C_{18} column (4.6 × 150 mm, 3.5 µm particle size, Phenomenex, Torrance, CA), a Nova-Pak C_{18} Guard column (4 µm; Waters, Inc., Ireland). An isocratic elution was used to separate the compounds. The mobile phase consisted of 50% 10mM monobasic potassium phosphate, 40% acetonitrile and 10% methanol without PH adjustment. The eluate was introduced, at 0.8 ml/min to the UV detector with a run time of 25 min. Under these conditions, the retention times of letrozole, estradiol, EDDP, testosterone, methadone, norgestrol and EMDP were approximately 3, 8, 10, 12, 15, 20 and 35 min, respectively.

Peak areas for each peak were obtained from an integrator, and peak area ratios with internal standard were calculated. Standard curves were estimated by linear regression of peak area ratios. Quantification of samples was carried out by applying the linear regression equation of the standard curve to the peak area ratio. The microsomal activity data represent individual data points or the mean of duplicate assays. The limit of quantification for estradiol was 2.5 pmol on column, with intra- and inter-day coefficients of variation of 2.4% and 5.3% respectively. The limit of quantification of EDDP was 5 pmol on column, with intra- and inter-day coefficients of variation of 5.5% and 7.3% respectively.

LC-MS/MS assays for plasma and urinary methadone, EDDP and EMDP

HPLC with tandem mass spectrometry detection (LC-MS/MS) assays were developed for the quantification of plasma and urinary methadone and its major metabolites, EDDP and EMDP. Each plasma and urine sample (1 ml) was extracted by

adding 500 µL of 1M glycine-HCl buffer (pH 3.0) and 6 mL of methyl tert-butyl ether. Nevirapine (100 µl of 1 µg/ml) was added to each sample as an internal standard. This mixture was mixed on a reciprocal shaker (Eberbach, Ann Arbor, MI) for 5 min and then centrifuged at about 3,000 rcf for 15 min. The organic layer was transferred to 13 × 100-mm glass culture tubes and evaporated to dryness. The resulting residue was reconstituted with mobile phase (50% 20 mM ammonium acetate and 50% acetonitrile without pH adjustment) and analyzed immediately. The LC-MS/MS assay was performed on an Applied Biosystems (Foster City, CA) model API 2000 triple-quadrupole mass spectrometer, coupled with a Shimadzu (Addison, IL) HPLC system consisting of a model LC-20AB binary solvent delivery pump and model SIL-20A HT autosampler. The separation system was composed of a Luna 3 µm C_{18}-2 column (100 × 2.00 mm i.d.; Phenomenex, Torrance, CA) and a nitrile guard column (4 × 3.0 mm; Phenomenex). The eluate was introduced, without splitting, at 0.200 mL/min to the electrospray ionization source. The electrospray voltage was set at + 2500 mV and the dwell time at 100 ms per detection channel with unit mass resolution on the quadrupole 1 and 3 mass analyzers. Optimal gas pressures for all of the analytes were: nitrogen nebulizer gas 20.00 psi, turbo/heater gas 0.00 psi, curtain gas 20.00 psi and collision gas 2.00 psi. All data were collected in the positive ion mode with the temperature of the interface set at 450 °C. Under these conditions, nevirapine, methadone, EDDP and EMDP were detected at the retention times of approximately 3, 6, 5, and 10 min, respectively, and were quantified using m / z values (Q3 / Q1) at 226.0 / 267, 265.2 / 310, 234.1 / 278 and 220.2 / 264 respectively. Peak areas for each peak were obtained, and peak area ratios with internal standard were calculated. Quantification of samples was carried out by applying the

linear regression equation of the standard curve to the peak area ratio. Each analytical run included calibration samples and quality control samples at the concentration range of 0.1 - 200 ng/ml for methadone, EDDP and EMDP. Using these methods, the limits of quantification (LOQs) for methadone, EDDP and EMDP were 0.1, 0.2 and 0.1 ng/ml respectively, with intra-day and inter-day coefficients of variation of less than 5 % and less than 12 % respectively for all three compounds, when measured above the LOQs.

HPLC-UV-fluorescence assays for plasma letrozole

Plasma letrozole concentrations were measured using HPLC assays with ultraviolet and fluorescence detection as described below. Baseline plasma samples (200 µl) were made alkaline by adding 500 µL of 1 M glycine-NaOH buffer (pH 11.3) and extracted by adding 6 mL of ethyl acetate. Desmethyldiazepam (100 µl of 1000 ng/ml) was used as internal standard. All samples were mixed, centrifuged and transferred as described above, and then reconstituted with mobile phase (70% 10 mM monobasic potassium phosphate, 30% acetonitrile, pH adjusted to 6.5) and analyzed immediately. The HPLC system was controlled by CLASS-VP version 7.1.1 SP1 Chromatographic Software (Shimadzu Scientific Instruments Inc., Columbia, MD) and included a Shimadzu solvent delivery module SCL-10A VP, an autoinjector SIL-10AD VP, a spectrofluorometric detector RF-10A XL (set at an excitation wavelength of 230 nm and emission wavelength of 295 nm), an ultraviolet detector SPD-10A VP (set at a wavelength of 234 nm, 0.1 AUFS) and a system controller SCL-10A VP (Shimadzu, Kyoto, Japan). The eluate was directed at 1 ml/min through a Zorbax SB-C18 3.5-µm C_{18} column (150 × 4.6 mm i.d.; Agilent Technologies, Santa Clara, CA) coupled with a

Nova-Pak C_{18} Guard column (4 µm; Waters, Inc., Ireland) with a run time of 32 min. Under these conditions, the retention times of letrozole and desmethyldiazepam were approximately 17 and 27 min, respectively. The limit of quantification for letrozole was 12.5 ng/ml, with intra-day and inter-day coefficients of variation of less than 4.3% and less than 8.1% respectively.

Fluorescent assay for inhibition of aromatase in vitro

The activity of recombinant human aromatase was determined by measuring the conversion rate of a fluorometric substrate, 7-methoxy-4-trifluoromethylcoumarin (MFC), to its fluorescent metabolite, 7-hydroxytrifluoromethylcoumarin (HFC). Experimental procedures were consistent with the methodology described for high-throughput screening of a human cytochrome P450 inhibitor (Stresser 2004). All incubations were carried out using incubation times and protein concentrations that were within the linear range for reaction velocity. Experiments involving tamoxifen and its metabolites were carried out under dim light to minimize photodegradation. MFC and inhibitors were prepared in acetonitrile solutions. A series of concentrations of inhibitor in a volume of 4 µl were mixed with 96 µl of NADPH-Cofactor Mix (16.3 µM NADP, 828 µM glucose-6-phosphate, 828 µM $MgCl_2$, and 0.4 U/ml glucose 6-phosphate dehydrogenase), and prewarmed for 10 min at 37 °C. MFC and recombinant human aromatase were mixed with 0.1 M potassium phosphate buffer (pH 7.4), and then added to an Enzyme/Substrate Mix. Reactions were initiated by adding 100 µl of Enzyme / Substrate Mix to bring the incubation volume to 200 µl. Final MFC concentration was typically set at 25 µM. When multiple substrate concentrations were tested in order to

characterize detailed kinetics of enzyme inhibition, final MFC concentrations of 10, 15, 20 and 25 µM were used. Final recombinant aromatase concentration was 7.5 nM. After incubation for 30 min at 37 °C, all reactions were stopped by adding 75 µl of acetonitrile / 0.1 M tris base. When aromatase inhibition was tested using human placental microsomes, experimental conditions were the same as described above except that the final total protein concentration was 0.12 mg/ml. The generation of HFC was determined immediately by measuring fluorescence response (excitation 400 nm, emission 540 nm) using a BioTek (Winooski, VT) Synergy 2 fluorometric plate reader. The activity of placental human aromatase was determined using the same methods with the exception that final protein concentration was 0.06 mg/ml. Standard curves were constructed using fluorescent metabolite HFC standard. Quantification of samples was carried out by applying the linear regression equation of the standard curve to the fluorescence response. The limit of quantification for HFC was 0.02 µM in a final volume of 200 µl, with intra- and inter-day coefficients of variation of 6.2% and 8.4% respectively.

Mechanism-based inhibition of aromatase in vitro

Recombinant aromatase was preincubated with various concentrations of tested inhibitor. All preincubations contained tested inhibitor, 0.1 µM aromatase and 100mM sodium phosphate buffer (pH = 7.4), NADPH-generating system (1.3 mM NADP, 3.3 mM glucose-6-phosphate, 3.3 mM MgCl2, and 0.4 U/ml glucose 6-phosphate dehydrogenase) in a final volume of 250 µl. Preincubations were initiated and carried out in the same way as described for the microsomal incubation conditions described above. After a period of time, each 250 µl preincubation mixture was diluted 10 times with a

solution containing testosterone, sodium phosphate buffer and NADPH-generating system to reach a final incubation mixture of 50 μM testosterone and 0.01 μM aromatase. The dilution was to eliminate competitive inhibition as a possible cause of the inhibitory effect. This incubation mix was then incubated at 37 °C for 10 min. The reaction was terminated the same way as described above. The extent of inactivation of aromatase, expressed as the percent activity remaining after preincubation, was determined by measuring the conversion rate of testosterone to estradiol.

Inhibition of testosterone metabolism by aromatase in vitro

The activity of aromatase was determined by measuring the rate of conversion of testosterone to estradiol. All incubations were carried out using incubation times and protein concentrations that were within the linear range for reaction velocity. Testosterone and the tested inhibitors were prepared in methanol. All experiments were performed under dim light and in brown, gall tubes to minimize photodegradation of tamoxifen and its metabolites.

For reversible inhibition studies, testosterone and inhibitor were mixed at the appropriate concentrations, and methanol was removed by drying under speed vacuum before the incubation. All incubations contained recombinant human aromatase in 100 mM sodium phosphate buffer (pH 7.4), with a NADPH-generating system (1.3 mM NADP, 3.3 mM glucose-6-phosphate, 3.3 mM $MgCl_2$, and 0.4 U/ml glucose 6-phosphate dehydrogenase) in a final volume of 250 μl. The reaction was prewarmed for 5 min at 37 °C, initiated by the addition of the NADPH-generating system, and incubated at 37 °C for 10 min. Final aromatase concentration was 50 nM. Final testosterone concentrations of 1,

2, 4 and 8 µM were tested. All reactions were terminated by the addition of 20 µl of 60% (w / v) perchloric acid, followed by immediate vortexing and placement of the tubes on ice. The fluorometric substrate, MFC was tested under these same conditions in order to compare IC_{50} values of tested inhibitors with a different substrate. For studies designed to test for irreversible inhibition, experiments were carried out as described above in "Mechanism-based inhibition of aromatase in vitro".

Inhibition of recombinant human CYP isoforms

The activity of each recombinant human CYP isoform was determined by measuring the conversion rate of a fluorometric substrate to its fluorescent metabolite. Aromatase and CYP2C9 activities were determined using the metabolism of 7-methoxy-4-trifluoromethylcoumarin (MFC) to 7-hydroxytrifluoromethylcoumarin. CYP2C19 activity was determined using the metabolism of 3-cyano-7-ethoxycoumarin (CEC) to 3-cyano-7-hydroxycoumarin. CYP2D6 activity was determined using the metabolism of 3-[2-(N,N-diethyl-N-methylamino)ethyl]-7-methoxy-4-methylcoumarin (AMMC) to 3-[2-(N,N-diethylamino)ethyl]-7-methoxy-4-methylcoumarin. Experimental procedures were consistent with the published methodology (Stresser 2004). All incubations were carried out using incubation times and protein concentrations that were within the linear range for reaction velocity. Substrates and inhibitors were prepared in acetonitrile. A series of concentrations of inhibitor in a volume of 4 µl were mixed with 96 µl of NADPH-Cofactor Mix (16.3 µM NADP, 828 µM glucose-6-phosphate, 828 µM $MgCl_2$, and 0.4 U/ml glucose 6-phosphate dehydrogenase), and prewarmed for 10 min at 37 °C. Enzyme / Substrate Mix was prepared with fluorometric substrate, recombinant human CYP

isoform and 0.1 M potassium phosphate buffer (pH 7.4). Reactions were initiated by adding 100 µl of Enzyme/Substrate Mix to bring the incubation volume to 200 µl. The optimal final recombinant enzyme concentrations, substrate concentrations and incubation times were: 7.5 nM AROMATASE + 25 µM MFC for 30 min, 15 nM CYP2C9 + 150 µM MFC for 45 min, 7.5 nM CYP2C19 + 25 µM CEC for 30 min, and 7.5 nM CYP2D6 + 1.5 µM AMMC for 30 min. All reactions were stopped by adding 75 µl of acetonitrile / 0.1 M tris base. The generation of fluorescent metabolites was determined immediately by measuring fluorescent response using a BioTek (Winooski, VT) Synergy 2 fluorometric plate reader. Excitation - emission wavelengths were 400 - 540 nm for the MFC metabolite or 400 - 460 nm for the CEC and AMMC metabolites. Standard curves were constructed using the appropriate fluorescent metabolite standards. Quantification of samples was carried out by applying the linear regression equation of the standard curve to the fluorescence response. The limits of quantification for the metabolites of MFC, CEC and AMMC were 4 pmol, 0.1 pmol and 0.8 pmol in a final volume of 200 µl respectively, with intra- and inter-assay coefficients of variation of less than 10%.

Inhibition of specific CYP isoforms using pooled HLMs

Inhibition of individual CYP isoforms was studied as previously described (Jeong et al. 2009) with the modification that the formation rates of 4-hydroxybupropion from bupropion, of 5′-hydroxyomeprazole from omeprazole and of 6-β hydroxytestosterone from testosterone served as markers of CYP2B6, CYP2C19 and CYP3A activity respectively. A single isoform-specific substrate concentration at the respective K_m value

was incubated at 37 °C in duplicate with pooled HLMs and the a NADPH-generating system (1.3 mM NADP, 3.3 mM glucose-6-phosphate, 3.3 mM $MgCl_2$, and 0.4 U/ml glucose 6-phosphate dehydrogenase) in the absence or the presence of tested inhibitors. The activity of specific CYP isoform was determined by measuring the formation rate of corresponding metabolite from probe drug in pooled HLMs. All incubations were carried out using incubation time and protein concentrations that were within the linear range for reaction velocity. An incubation mixture that consisted of substrate probes, HLMs, and 100 mM phosphate reaction buffer (pH 7.4) was pre-warmed for 5 min at 37 °C. The reaction was initiated by the addition of the NADPH-generating system, and incubated at 37 °C for 15 min. The final protein concentration of pooled HLMs was 0.25 mg/ml. All reactions were terminated by the addition of 500 μl of acetonitrile, followed by immediate vortex and placement of the tubes on ice. All samples were extracted immediately after the incubations were carried out. The quantification methods for metabolite formation were the same as those described in published papers (Jeong et al. 2009; Lu, Ferlito et al. 2011; Lu, Xu et al. 2011).

Computerized molecular modeling

"All tamoxifen metabolite structures were constructed with Sybyl 7.1 software and their energies minimized to 0.01 kcal/mol by the Powell method, using Gasteiger-Hückel charges and the Tripos force field. The energy-minimized structures were docked into the androgen binding pocket in aromatase after removal of the structure of the natural ligand. The parameters were set as the default values for protein-ligand docking program GOLD. The maximum distance between hydrogen bond donors and acceptors

for hydrogen bonding was set to 3.5 Å. After docking, the lowest-energy docking solutions of compounds of interest were merged into the ligand–free protein structure. In the case of (Z)-norendoxifen, the amino side chain was rotated manually to place the nitrogen atom within hydrogen bonding distance to the Ala306 carbonyl oxygen, which ultimately resulted in a more favorable calculated binding energy after energy minimization. The structures of the new ligand–protein complexes were subsequently subjected to energy minimization using the Amber force field with Amber charges. During the energy minimizations, the structures of the compounds of interest and a surrounding 10 Å sphere of the protein were allowed to move. The structure of the remaining protein was kept frozen. The energy minimizations were performed using the Powell method with a 0.05 kcal/(mol Å) energy gradient convergence criterion and a distance-dependent dielectric function." Note: Described by co-investigators in Mark Cushman Lab at Purdue University; quoted from (Lu, Xu et al. 2011).

Protocol for clinical trial: effects of aromatase inhibition on methadone disposition

Specific Aim:

To test the hypothesis that methadone is significantly metabolized by aromatase in vivo by measuring single dose methadone pharmacokinetics in healthy post-menopausal female volunteers in the presence and absence of the selective aromatase inhibitor letrozole.

Research Design:

This study will be conducted at the Indiana University School of Medicine Clinical Research Center (ICRC). This is a single-site, acute-dose and three-period design to determine the effect of the administration of the aromatase inhibitor letrozole given at a dose of 2.5 mg daily by mouth for 7 days, on single dose methadone pharmacokinetics. The specific procedures to be carried out and their sequence in time are detailed in Figure 3.4.

Letrozole specifically and potently reduces the activity of aromatase, with its maximal effect on serum estrogen concentration being evident after five days (FDA letrozole label). We therefore conservatively anticipate that aromatase will be completely inhibited after 7 days of treatment.

Previous investigators studying drug interactions with methadone have successfully used a single dose of intravenous racemic methadone (6.0 mg, 5.4 mg free base) administered intravenously, followed by pharmacokinetic sampling for the measurement of serum methadone concentrations for 96 hours after the dose, using sampling at 30 min, and then 1, 2, 4, 8, 12, 24, 48, 72 and 96 hours after the dose in normal volunteers. Since the terminal elimination phase of methadone clearance can be accurately estimated by 72 hours, we will use a pharmacokinetic sampling strategy involving collections of blood between 0 and 72 hours. In this particular study we will be administering 2 mg of methadone IV. After methadone has been cleared from the body, daily dosing of letrozole will begin on the 8^{th} day after the first methadone dose. The same procedure involving a single intravenous dose of methadone will be repeated on the 15^{th} day of the study after pretreatment with letrozole for 7 days.

Patient Selection:

A total of 15 normal volunteers who satisfy the inclusion and exclusion criteria below will be enrolled in this trial after a prescreening visit.

Inclusion Criteria:

1. Subjects must weigh at least 110 pounds.
2. 45 - 70 years of age.
3. Post-menopausal as defined by more than one year without menses, or after surgical oophorectomy. For women who have undergone a partial surgical hysterectomy and are age 55 or less, an estradiol level will be done to confirm post menopausal status.
4. Subjects must be capable of satisfying protocol requirements and be able to provide written informed consent.
5. Agree to avoid the use of alcohol during the period of the study.

Exclusion Criteria:

1. Subjects must not have a history of intolerance or allergy to the study drugs: methadone or letrozole.
2. A diagnosis of asthma, chronic obstructive pulmonary disease or cor pulmonale, severe obesity with a weight over 300 lbs, or sleep apnea syndrome.
3. Renal insufficiency as indicated by a serum creatinine greater than 1.4.
4. Anemia as defined by a hematocrit of below 30%.
5. Elevation of serum liver enzymes outside the normal range indicating clinically significant hepatic dysfunction.
6. Subjects with low serum potassium and magnesium levels.

7. Have donated blood to the blood bank within the last 2 months.
8. Have taken part in an investigational drug research study within the last 2 months.
9. Increased electrocardiographic QT interval as measured by a QTc (Bazette) of more than 480 msecs.
10. Subjects taking drugs that are known to possibly prolong the QT interval.

Study Procedures:

Screening: After a signed written informed consent is obtained from the subject, a detailed health history will be collected in addition to blood collection, vital signs and a 12 lead electrocardiogram. 10 cc of blood will be collected for genotyping, CBC/diff/plts, Comprehensive Metabolic Panel and serum estradiol. Since methadone has been associated with prolongation of the QT interval when given at high doses intravenously, and there are clear FDA reports of torsades de pointes arrhythmia in patients treated with methadone, a resting electrocardiogram will be obtained to ensure that patients are not placed at risk for arrhythmia by a prolonged baseline electrocardiographic QT interval. The screening will be carried out no later than 4 weeks prior to the study.

Period 1 (Control): Once the screening is completed, qualifying subjects will be admitted to the ICRC at about 7 AM for approximately 25 hours (day 1), after an overnight fast of at least 8 hours.

Following predose blood and urine sampling, and the insertion of a forearm intravenous catheter, subjects will be administered 250 cc of normal saline and then will receive methadone 2.0 mg (5.4 mg free base) IV. After methadone administration, eight samples of blood (~ 10 cc each) will be collected over the next 72 hours according to the

following schedule: 1, 2, 4, 8, 12, 24, 48, and 72 hours after the dose. After the 24 hour sample has been collected, patients will be discharged from the unit. Subjects will be instructed to return again at 48 and 72 hours after the dose for additional single blood draws. Upon return for the 48 and 72 hour blood draws, subjects will be asked to return within a window of plus or minus 2 hours from the assigned time. Similarly the 12 hour urine collection will be stopped at 12 hours after methadone dosing and the exact time of the last urine collection will be recorded. At the 72 hour visit, patients will be given an 11 day supply of letrozole, to be taken daily starting on Day 8, and continuing through Day 18. They will be instructed to take a single dose of letrozole (2.5 mg) each morning at the same time starting on Day 8, and to return to the ICRC at approximately 7 AM on Day 15 for approximately 25 hours after an overnight fast of at least 8 hours.

Methadone Washout: Patients will not return to the ICRC until Day 15. In the interim, they will simply begin talking letrozole tablets once daily beginning on Day 8.

Period 2 (Letrozole Treatment): The same procedures as described above for Day 1 - 4 will be carried out on Day 15 - 18 of the study, except that patients will continue to take a single letrozole tablet every morning until Day 18, when the last dose of letrozole will be taken in the morning. Note: On Day 15, subjects will be asked to hold their letrozole dosing until their arrival to the ICRC and will then be given the letrozole an hour after the methadone dose that day. In order to assess patient compliance with daily letrozole dosing, the blood drawn immediately before the dose of methadone on Day 15 will be used to measure letrozole serum concentrations. Since methadone has highly variable inter-individual clearance, serum methadone concentrations will also be

measured in the blood samples obtained on Day 15 to ensure that no methadone remains in the blood before the pharmacokinetic sampling done in period 2.

Subjects who withdraw from the study or are terminated per investigator's discretion will be replaced for a total of 15 normal volunteers who have completed all 18 days of the study.

Study Drugs: Methadone will be supplied by the Indiana University Hospital Inpatient Pharmacy. A single batch of letrozole 2.5 mg pills to be used for the whole study will also be purchased from the Indiana University Hospital Pharmacies.

Statistics:

Statistical comparisons between the 15 subjects at baseline and after letrozole administration for each of the following serum methadone pharmacokinetic indices will be carried out: AUC, AUC_{inf}, terminal elimination half life, clearance and clearance/kg will be compared between the two periods using a paired student's t-test. The ratios of the urinary concentrations of EDDP and EMDP to urinary methadone will also be compared between the two periods using a paired student's t-test.

Power: Using this design with 15 patients, and a coefficient of variation of 40% in the AUC of this dose of intravenous methadone, and using a two-tailed paired-test, we will have 90% power to detect a change of 33% or more in the AUC of methadone, with an α of 0.05. Such a 33% change would indicate that aromatase is responsible for 33% of methadone clearance.

Procedures to Minimize the Potential Risks of This Study:

1. An electrocardiogram will be performed as part of screening, and subjects with abnormal electrocardiograms will be excluded from the study.
2. Phlebotomy will follow approved hospital and/or nursing policies and procedures.
3. Trained personnel will perform blood and urine sampling.
4. Prior to administration of methadone, subjects will be given 250 cc of normal saline.
5. All subjects will be under close supervision by medical staff.
6. Adverse events will be evaluated & treated immediately, if necessary.
7. Parameters for Narcan adminstration will be included in the doctor's orders which are different than Clarian's standard Narcan policy, These parameters will offer a more sensitive reaction to methadone overdose and will be specific only to this study. They include:
    a. If RR <10, add O_2 to keep O_2 sats > 92%.
    b. If RR <8 or O_2 sats < 90%, administer Narcan.
    c. If Narcan is administered, subject will be assessed by a physician at time of adminstration as well as every hour until stable.
    d. If Narcan is administered, continue VS every 10 minutes until stable.
8. Although methadone does not meet Clarian's definition of 'conscious sedation', we will initiate the 'conscious sedation' policy which includes continuous pulse ox monitoring as well as frequent VS assessments.
9. Subject will be required to be seen and assessed by a physician prior to discharge.

10. Subjects will be required to spend the night on Day 1 and 15. Prior to discharge the next morning, subject will be assessed by a physician and then released to self per MD approval.
11. Information in the study records will be kept confidential. Any reporting of data will not include subject names. This information will not be given to any 3rd party or used for other purposes without the written permission of the subject.

Note: Modified from Indiana University IRB approved protocol which I co-wrote (Flockhart and Lu 2010).

APPENDIX

Republication Permissions

BREAST CANCER ACTION

November 4, 2011

Wenjie Jessie Lu
Division of Clinical Pharmacology
Indiana University School of Medicine

Dear Ms. Lu,

We are pleased to be able to grant permission for you to reproduce the figure entitled: "Women's experiences with aromatase inhibitors" from the Breast Cancer Action report, "Side effects revisited: women's experiences with aromatase inhibitors." in your PhD thesis to be published by Indiana University.

We wish you much success with your work.

Yours sincerely,

Joyce Bichler, ACSW
Deputy Director

55 New Montgomery Street, Suite 323 San Francisco, California 94105
Tel: 415.243.9301 Toll free: 1.877.2STOPBC Fax: 415-243-3996
Web: www.bcaction.org www.thinkbeforeyoupink.org Email: info@bcaction.org

The NEW ENGLAND JOURNAL of MEDICINE

Permission to Use NEJM Material in a Thesis or Dissertation

This permission applies only to copyrighted material that the Massachusetts Medical Society owns, and not to copyrighted text or illustrations from other sources.

All content reproduced from copyrighted material owned by the Massachusetts Medical Society (MMS) remains the full and exclusive copyrighted property of the MMS. The right to grant to a third party is reserved solely by the MMS.

Copyrighted MMS content may not be used in any manner that implies endorsement, sponsorship, or promotion of any entity, product or service by the MMS or its publications. The MMS cannot authorize use of authors' names on promotional materials; such approval must be obtained directly from authors.

The *New England Journal of Medicine* (and its logo design) are registered trademarks of the Massachusetts Medical Society. We do not grant permission for our logo, cover, or brand identity to be used in materials produced by other organizations. NEJM does not issue grants of permission for blanket use of its material. Non-exclusive grants are issued for identified content to be used in a specific manner. We do provide worldwide rights.

MODIFICATIONS/ADAPTATIONS

Grants of permission are issued for the material to be used as originally published by MMS. MMS does not approve adaptations or modifications.

Formatting and stylistic changes and any explanatory material or figure legends used by the requestor must accurately reflect the material as originally published in the *New England Journal of Medicine*.

*This grant covers the right to use the material in print and electronic formats. Figures/Tables that contain text, may be translated.

REFERENCES

Abushahin, F., K. N. Goldman, E. Barbieri, M. Milad, A. Rademaker, and S. E. Bulun. 2011. Aromatase inhibition for refractory endometriosis-related chronic pelvic pain. *Fertil Steril*.

Adams, L. S., Y. Zhang, N. P. Seeram, D. Heber, and S. Chen. 2010. Pomegranate ellagitannin-derived compounds exhibit antiproliferative and antiaromatase activity in breast cancer cells in vitro. *Cancer Prev Res (Phila)* 3 (1):108-13.

Ahmad, A., S. M. Ali, M. U. Ahmad, S. Sheikh, and I. Ahmad. 2010. Orally administered endoxifen is a new therapeutic agent for breast cancer. *Breast Cancer Res Treat* 122 (2):579-84.

Ahmad, A., S. Shahabuddin, S. Sheikh, P. Kale, M. Krishnappa, R. C. Rane, and I. Ahmad. 2010. Endoxifen, a new cornerstone of breast cancer therapy: demonstration of safety, tolerability, and systemic bioavailability in healthy human subjects. *Clin Pharmacol Ther* 88 (6):814-7.

Ahsan, H., A. S. Whittemore, Y. Chen, R. T. Senie, S. P. Hamilton, Q. Wang, I. Gurvich, and R. M. Santella. 2005. Variants in estrogen-biosynthesis genes CYP17 and CYP19 and breast cancer risk: a family-based genetic association study. *Breast Cancer Res* 7 (1):R71-81.

Aiginger, P., H. Kolbe, J. Kuhbock, J. Spona, and G. Geyer. 1981. The endocrinology of testicular germinal cell tumors. *Acta Endocrinol (Copenh)* 97 (3):419-26.

Aihara, T., Y. Takatsuka, S. Ohsumi, K. Aogi, Y. Hozumi, S. Imoto, H. Mukai, H. Iwata, T. Watanabe, C. Shimizu, K. Nakagami, M. Tamura, T. Ito, N. Masuda, N. Ogino, K. Hisamatsu, S. Mitsuyama, H. Abe, S. Tanaka, T. Yamaguchi, and Y. Ohashi. 2010. Phase III randomized adjuvant study of tamoxifen alone versus sequential tamoxifen and anastrozole in Japanese postmenopausal women with hormone-responsive breast cancer: N-SAS BC03 study. *Breast Cancer Res Treat* 121 (2):379-87.

Amir, E., B. Seruga, S. Niraula, L. Carlsson, and A. Ocana. 2011. Toxicity of Adjuvant Endocrine Therapy in Postmenopausal Breast Cancer Patients: A Systematic Review and Meta-analysis. *J Natl Cancer Inst* 103 (17):1299-309.

Backstrom, T. 1995. Symptoms related to the menopause and sex steroid treatments. *Ciba Found Symp* 191:171-80; discussion 180-6.

Bailey, D. G., J. M. Arnold, C. Munoz, and J. D. Spence. 1993. Grapefruit juice--felodipine interaction: mechanism, predictability, and effect of naringin. *Clin Pharmacol Ther* 53 (6):637-42.

Bailey, D. G., G. K. Dresser, and J. R. Bend. 2003. Bergamottin, lime juice, and red wine as inhibitors of cytochrome P450 3A4 activity: comparison with grapefruit juice. *Clin Pharmacol Ther* 73 (6):529-37.

Bailey, D. G., J. Malcolm, O. Arnold, and J. D. Spence. 2004. Grapefruit juice-drug interactions. 1998. *Br J Clin Pharmacol* 58 (7):S831-40; discussion S841-3.

Bajetta, E., L. Ferrari, L. Celio, L. Mariani, R. Miceli, A. Di Leo, N. Zilembo, R. Buzzoni, I. Spagnoli, A. Martinetti, E. Bichisao, and E. Seregni. 1997. The aromatase inhibitor letrozole in advanced breast cancer: effects on serum insulin-like growth factor (IGF)-I and IGF-binding protein-3 levels. *J Steroid Biochem Mol Biol* 63 (4-6):261-7.

Baselt, R. C., and L. J. Casarett. 1972. Urinary excretion of methadone in man. *Clin Pharmacol Ther* 13 (1):64-70.

Bear, W. L., and R. W. Teel. 2000. Effects of citrus phytochemicals on liver and lung cytochrome P450 activity and on the in vitro metabolism of the tobacco-specific nitrosamine NNK. *Anticancer Res* 20 (5A):3323-9.

Belgorosky, A., G. Guercio, C. Pepe, N. Saraco, and M. A. Rivarola. 2009. Genetic and clinical spectrum of aromatase deficiency in infancy, childhood and adolescence. *Horm Res* 72 (6):321-30.

Benmebarek, M., C. Devaud, M. Gex-Fabry, K. Powell Golay, C. Brogli, P. Baumann, B. Gravier, and C. B. Eap. 2004. Effects of grapefruit juice on the pharmacokinetics of the enantiomers of methadone. *Clin Pharmacol Ther* 76 (1):55-63.

Berthou, F., Y. Dreano, C. Belloc, L. Kangas, J. C. Gautier, and P. Beaune. 1994. Involvement of cytochrome P450 3A enzyme family in the major metabolic pathways of toremifene in human liver microsomes. *Biochem Pharmacol* 47 (10):1883-95.

Borges, S., Z. Desta, L. Li, T. C. Skaar, B. A. Ward, A. Nguyen, Y. Jin, A. M. Storniolo, D. M. Nikoloff, L. Wu, G. Hillman, D. F. Hayes, V. Stearns, and D. A. Flockhart. 2006. Quantitative effect of CYP2D6 genotype and inhibitors on tamoxifen metabolism: implication for optimization of breast cancer treatment. *Clin Pharmacol Ther* 80 (1):61-74.

Bouvard, B., E. Hoppe, P. Soulie, M. Georgin-Mege, E. Jadaud, S. Abadie-Lacourtoisie, A. Petit Le Manac'h, A. Laffitte, R. Levasseur, M. Audran, D. Chappard, and E. Legrand. 2011. High prevalence of vertebral fractures in women with breast cancer starting aromatase inhibitor therapy. *Ann Oncol*.

Bulun, S. E. 2000. Aromatase deficiency and estrogen resistance: from molecular genetics to clinic. *Semin Reprod Med* 18 (1):31-9.

Bulun, S. E., L. S. Noble, K. Takayama, M. D. Michael, V. Agarwal, C. Fisher, Y. Zhao, M. M. Hinshelwood, Y. Ito, and E. R. Simpson. 1997. Endocrine disorders associated with inappropriately high aromatase expression. *J Steroid Biochem Mol Biol* 61 (3-6):133-9.

Bulun, S. E., S. Sebastian, K. Takayama, T. Suzuki, H. Sasano, and M. Shozu. 2003. The human CYP19 (aromatase P450) gene: update on physiologic roles and genomic organization of promoters. *J Steroid Biochem Mol Biol* 86 (3-5):219-24.

Bulun, S. E., and E. R. Simpson. 2008. Aromatase expression in women's cancers. *Adv Exp Med Biol* 630:112-32.

Burstein, H. J., A. A. Prestrud, J. Seidenfeld, H. Anderson, T. A. Buchholz, N. E. Davidson, K. E. Gelmon, S. H. Giordano, C. A. Hudis, J. Malin, E. P. Mamounas, D. Rowden, A. J. Solky, M. R. Sowers, V. Stearns, E. P. Winer, M. R. Somerfield, and J. J. Griggs. 2010. American Society of Clinical Oncology clinical practice guideline: update on adjuvant endocrine therapy for women with hormone receptor-positive breast cancer. *J Clin Oncol* 28 (23):3784-96.

Caccamese, S., S. Bianca, and D. Santo. 2007. Racemization at C-2 of naringin in sour oranges with increasing maturity determined by chiral high-performance liquid chromatography. *J Agric Food Chem* 55 (10):3816-22.

Caccamese, S., and R. Chillemi. 2010. Racemization at C-2 of naringin in pummelo (Citrus grandis) with increasing maturity determined by chiral high-performance liquid chromatography. *J Chromatogr A* 1217 (7):1089-93.

Caccamese, S., L. Manna, and G. Scivoli. 2003. Chiral HPLC separation and CD spectra of the C-2 diastereomers of naringin in grapefruit during maturation. *Chirality* 15 (8):661-7.

Carabaza, A., F. Cabre, A. M. Garcia, E. Rotllan, M. L. Garcia, and D. Mauleon. 1997. Stereoselective inhibition of rat brain cyclooxygenase by dexketoprofen. *Chirality* 9 (3):281-5.

Carruba, G. 2009. Aromatase in nontumoral and malignant human liver tissues and cells. *Ann N Y Acad Sci* 1155:187-93.

Chang, Y., W. B. Fang, S. N. Lin, and D. E. Moody. 2011. Stereo-selective metabolism of methadone by human liver microsomes and cDNA-expressed cytochrome P450s: a reconciliation. *Basic Clin Pharmacol Toxicol* 108 (1):55-62.

Chen, S. 1998. Aromatase and breast cancer. *Front Biosci* 3:d922-33.

Chen, S., S. R. Oh, S. Phung, G. Hur, J. J. Ye, S. L. Kwok, G. E. Shrode, M. Belury, L. S. Adams, and D. Williams. 2006. Anti-aromatase activity of phytochemicals in white button mushrooms (Agaricus bisporus). *Cancer Res* 66 (24):12026-34.

Cheshenko, K., F. Pakdel, H. Segner, O. Kah, and R. I. Eggen. 2008. Interference of endocrine disrupting chemicals with aromatase CYP19 expression or activity, and consequences for reproduction of teleost fish. *Gen Comp Endocrinol* 155 (1):31-62.

Chlebowski, R. T., D. E. Collyar, M. R. Somerfield, and D. G. Pfister. 1999. American Society of Clinical Oncology technology assessment on breast cancer risk reduction strategies: tamoxifen and raloxifene. *J Clin Oncol* 17 (6):1939-55.

Ciolino, H. P., Z. Dai, and V. Nair. 2011. Retinol inhibits aromatase activity and expression in vitro. *J Nutr Biochem* 22 (6):522-6.

Ciolino, H. P., T. T. Wang, and N. Sathyamoorthy. 2000. Inhibition of aromatase activity and expression in MCF-7 cells by the chemopreventive retinoid N-(4-hydroxy-phenyl)-retinamide. *Br J Cancer* 83 (3):333-7.

Crettol, S., J. J. Deglon, J. Besson, M. Croquette-Krokkar, I. Gothuey, R. Hammig, M. Monnat, H. Huttemann, P. Baumann, and C. B. Eap. 2005. Methadone enantiomer plasma levels, CYP2B6, CYP2C19, and CYP2C9 genotypes, and response to treatment. *Clin Pharmacol Ther* 78 (6):593-604.

Crew, K. D., H. Greenlee, J. Capodice, G. Raptis, L. Brafman, D. Fuentes, A. Sierra, and D. L. Hershman. 2007. Prevalence of joint symptoms in postmenopausal women taking aromatase inhibitors for early-stage breast cancer. *J Clin Oncol* 25 (25):3877-83.

Crossley, R. 1992. The relevance of chirality to the study of biological activity. *Tetrahedron* 48:8155-8178.

Cuzick, J., I. Sestak, M. Baum, A. Buzdar, A. Howell, M. Dowsett, and J. F. Forbes. 2010. Effect of anastrozole and tamoxifen as adjuvant treatment for early-stage breast cancer: 10-year analysis of the ATAC trial. *Lancet Oncol* 11 (12):1135-1141.

Czajka-Oraniec, I., and E. R. Simpson. 2010. Aromatase research and its clinical significance. *Endokrynol Pol* 61 (1):126-34.

da Rocha, A. B., D. R. Mans, E. A. Bernard, C. Ruschel, A. F. Logullo, L. A. Wetmore, A. Leyva, and G. Schwartsmann. 1999. Tamoxifen inhibits particulate-associated protein kinase C activity, and sensitises cultured human glioblastoma cells not to etoposide but to gamma-radiation and BCNU. *Eur J Cancer* 35 (5):833-9.

Deapen, D., L. Liu, C. Perkins, L. Bernstein, and R. K. Ross. 2002. Rapidly rising breast cancer incidence rates among Asian-American women. *Int J Cancer* 99 (5):747-50.

Deshmukh, S. V., T. N. Nanovskaya, and M. S. Ahmed. 2003. Aromatase is the major enzyme metabolizing buprenorphine in human placenta. *J Pharmacol Exp Ther* 306 (3):1099-105.

Desta, Z., B. A. Ward, N. V. Soukhova, and D. A. Flockhart. 2004. Comprehensive evaluation of tamoxifen sequential biotransformation by the human cytochrome P450 system in vitro: prominent roles for CYP3A and CYP2D6. *J Pharmacol Exp Ther* 310 (3):1062-75.

Dilmaghanian, S., J. G. Gerber, S. G. Filler, A. Sanchez, and J. Gal. 2004. Enantioselectivity of inhibition of cytochrome P450 3A4 (CYP3A4) by ketoconazole: Testosterone and methadone as substrates. *Chirality* 16 (2):79-85.

Doering, I. L., and E. Richter. 2009. Inhibition of human aromatase by myosmine. *Drug Metab Lett* 3 (2):83-6.

Dresser, G. K., and D. G. Bailey. 2003. The effects of fruit juices on drug disposition: a new model for drug interactions. *Eur J Clin Invest* 33 Suppl 2:10-6.

Du, G., L. Jin, X. Han, Z. Song, H. Zhang, and W. Liang. 2009. Naringenin: a potential immunomodulator for inhibiting lung fibrosis and metastasis. *Cancer Res* 69 (7):3205-12.

Eap, C. B., T. Buclin, and P. Baumann. 2002. Interindividual variability of the clinical pharmacokinetics of methadone: implications for the treatment of opioid dependence. *Clin Pharmacokinet* 41 (14):1153-93.

Eap, C. B., E. Lessard, P. Baumann, M. Brawand-Amey, M. A. Yessine, G. O'Hara, and J. Turgeon. 2003. Role of CYP2D6 in the stereoselective disposition of venlafaxine in humans. *Pharmacogenetics* 13 (1):39-47.

Early Breast Cancer Trialists' Collaborative Group, EBCTCG 2005. Effects of chemotherapy and hormonal therapy for early breast cancer on recurrence and 15-year survival: an overview of the randomised trials. *Lancet* 365 (9472):1687-717.

Eng, E. T., J. Ye, D. Williams, S. Phung, R. E. Moore, M. K. Young, U. Gruntmanis, G. Braunstein, and S. Chen. 2003. Suppression of estrogen biosynthesis by procyanidin dimers in red wine and grape seeds. *Cancer Res* 63 (23):8516-22.

Erlund, I., E. Meririnne, G. Alfthan, and A. Aro. 2001. Plasma kinetics and urinary excretion of the flavanones naringenin and hesperetin in humans after ingestion of orange juice and grapefruit juice. *J Nutr* 131 (2):235-41.

Ferlay, J., H. R. Shin, F. Bray, D. Forman, C. Mathers, and D. M. Parkin. 2010. Estimates of worldwide burden of cancer in 2008: GLOBOCAN 2008. *Int J Cancer* 127 (12):2893-917.

Fisher, B., J. P. Costantino, D. L. Wickerham, R. S. Cecchini, W. M. Cronin, A. Robidoux, T. B. Bevers, M. T. Kavanah, J. N. Atkins, R. G. Margolese, C. D. Runowicz, J. M. James, L. G. Ford, and N. Wolmark. 2005. Tamoxifen for the prevention of breast cancer: current status of the National Surgical Adjuvant Breast and Bowel Project P-1 study. *J Natl Cancer Inst* 97 (22):1652-62.

Flockhart, D. A., and W. J. Lu. 2010. Inhibition of methadone metabolism by the aromatase (CYP19) inhibitor, letrozole. *Clinical protocol approved by the Indiana University IRB.*

Flockhart, D. A., T. Skaar, D. S. Berlin, T. E. Klein, and A. T. Nguyen. 2009. Clinically available pharmacogenomics tests. *Clin Pharmacol Ther* 86 (1):109-13.

Foster, D. J., A. A. Somogyi, and F. Bochner. 1999. Methadone N-demethylation in human liver microsomes: lack of stereoselectivity and involvement of CYP3A4. *Br J Clin Pharmacol* 47 (4):403-12.

Fredheim, O. M., K. Moksnes, P. C. Borchgrevink, S. Kaasa, and O. Dale. 2008. Clinical pharmacology of methadone for pain. *Acta Anaesthesiol Scand* 52 (7):879-89.

Fuhr, U. 1998. Drug interactions with grapefruit juice. Extent, probable mechanism and clinical relevance. *Drug Saf* 18 (4):251-72.

Furr, B. J., and V. C. Jordan. 1984. The pharmacology and clinical uses of tamoxifen. *Pharmacol Ther* 25 (2):127-205.

Gennari, L., L. Masi, D. Merlotti, L. Picariello, A. Falchetti, A. Tanini, C. Mavilia, F. Del Monte, S. Gonnelli, B. Lucani, C. Gennari, and M. L. Brandi. 2004. A polymorphic CYP19 TTTA repeat influences aromatase activity and estrogen levels in elderly men: effects on bone metabolism. *J Clin Endocrinol Metab* 89 (6):2803-10.

Ghosh, D., J. Griswold, M. Erman, and W. Pangborn. 2010. X-ray structure of human aromatase reveals an androgen-specific active site. *J Steroid Biochem Mol Biol* 118 (4-5):197-202.

Goetz, M. P., J. M. Rae, V. J. Suman, S. L. Safgren, M. M. Ames, D. W. Visscher, C. Reynolds, F. J. Couch, W. L. Lingle, D. A. Flockhart, Z. Desta, E. A. Perez, and J. N. Ingle. 2005. Pharmacogenetics of tamoxifen biotransformation is associated with clinical outcomes of efficacy and hot flashes. *J Clin Oncol* 23 (36):9312-8.

Gonzalez, Frank J., and Robert H. Tukey. 2006. Drug Metabolism. In *Goodman & Gilman's The Pharmacological Basis of Therapeutics* edited by L. L. Brunton: McGraw-Hill. 75-77.

Goss, P. E., J. N. Ingle, J. E. Ales-Martinez, A. M. Cheung, R. T. Chlebowski, J. Wactawski-Wende, A. McTiernan, J. Robbins, K. C. Johnson, L. W. Martin, E. Winquist, G. E. Sarto, J. E. Garber, C. J. Fabian, P. Pujol, E. Maunsell, P. Farmer, K. A. Gelmon, D. Tu, and H. Richardson. 2011. Exemestane for breast-cancer prevention in postmenopausal women. *N Engl J Med* 364 (25):2381-91.

Grow, D. R. 2002. Metabolism of endogenous and exogenous reproductive hormones. *Obstet Gynecol Clin North Am* 29 (3):425-36.

Guengerich, F. P., and D. H. Kim. 1990. In vitro inhibition of dihydropyridine oxidation and aflatoxin B1 activation in human liver microsomes by naringenin and other flavonoids. *Carcinogenesis* 11 (12):2275-9.

Hallinan, R., A. Byrne, K. Agho, C. G. McMahon, P. Tynan, and J. Attia. 2009. Hypogonadism in men receiving methadone and buprenorphine maintenance treatment. *Int J Androl* 32 (2):131-9.

Hamman, M. A., G. A. Thompson, and S. D. Hall. 1997. Regioselective and stereoselective metabolism of ibuprofen by human cytochrome P450 2C. *Biochem Pharmacol* 54 (1):33-41.

Hammond, M. E., D. F. Hayes, A. C. Wolff, P. B. Mangu, and S. Temin. 2010. American society of clinical oncology/college of american pathologists guideline recommendations for immunohistochemical testing of estrogen and progesterone receptors in breast cancer. *J Oncol Pract* 6 (4):195-7.

Hammoud, A. O., J. Griffin, A. W. Meikle, M. Gibson, C. M. Peterson, and D. T. Carrell. 2010. Association of aromatase (TTTAn) repeat polymorphism length and the relationship between obesity and decreased sperm concentration. *Hum Reprod* 25 (12):3146-51.

Hao, C. F., N. Zhang, Q. Qu, X. Wang, H. F. Gu, and Z. J. Chen. 2010. Evaluation of the association between the CYP19 Tetranucleotide (TTTA)n polymorphism and polycystic ovarian syndrome(PCOS) in Han Chinese women. *Neuro Endocrinol Lett* 31 (3):370-4.

Henry, N. L., J. T. Giles, D. Ang, M. Mohan, D. Dadabhoy, J. Robarge, J. Hayden, S. Lemler, K. Shahverdi, P. Powers, L. Li, D. Flockhart, V. Stearns, D. F. Hayes, A. M. Storniolo, and D. J. Clauw. 2008. Prospective characterization of musculoskeletal symptoms in early stage breast cancer patients treated with aromatase inhibitors. *Breast Cancer Res Treat* 111 (2):365-72.

Henry, N. L., J. T. Giles, and V. Stearns. 2008. Aromatase inhibitor-associated musculoskeletal symptoms: etiology and strategies for management. *Oncology (Williston Park)* 22 (12):1401-8.

Henry, N. L., J. A. Jacobson, M. Banerjee, J. Hayden, J. B. Smerage, C. Van Poznak, A. M. Storniolo, V. Stearns, and D. F. Hayes. 2010. A prospective study of aromatase inhibitor-associated musculoskeletal symptoms and abnormalities on serial high-resolution wrist ultrasonography. *Cancer* 116 (18):4360-7.

Henry, N. L., J. M. Rae, L. Li, F. Azzouz, T. C. Skaar, Z. Desta, M. J. Sikora, S. Philips, A. T. Nguyen, A. M. Storniolo, D. F. Hayes, D. A. Flockhart, and V. Stearns. 2009. Association between CYP2D6 genotype and tamoxifen-induced hot flashes in a prospective cohort. *Breast Cancer Res Treat* 117 (3):571-5.

Hershman, D. L., L. H. Kushi, T. Shao, D. Buono, A. Kershenbaum, W. Y. Tsai, L. Fehrenbacher, S. Lin Gomez, S. Miles, and A. I. Neugut. 2010. Early discontinuation and nonadherence to adjuvant hormonal therapy in a cohort of 8,769 early-stage breast cancer patients. *J Clin Oncol* 28 (27):4120-8.

Hieronymus, T. L., T. N. Nanovskaya, S. V. Deshmukh, R. Vargas, G. D. Hankins, and M. S. Ahmed. 2006. Methadone metabolism by early gestational age placentas. *Am J Perinatol* 23 (5):287-94.

Higgins, M. J., J. M. Rae, D. A. Flockhart, D. F. Hayes, and V. Stearns. 2009. Pharmacogenetics of tamoxifen: who should undergo CYP2D6 genetic testing? *J Natl Compr Canc Netw* 7 (2):203-13.

Higgins, M. J., and V. Stearns. 2010. CYP2D6 polymorphisms and tamoxifen metabolism: clinical relevance. *Curr Oncol Rep* 12 (1):7-15.

Ho, P. C., D. J. Saville, and S. Wanwimolruk. 2001. Inhibition of human CYP3A4 activity by grapefruit flavonoids, furanocoumarins and related compounds. *J Pharm Pharm Sci* 4 (3):217-27.

Hollenberg, P. F., U. M. Kent, and N. N. Bumpus. 2008. Mechanism-based inactivation of human cytochromes p450s: experimental characterization, reactive intermediates, and clinical implications. *Chem Res Toxicol* 21 (1):189-205.

Howell, A., J. Cuzick, M. Baum, A. Buzdar, M. Dowsett, J. F. Forbes, G. Hoctin-Boes, J. Houghton, G. Y. Locker, and J. S. Tobias. 2005. Results of the ATAC (Arimidex, Tamoxifen, Alone or in Combination) trial after completion of 5 years' adjuvant treatment for breast cancer. *Lancet* 365 (9453):60-2.

Howell, A., and M. Dowsett. 1997. Recent advances in endocrine therapy of breast cancer. *BMJ* 315 (7112):863-6.

Hung, C. C., M. H. Chiou, B. H. Huang, Y. W. Hsieh, T. J. Hsieh, C. L. Huang, and H. Y. Lane. 2011. Impact of genetic polymorphisms in ABCB1, CYP2B6, OPRM1, ANKK1 and DRD2 genes on methadone therapy in Han Chinese patients. *Pharmacogenomics*.

Hutt, AJ 2006. Drug chirality and its pharmacological consequences. In *Introduction to the Principles of Drug Design and Action*, edited by H. Smith. Boca Raton FL: CRC Press.

Ingle, J. N., D. J. Schaid, P. E. Goss, M. Liu, T. Mushiroda, J. A. Chapman, M. Kubo, G. D. Jenkins, A. Batzler, L. Shepherd, J. Pater, L. Wang, M. J. Ellis, V. Stearns, D. C. Rohrer, M. P. Goetz, K. I. Pritchard, D. A. Flockhart, Y. Nakamura, and R. M. Weinshilboum. 2010. Genome-wide associations and functional genomic studies of musculoskeletal adverse events in women receiving aromatase inhibitors. *J Clin Oncol* 28 (31):4674-82.

Inturrisi, C. E., W. A. Colburn, R. F. Kaiko, R. W. Houde, and K. M. Foley. 1987. Pharmacokinetics and pharmacodynamics of methadone in patients with chronic pain. *Clin Pharmacol Ther* 41 (4):392-401.

Iribarne, C., Y. Dreano, L. G. Bardou, J. F. Menez, and F. Berthou. 1997. Interaction of methadone with substrates of human hepatic cytochrome P450 3A4. *Toxicology* 117 (1):13-23.

Jeong, S., M. M. Woo, D. A. Flockhart, and Z. Desta. 2009. Inhibition of drug metabolizing cytochrome P450s by the aromatase inhibitor drug letrozole and its major oxidative metabolite 4,4'-methanol-bisbenzonitrile in vitro. *Cancer Chemother Pharmacol* 64 (5):867-75.

Jin, Y., Z. Desta, V. Stearns, B. Ward, H. Ho, K. H. Lee, T. Skaar, A. M. Storniolo, L. Li, A. Araba, R. Blanchard, A. Nguyen, L. Ullmer, J. Hayden, S. Lemler, R. M. Weinshilboum, J. M. Rae, D. F. Hayes, and D. A. Flockhart. 2005. CYP2D6 genotype, antidepressant use, and tamoxifen metabolism during adjuvant breast cancer treatment. *J Natl Cancer Inst* 97 (1):30-9.

Johnson, M. D., H. Zuo, K. H. Lee, J. P. Trebley, J. M. Rae, R. V. Weatherman, Z. Desta, D. A. Flockhart, and T. C. Skaar. 2004. Pharmacological characterization of 4-hydroxy-N-desmethyl tamoxifen, a novel active metabolite of tamoxifen. *Breast Cancer Res Treat* 85 (2):151-9.

Jones, D. R., J. C. Gorski, M. A. Hamman, B. S. Mayhew, S. Rider, and S. D. Hall. 1999. Diltiazem inhibition of cytochrome P-450 3A activity is due to metabolite intermediate complex formation. *J Pharmacol Exp Ther* 290 (3):1116-25.

Jongen, V. H., H. Hollema, A. G. Van Der Zee, and M. J. Heineman. 2006. Aromatase in the context of breast and endometrial cancer. A review. *Minerva Endocrinol* 31 (1):47-60.

Jordan, V. C. 1982. Metabolites of tamoxifen in animals and man: identification, pharmacology, and significance. *Breast Cancer Res Treat* 2 (2):123-38.

Jordan, V. C. 2007. New insights into the metabolism of tamoxifen and its role in the treatment and prevention of breast cancer. *Steroids* 72 (13):829-42.

Kalgutkar, A. S., R. S. Obach, and T. S. Maurer. 2007. Mechanism-based inactivation of cytochrome P450 enzymes: chemical mechanisms, structure-activity relationships and relationship to clinical drug-drug interactions and idiosyncratic adverse drug reactions. *Curr Drug Metab* 8 (5):407-47.

Kamden, KL, Y Kreutz, L Li, and Z Desta. 2011. CYP2A6 genetic variants, body mass index and age are associated with letrozole plasma concentrations in postmenopausal women with breast cancer. *Clinical Pharmacology & Therapeutics*.

Katzenellenbogen, B. S., I. Choi, R. Delage-Mourroux, T. R. Ediger, P. G. Martini, M. Montano, J. Sun, K. Weis, and J. A. Katzenellenbogen. 2000. Molecular mechanisms of estrogen action: selective ligands and receptor pharmacology. *J Steroid Biochem Mol Biol* 74 (5):279-85.

Kharasch, E. D., P. S. Bedynek, S. Park, D. Whittington, A. Walker, and C. Hoffer. 2008. Mechanism of ritonavir changes in methadone pharmacokinetics and pharmacodynamics: I. Evidence against CYP3A mediation of methadone clearance. *Clin Pharmacol Ther* 84 (4):497-505.

Kharasch, E. D., C. Hoffer, D. Whittington, and P. Sheffels. 2004. Role of hepatic and intestinal cytochrome P450 3A and 2B6 in the metabolism, disposition, and miotic effects of methadone. *Clin Pharmacol Ther* 76 (3):250-69.

Kharasch, E. D., C. Hoffer, D. Whittington, A. Walker, and P. S. Bedynek. 2009. Methadone pharmacokinetics are independent of cytochrome P4503A (CYP3A) activity and gastrointestinal drug transport: insights from methadone interactions with ritonavir/indinavir. *Anesthesiology* 110 (3):660-72.

Kim, T. W., D. P. Alford, A. Malabanan, M. F. Holick, and J. H. Samet. 2006. Low bone density in patients receiving methadone maintenance treatment. *Drug Alcohol Depend* 85 (3):258-62.

Kisanga, E. R., J. Gjerde, A. Guerrieri-Gonzaga, F. Pigatto, A. Pesci-Feltri, C. Robertson, D. Serrano, G. Pelosi, A. Decensi, and E. A. Lien. 2004. Tamoxifen and metabolite concentrations in serum and breast cancer tissue during three dose regimens in a randomized preoperative trial. *Clin Cancer Res* 10 (7):2336-43.

Kleber, H. D. 2008. Methadone maintenance 4 decades later: thousands of lives saved but still controversial. *JAMA* 300 (19):2303-5.

Krantz, M. J., I. B. Kutinsky, A. D. Robertson, and P. S. Mehler. 2003. Dose-related effects of methadone on QT prolongation in a series of patients with torsade de pointes. *Pharmacotherapy* 23 (6):802-5.

Kremer, J. M., J. Wilting, and L. H. Janssen. 1988. Drug binding to human alpha-1-acid glycoprotein in health and disease. *Pharmacol Rev* 40 (1):1-47.

Kreutz, R. P., E. J. Stanek, R. Aubert, J. Yao, J. A. Breall, Z. Desta, T. C. Skaar, J. R. Teagarden, F. W. Frueh, R. S. Epstein, and D. A. Flockhart. 2010. Impact of proton pump inhibitors on the effectiveness of clopidogrel after coronary stent placement: the clopidogrel Medco outcomes study. *Pharmacotherapy* 30 (8):787-96.

Krishnan, A. V., and D. Feldman. 2011. Mechanisms of the anti-cancer and anti-inflammatory actions of vitamin D. *Annu Rev Pharmacol Toxicol* 51:311-36.

Kristensen, V. N., N. Harada, N. Yoshimura, E. Haraldsen, P. E. Lonning, B. Erikstein, R. Karesen, T. Kristensen, and A. L. Borresen-Dale. 2000. Genetic variants of CYP19 (aromatase) and breast cancer risk. *Oncogene* 19 (10):1329-33.

Labrie, F., A. Belanger, L. Cusan, J. L. Gomez, and B. Candas. 1997. Marked decline in serum concentrations of adrenal C19 sex steroid precursors and conjugated androgen metabolites during aging. *J Clin Endocrinol Metab* 82 (8):2396-402.

Land, S. R., D. L. Wickerham, J. P. Costantino, M. W. Ritter, V. G. Vogel, M. Lee, E. R. Pajon, J. L. Wade, 3rd, S. Dakhil, J. B. Lockhart, Jr., N. Wolmark, and P. A. Ganz. 2006. Patient-reported symptoms and quality of life during treatment with tamoxifen or raloxifene for breast cancer prevention: the NSABP Study of Tamoxifen and Raloxifene (STAR) P-2 trial. *JAMA* 295 (23):2742-51.

Leder, B. Z., J. L. Rohrer, S. D. Rubin, J. Gallo, and C. Longcope. 2004. Effects of aromatase inhibition in elderly men with low or borderline-low serum testosterone levels. *J Clin Endocrinol Metab* 89 (3):1174-80.

Lee, M., D. I. Min, Y. M. Ku, and M. Flanigan. 2001. Effect of grapefruit juice on pharmacokinetics of microemulsion cyclosporine in African American subjects compared with Caucasian subjects: does ethnic difference matter? *J Clin Pharmacol* 41 (3):317-23.

Levine, B., S. C. Wu, A. Dixon, and J. E. Smialek. 1995. Site dependence of postmortem blood methadone concentrations. *Am J Forensic Med Pathol* 16 (2):97-100.

Lien, E. A., E. Solheim, O. A. Lea, S. Lundgren, S. Kvinnsland, and P. M. Ueland. 1989. Distribution of 4-hydroxy-N-desmethyltamoxifen and other tamoxifen metabolites in human biological fluids during tamoxifen treatment. *Cancer Res* 49 (8):2175-83.

Lien, E. A., E. Solheim, and P. M. Ueland. 1991. Distribution of tamoxifen and its metabolites in rat and human tissues during steady-state treatment. *Cancer Res* 51 (18):4837-44.

Lien, E. A., K. Wester, P. E. Lonning, E. Solheim, and P. M. Ueland. 1991. Distribution of tamoxifen and metabolites into brain tissue and brain metastases in breast cancer patients. *Br J Cancer* 63 (4):641-5.

Lim, Y. C., Z. Desta, D. A. Flockhart, and T. C. Skaar. 2005. Endoxifen (4-hydroxy-N-desmethyl-tamoxifen) has anti-estrogenic effects in breast cancer cells with potency similar to 4-hydroxy-tamoxifen. *Cancer Chemother Pharmacol* 55 (5):471-8.

Liu, K. H., M. J. Kim, J. H. Shon, Y. S. Moon, S. Y. Seol, W. Kang, I. J. Cha, and J. G. Shin. 2005. Stereoselective inhibition of cytochrome P450 forms by lansoprazole and omeprazole in vitro. *Xenobiotica* 35 (1):27-38.

Liu, Z. Q., Y. Shu, S. L. Huang, L. S. Wang, N. He, and H. H. Zhou. 2001. Effects of CYP2C19 genotype and CYP2C9 on fluoxetine N-demethylation in human liver microsomes. *Acta Pharmacol Sin* 22 (1):85-90.

Lo, R., L. Burgoon, L. Macpherson, S. Ahmed, and J. Matthews. 2010. Estrogen receptor-dependent regulation of CYP2B6 in human breast cancer cells. *Biochim Biophys Acta* 1799 (5-6):469-79.

Lonning, P. E., D. C. Johannessen, E. A. Lien, D. Ekse, T. Fotsis, and H. Adlercreutz. 1995. Influence of tamoxifen on sex hormones, gonadotrophins and sex hormone binding globulin in postmenopausal breast cancer patients. *J Steroid Biochem Mol Biol* 52 (5):491-6.

Love, R. R., B. D. Nguyen, C. B. Nguyen, V. D. Nguyen, and T. C. Havighurst. 1999. Symptoms associated with oophorectomy and tamoxifen treatment for breast cancer in premenopausal Vietnamese women. *Breast Cancer Res Treat* 58 (3):281-6.

Lu, W. J. , W. Zhou, Y. Kreutz, and D. A. Flockhart. 2011. Methadone adverse reaction presenting with large increase in plasma methadone binding: a case series. *Journal of Medical Case Report* 5:513.

Lu, W. J., R. Bies, L. K. Kamden, Z. Desta, and D. A. Flockhart. 2010. Methadone: a substrate and mechanism-based inhibitor of CYP19 (aromatase). *Drug Metab Dispos* 38 (8):1308-13.

Lu, W. J., Z. Desta, and D. A. Flockhart. 2011. Tamoxifen metabolites as active inhibitors of aromatase in the treatment of breast cancer. *Breast Cancer Res Treat*.

Lu, W. J., V. Ferlito, C. Xu, D. A. Flockhart, and S. Caccamese. 2011. Enantiomers of naringenin as pleiotropic, stereoselective inhibitors of cytochrome P450 isoforms. *Chirality*.

Lu, W. J., N. Thong, and D. A. Flockhart. 2011. Reduced methadone clearance during aromatase inhibition. (submitted for publication).

Lu, W. J., C. Xu, Z. Pei, A. S. Mayhoub, M. Cushman, and D. A. Flockhart. 2011. The tamoxifen metabolite norendoxifen is a potent and selective inhibitor of aromatase (CYP19) and a potential lead compound for novel therapeutic agents. *Breast Cancer Res Treat*.

Ma, C. X., A. A. Adjei, O. E. Salavaggione, J. Coronel, L. Pelleymounter, L. Wang, B. W. Eckloff, D. Schaid, E. D. Wieben, and R. M. Weinshilboum. 2005. Human aromatase: gene resequencing and functional genomics. *Cancer Res* 65 (23):11071-82.

Ma, X., X. Qi, C. Chen, H. Lin, H. Xiong, Y. Li, and J. Jiang. 2010. Association between CYP19 polymorphisms and breast cancer risk: results from 10,592 cases and 11,720 controls. *Breast Cancer Res Treat* 122 (2):495-501.

Manthey, J. A., K. Grohmann, and N. Guthrie. 2001. Biological properties of citrus flavonoids pertaining to cancer and inflammation. *Curr Med Chem* 8 (2):135-53.

Mao, J. J., H. I. Su, R. Feng, M. L. Donelson, R. Aplenc, T. R. Rebbeck, F. Stanczyk, and A. Demichele. 2011. Association of functional polymorphisms in CYP19A1 with aromatase inhibitor associated arthralgia in breast cancer survivors. *Breast Cancer Res* 13 (1):R8.

Marsh, E. E., N. D. Shaw, K. M. Klingman, T. O. Tiamfook-Morgan, M. A. Yialamas, P. M. Sluss, and J. E. Hall. 2011. Estrogen Levels Are Higher across the Menstrual Cycle in African-American Women Compared with Caucasian Women. *J Clin Endocrinol Metab*.

Masi, L., L. Becherini, L. Gennari, A. Amedei, E. Colli, A. Falchetti, M. Farci, S. Silvestri, S. Gonnelli, and M. L. Brandi. 2001. Polymorphism of the aromatase gene in postmenopausal Italian women: distribution and correlation with bone mass and fracture risk. *J Clin Endocrinol Metab* 86 (5):2263-9.

McCowan, C., J. Shearer, P. T. Donnan, J. A. Dewar, M. Crilly, A. M. Thompson, and T. P. Fahey. 2008. Cohort study examining tamoxifen adherence and its relationship to mortality in women with breast cancer. *Br J Cancer* 99 (11):1763-8.

Miners, J. O., S. Coulter, R. H. Tukey, M. E. Veronese, and D. J. Birkett. 1996. Cytochromes P450, 1A2, and 2C9 are responsible for the human hepatic O-demethylation of R- and S-naproxen. *Biochem Pharmacol* 51 (8):1003-8.

Miyoshi, Y., and S. Noguchi. 2003. Polymorphisms of estrogen synthesizing and metabolizing genes and breast cancer risk in Japanese women. *Biomed Pharmacother* 57 (10):471-81.

Mnif, W., J. M. Pascussi, A. Pillon, A. Escande, A. Bartegi, J. C. Nicolas, V. Cavailles, M. J. Duchesne, and P. Balaguer. 2007. Estrogens and antiestrogens activate hPXR. *Toxicol Lett* 170 (1):19-29.

Morales, L., P. Neven, D. Timmerman, M. R. Christiaens, I. Vergote, E. Van Limbergen, A. Carbonez, S. Van Huffel, L. Ameye, and R. Paridaens. 2004. Acute effects of tamoxifen and third-generation aromatase inhibitors on menopausal symptoms of breast cancer patients. *Anticancer Drugs* 15 (8):753-60.

Mortimer, J. E., S. W. Flatt, B. A. Parker, E. B. Gold, L. Wasserman, L. Natarajan, and J. P. Pierce. 2008. Tamoxifen, hot flashes and recurrence in breast cancer. *Breast Cancer Res Treat* 108 (3):421-6.

Morton, E. B. 2007. Methadone pharmacology. *Ph.D. thesis, University of Adelaide, Adelaide, South Australia.*

Muftuoglu, Y., and G. Mustata. 2010. Pharmacophore modeling strategies for the development of novel nonsteroidal inhibitors of human aromatase (CYP19). *Bioorg Med Chem Lett* 20 (10):3050-64.

Muralidharan, G., E. M. Hawes, G. McKay, E. D. Korchinski, and K. K. Midha. 1991. Quinidine but not quinine inhibits in man the oxidative metabolic routes of methoxyphenamine which involve debrisoquine 4-hydroxylase. *Eur J Clin Pharmacol* 41 (5):471-4.

Nanovskaya, T. N., S. V. Deshmukh, I. A. Nekhayeva, O. L. Zharikova, G. D. Hankins, and M. S. Ahmed. 2004. Methadone metabolism by human placenta. *Biochem Pharmacol* 68 (3):583-91.

Nelson, D. R., D. C. Zeldin, S. M. Hoffman, L. J. Maltais, H. M. Wain, and D. W. Nebert. 2004. Comparison of cytochrome P450 (CYP) genes from the mouse and human genomes, including nomenclature recommendations for genes, pseudogenes and alternative-splice variants. *Pharmacogenetics* 14 (1):1-18.

Nilsson, M. I., E. Widerlov, U. Meresaar, and E. Anggard. 1982. Effect of urinary pH on the disposition of methadone in man. *Eur J Clin Pharmacol* 22 (4):337-42.

Nowell, S. A., J. Ahn, J. M. Rae, J. O. Scheys, A. Trovato, C. Sweeney, S. L. MacLeod, F. F. Kadlubar, and C. B. Ambrosone. 2005. Association of genetic variation in tamoxifen-metabolizing enzymes with overall survival and recurrence of disease in breast cancer patients. *Breast Cancer Res Treat* 91 (3):249-58.

Oberguggenberger, A., M. Hubalek, M. Sztankay, V. Meraner, B. Beer, H. Oberacher, J. Giesinger, G. Kemmler, D. Egle, E. M. Gamper, B. Sperner-Unterweger, and B. Holzner. 2011. Is the toxicity of adjuvant aromatase inhibitor therapy underestimated? Complementary information from patient-reported outcomes (PROs). *Breast Cancer Res Treat*.

Ortiz de Montellano, P. R., B. A. Mico, J. M. Mathews, K. L. Kunze, G. T. Miwa, and A. Y. Lu. 1981. Selective inactivation of cytochrome P-450 isozymes by suicide substrates. *Arch Biochem Biophys* 210 (2):717-28.

Osawa, Y., T. Higashiyama, Y. Shimizu, and C. Yarborough. 1993. Multiple functions of aromatase and the active site structure; aromatase is the placental estrogen 2-hydroxylase. *J Steroid Biochem Mol Biol* 44 (4-6):469-80.

Osawa, Y., T. Higashiyama, Y. Toma, and C. Yarborough. 1997. Diverse function of aromatase and the N-terminal sequence deleted form. *J Steroid Biochem Mol Biol* 61 (3-6):117-26.

Osborne, C. K., H. Zhao, and S. A. Fuqua. 2000. Selective estrogen receptor modulators: structure, function, and clinical use. *J Clin Oncol* 18 (17):3172-86.

Paar, W. D., S. Poche, J. Gerloff, and H. J. Dengler. 1997. Polymorphic CYP2D6 mediates O-demethylation of the opioid analgesic tramadol. *Eur J Clin Pharmacol* 53 (3-4):235-9.

Partridge, A. H., A. LaFountain, E. Mayer, B. S. Taylor, E. Winer, and A. Asnis-Alibozek. 2008. Adherence to initial adjuvant anastrozole therapy among women with early-stage breast cancer. *J Clin Oncol* 26 (4):556-62.

Payne, E. J., E. Ingley, I. M. Dick, S. G. Wilson, C. S. Bond, and R. L. Prince. 2009. In vitro kinetic properties of the Thr201Met variant of human aromatase gene CYP19A1: functional responses to substrate and product inhibition and enzyme inhibitors. *J Clin Endocrinol Metab* 94 (8):2998-3002.

Pohland, A., H. E. Boaz, and H. R. Sullivan. 1971. Synthesis and identification of metabolites resulting from the biotransformation of DL-methadone in man and in the rat. *J Med Chem* 14 (3):194-7.

Pond, S. M., M. J. Kreek, T. G. Tong, J. Raghunath, and N. L. Benowitz. 1985. Altered methadone pharmacokinetics in methadone-maintained pregnant women. *J Pharmacol Exp Ther* 233 (1):1-6.

Pritts, E. A. 2010. Letrozole for ovulation induction and controlled ovarian hyperstimulation. *Curr Opin Obstet Gynecol* 22 (4):289-94.

Punetha, A., K. Shanmugam, and D. Sundar. 2011. Insight into the enzyme-inhibitor interactions of the first experimentally determined human aromatase. *J Biomol Struct Dyn* 28 (5):759-71.

Rettie, A. E., K. R. Korzekwa, K. L. Kunze, R. F. Lawrence, A. C. Eddy, T. Aoyama, H. V. Gelboin, F. J. Gonzalez, and W. F. Trager. 1992. Hydroxylation of warfarin by human cDNA-expressed cytochrome P-450: a role for P-4502C9 in the etiology of (S)-warfarin-drug interactions. *Chem Res Toxicol* 5 (1):54-9.

Rochira, V., and C. Carani. 2009. Aromatase deficiency in men: a clinical perspective. *Nat Rev Endocrinol* 5 (10):559-68.

Romach, M. K., K. M. Piafsky, J. G. Abel, V. Khouw, and E. M. Sellers. 1981. Methadone binding to orosomucoid (alpha 1-acid glycoprotein): determinant of free fraction in plasma. *Clin Pharmacol Ther* 29 (2):211-7.

Rowland, M., and T. N. Tozer. 1995. *Clinical pharmacokinetics: concepts and applications*. 3rd ed: Lippincott Williams & Wilkins.

Sanderson, J. T. 2006. The steroid hormone biosynthesis pathway as a target for endocrine-disrupting chemicals. *Toxicol Sci* 94 (1):3-21.

Sano, Y., K. Suzuki, K. Arai, S. Okinaga, and B. I. Tamaoki. 1981. Changes in enzyme activities related to steroidogenesis in human ovaries during the menstrual cycle. *J Clin Endocrinol Metab* 52 (5):994-1001.

Santen, R. J., H. Brodie, E. R. Simpson, P. K. Siiteri, and A. Brodie. 2009. History of aromatase: saga of an important biological mediator and therapeutic target. *Endocr Rev* 30 (4):343-75.

Saylam, B., O. Efesoy, and S. Cayan. 2011. The effect of aromatase inhibitor letrozole on body mass index, serum hormones, and sperm parameters in infertile men. *Fertil Steril* 95 (2):809-11.

Sebastian, S., and S. E. Bulun. 2001. A highly complex organization of the regulatory region of the human CYP19 (aromatase) gene revealed by the Human Genome Project. *J Clin Endocrinol Metab* 86 (10):4600-2.

Segel, I. H. 1993. *Enzyme kinetics*: Wiley.

Senay, E. C. 1985. Methadone maintenance treatment. *Int J Addict* 20 (6-7):803-21.

Serane, V. T., and O. Kurian. 2008. Neonatal abstinence syndrome. *Indian J Pediatr* 75 (9):911-4.

Shin, J. G., K. Kane, and D. A. Flockhart. 2001. Potent inhibition of CYP2D6 by haloperidol metabolites: stereoselective inhibition by reduced haloperidol. *Br J Clin Pharmacol* 51 (1):45-52.

Shiran, M. R., M. S. Lennard, M. Z. Iqbal, O. Lagundoye, N. Seivewright, G. T. Tucker, and A. Rostami-Hodjegan. 2009. Contribution of the activities of CYP3A, CYP2D6, CYP1A2 and other potential covariates to the disposition of methadone in patients undergoing methadone maintenance treatment. *Br J Clin Pharmacol* 67 (1):29-37.

Silverman, R. 1988. Mechanism based inactivation: chemistry and enzymology. *CRC Press, Boca Raton, FL*.

Simpson, E. R. 2003. Sources of estrogen and their importance. *J Steroid Biochem Mol Biol* 86 (3-5):225-30.

Simpson, E. R., C. Clyne, G. Rubin, W. C. Boon, K. Robertson, K. Britt, C. Speed, and M. Jones. 2002. Aromatase--a brief overview. *Annu Rev Physiol* 64:93-127.

Simpson, E. R., and S. R. Davis. 2001. Minireview: aromatase and the regulation of estrogen biosynthesis--some new perspectives. *Endocrinology* 142 (11):4589-94.

Sims, S. A., L. A. Snow, and C. A. Porucznik. 2007. Surveillance of methadone-related adverse drug events using multiple public health data sources. *J Biomed Inform* 40 (4):382-9.

Smith, I. E., and M. Dowsett. 2003. Aromatase inhibitors in breast cancer. *N Engl J Med* 348 (24):2431-42.

Somner, J., S. McLellan, J. Cheung, Y. T. Mak, M. L. Frost, K. M. Knapp, A. S. Wierzbicki, M. Wheeler, I. Fogelman, S. H. Ralston, and G. N. Hampson. 2004. Polymorphisms in the P450 c17 (17-hydroxylase/17,20-Lyase) and P450 c19 (aromatase) genes: association with serum sex steroid concentrations and bone mineral density in postmenopausal women. *J Clin Endocrinol Metab* 89 (1):344-51.

Stearns, V., M. D. Johnson, J. M. Rae, A. Morocho, A. Novielli, P. Bhargava, D. F. Hayes, Z. Desta, and D. A. Flockhart. 2003. Active tamoxifen metabolite plasma concentrations after coadministration of tamoxifen and the selective serotonin reuptake inhibitor paroxetine. *J Natl Cancer Inst* 95 (23):1758-64.

Stresser, David M. . 2004. High-throughput screening of human cytochrome P450 inhibitors using fluorometric substrates. In *Optimization in drug discovery: in vitro methods*, edited by Z. Yan and G. W. Caldwell.

Sullivan, H. R., and S. L. Due. 1973. Urinary metabolites of dl-methadone in maintenance subjects. *J Med Chem* 16 (8):909-13.

Sun, B., J. Hoshino, K. Jermihov, L. Marler, J. M. Pezzuto, A. D. Mesecar, and M. Cushman. 2010. Design, synthesis, and biological evaluation of resveratrol analogues as aromatase and quinone reductase 2 inhibitors for chemoprevention of cancer. *Bioorg Med Chem* 18 (14):5352-66.

Szeto, H. H., J. F. Clapp, 3rd, R. W. Larrow, J. Hewitt, C. E. Inturrisi, and L. I. Mann. 1981. Disposition of methadone in the ovine maternal-fetal unit. *Life Sci* 28 (19):2111-7.

Tahboub, R., and B. M. Arafah. 2009. Sex steroids and the thyroid. *Best Pract Res Clin Endocrinol Metab* 23 (6):769-80.

Taylor, W. C., and H. B. Muss. 2010. Recent advances: adjuvant therapy for older women with breast cancer. *Cancer J* 16 (4):289-93.

Thompson, A. M., A. Johnson, P. Quinlan, G. Hillman, M. Fontecha, S. E. Bray, C. A. Purdie, L. B. Jordan, R. Ferraldeschi, A. Latif, K. D. Hadfield, R. B. Clarke, L. Ashcroft, D. G. Evans, A. Howell, M. Nikoloff, J. Lawrence, and W. G. Newman. 2010. Comprehensive CYP2D6 genotype and adherence affect outcome in breast cancer patients treated with tamoxifen monotherapy. *Breast Cancer Res Treat*.

Thompson, P. W., and F. S. Pegley. 1991. A comparison of disability measured by the Stanford Health Assessment Questionnaire disability scales (HAQ) in male and female rheumatoid outpatients. *Br J Rheumatol* 30 (4):298-300.

Tian, F., H. Wu, Z. Li, N. Wang, J. Huang, C. Li, and F. Xie. 2009. Activated PKCalpha/ERK1/2 signaling inhibits tamoxifen-induced apoptosis in C6 cells. *Cancer Invest* 27 (7):802-8.

Toda, K., T. Okada, C. Miyaura, and T. Saibara. 2003. Fenofibrate, a ligand for PPARalpha, inhibits aromatase cytochrome P450 expression in the ovary of mouse. *J Lipid Res* 44 (2):265-70.

Toi, M., Y. Ohashi, A. Seow, T. Moriya, G. Tse, H. Sasano, B. W. Park, L. W. Chow, A. V. Laudico, C. H. Yip, E. Ueno, H. Ishiguro, and H. Bando. 2010. The Breast Cancer Working Group presentation was divided into three sections: the epidemiology, pathology and treatment of breast cancer. *Jpn J Clin Oncol* 40 Suppl 1:i13-18.

Totah, R. A., P. Sheffels, T. Roberts, D. Whittington, K. Thummel, and E. D. Kharasch. 2008. Role of CYP2B6 in stereoselective human methadone metabolism. *Anesthesiology* 108 (3):363-74.

Vaz, A. D. N. 2003. *Drug metabolizing enzymes: cytochrome P450 and other enzymes in drug discovery and development*: FontisMedia.

Verdonk, M. L., J. C. Cole, M. J. Hartshorn, C. W. Murray, and R. D. Taylor. 2003. Improved protein-ligand docking using GOLD. *Proteins* 52 (4):609-23.

Wang, H., R. Li, and Y. Hu. 2009. The alternative noncoding exons 1 of aromatase (Cyp19) gene modulate gene expression in a posttranscriptional manner. *Endocrinology* 150 (7):3301-7.

Wang, J. S., and C. L. DeVane. 2003. Involvement of CYP3A4, CYP2C8, and CYP2D6 in the metabolism of (R)- and (S)-methadone in vitro. *Drug Metab Dispos* 31 (6):742-7.

Wang, Q., H. Zhao, Q. Xiang, H. Ju, S. M. Han, L. Y. Wang, and B. Xu. 2009. Effect of Yikun Neiyi Wan on the expression of aromatase P450, COX-2, and ER related receptor in endometrial cells in vitro from patients with endometriosis. *J Tradit Chin Med* 29 (4):296-300.

Wang, S. C., I. K. Ho, H. H. Tsou, J. N. Tian, C. F. Hsiao, C. H. Chen, H. K. Tan, L. Lin, C. S. Wu, L. W. Su, C. L. Huang, Y. H. Yang, M. L. Liu, K. M. Lin, C. Y. Chen, S. C. Liu, H. Y. Wu, H. W. Chan, M. H. Tsai, P. S. Lin, and Y. L. Liu. 2011. CYP2B6 Polymorphisms Influence the Plasma Concentration and Clearance of the Methadone S-Enantiomer. *J Clin Psychopharmacol* 31 (4):463-469.

Wegman, P., S. Elingarami, J. Carstensen, O. Stal, B. Nordenskjold, and S. Wingren. 2007. Genetic variants of CYP3A5, CYP2D6, SULT1A1, UGT2B15 and tamoxifen response in postmenopausal patients with breast cancer. *Breast Cancer Res* 9 (1):R7.

Weschules, D. J., K. T. Bain, and S. Richeimer. 2008. Actual and potential drug interactions associated with methadone. *Pain Med* 9 (3):315-44.

Wilkinson, G. R. 2005. Drug metabolism and variability among patients in drug response. *N Engl J Med* 352 (21):2211-21.

Xita, N., A. Chatzikyriakidou, I. Stavrou, Ch Zois, I. Georgiou, and A. Tsatsoulis. 2010. The (TTTA)n polymorphism of aromatase (CYP19) gene is associated with age at menarche. *Hum Reprod* 25 (12):3129-33.

Yahiaoui, S., C. Pouget, J. Buxeraud, A. J. Chulia, and C. Fagnere. 2011. Lead optimization of 4-imidazolylflavans: new promising aromatase inhibitors. *Eur J Med Chem* 46 (6):2541-5.

Yanez, J. A., and N. M. Davies. 2005. Stereospecific high-performance liquid chromatographic analysis of naringenin in urine. *J Pharm Biomed Anal* 39 (1-2):164-9.

Young, J., S. E. Bulun, V. Agarwal, B. Couzinet, C. R. Mendelson, E. R. Simpson, and G. Schaison. 1996. Aromatase expression in a feminizing adrenocortical tumor. *J Clin Endocrinol Metab* 81 (9):3173-6.

Yousefi, M., W. Karmaus, L. M. Mudd, J. R. Landgraf, D. Mikucki, P. S. Haan, J. Zhang, and J. R. Osuch. 2011. Expression of CYP19 and CYP17 is associated with leg length, weight, and BMI. *Obesity (Silver Spring)* 19 (2):436-41.

Yue, Q. Y., C. Alm, J. O. Svensson, and J. Sawe. 1997. Quantification of the O- and N-demethylated and the glucuronidated metabolites of codeine relative to the debrisoquine metabolic ratio in urine in ultrarapid, rapid, and poor debrisoquine hydroxylators. *Ther Drug Monit* 19 (5):539-42.

Zharikova, O. L., S. V. Deshmukh, T. N. Nanovskaya, G. D. Hankins, and M. S. Ahmed. 2006. The effect of methadone and buprenorphine on human placental aromatase. *Biochem Pharmacol* 71 (8):1255-64.

Ziller, V., M. Kalder, U. S. Albert, W. Holzhauer, M. Ziller, U. Wagner, and P. Hadji. 2009. Adherence to adjuvant endocrine therapy in postmenopausal women with breast cancer. *Ann Oncol* 20 (3):431-6.

Zivian, M. T. , and B. Salgado. 2008. Side effects revisited: women's experiences with aromatase inhibitors. San Francisco, CA: A report from Breast Cancer Action.

CURRICULUM VITAE

Wenjie Lu

EDUCATION

2007 – 2012	Ph.D. Pharmacology Indiana University, USA
2003 – 2007	B.S. Biological Sciences Peking University, China

AWARDS AND HONORS

10/2011	Featured Young Investigator in Pharmaceutical Technology, USA
08/2011	Second Place Award in the 2011 Sigma Xi Graduate Biomedical Research Competition, Indiana University, USA
07/2011	Graduate Student Symposium Award in Pharmacokinetics, Pharmacodynamics, and Drug Metabolism and Clinical Pharmacology and Translational Research, American Association of Pharmaceutical Scientists (AAPS), USA
08/2007 – 07/2008	Indiana University Biomedical Gateway Fellowship, USA
05/2005 – 04/2006	Undergraduate Research Fellowship, President's Fund, Peking University, China
09/2004 – 07/2005	Outstanding Student Honor, Department of Life Science, Peking University, China
09/2003 – 07/2004	Outstanding Student Honor, Department of Chemistry and Molecular Engineering, Peking University, China
05/2002	National Biology Olympiad Prize, China

GRANT

11/1/10 – 10/31/12	Department of Defense, USA Breast Cancer Research Program Predoctoral Traineeship Award Principle Investigator: Wenjie Jessie Lu Title: "A New Role for Aromatase (CYP19) in Drug Disposition in Breast Cancer"

PUBLICATIONS

Original research articles:

1. **Wenjie Jessie Lu**, Cong Xu, Zifan Pei, Abdelrahman Salah Abbas Mayhoub, Mark Cushman, David A Flockhart. The tamoxifen metabolite norendoxifen is a potent and selective inhibitor of aromatase and a potential lead compound for novel therapeutic agents. Breast Cancer Research and Treatment, 2011. PMID: 21814747

2. **Wenjie Jessie Lu**, Valentina Ferlito, Cong Xu, David A Flockhart, Salvatore Caccamese. Enantiomers of naringenin as pleiotropic, stereoselective inhibitors of cytochrome P450 isoforms. Chirality, 2011. PMID: 21953762

3. **Wenjie Jessie Lu**, Zeruesenay Desta, David A Flockhart. Tamoxifen metabolites as active inhibitors of aromatase in the treatment of breast cancer. Breast Cancer Research and Treatment, 2011. PMID: 21390495

4. **Wenjie Jessie Lu**, Weidong Zhou, Yvonne Kreutz, David A Flockhart. Methadone adverse reaction presenting with large increase in plasma methadone binding: a case series. Journal of Medical Case Report, 2011, 5:513. PMID: 21985665

5. **Wenjie Jessie Lu**, Robert R Bies, Landry Kamden Kamden, Zeruesenay Desta, David A Flockhart. Methadone: a substrate and mechanism-based inhibitor of CYP19 (Aromatase). Drug Metabolism and Disposition, 2010 Aug; 38(8):1308-13. PMID: 20410453

6. **Wenjie Jessie Lu**, Nancy Thong, David A Flockhart. Reduced methadone clearance during aromatase inhibition. 2011 (submitted for publication)

Abstracts:

1. **Wenjie Jessie Lu**, Nancy Thong, David A Flockhart. "Reduced methadone clearance during aromatase inhibition". The 32nd Annual Meeting of the Japanese Society of Clinical Pharmacology and Therapeutics (JSCPT) and the JSCPT-KSCPT-ASCPT Joint Conference 2011, Hamamatsu, Japan, December 1, 2011. Abstract Nr 00008

2. **Wenjie Jessie Lu**, Claire Xu, Zifan Pei, David A Flockhart. "A structural basis for inhibition of aromatase by tamoxifen metabolites". The 2011 Annual Meeting and Exposition of the American Association of Pharmaceutical Scientists, Washington, DC, October 23-27, 2011

3. **Wenjie Jessie Lu**, David A Flockhart, Salvatore Caccamese: "Stereoisomers of naringenin as pleiotropic, selective inhibitors of cytochrome P450 isoforms". The 2011 Annual Meeting of the Canadian Society of Pharmacology and Therapeutics. Montreal, Canada, May 24-27, 2011. Journal of Population Therapeutics and Clinical Pharmacology, 2011 May; 18(2):e349

4. **Wenjie Jessie Lu**, Zeruesenay Desta, David A Flockhart: "Aromatase inhibition by active tamoxifen metabolites". In: Proceedings of the 102nd Annual Meeting of the American Association for Cancer Research. Orlando, FL, April 2-6, 2011. Abstract nr 4460

5. **Wenjie Jessie Lu**, Yvonne Kreutz, David A Flockhart.: "Case study of an adverse reaction to methadone during coadministration of letrozole". The 112th Annual Meeting of the American Society for Clinical Pharmacology and Therapeutics. Dallas, TX, March 2-5, 2011. Clinical Pharmacology & Therapeutics. 2011 Feb; 89 (S1) S26

6. **Wenjie Jessie Lu**, Landry Kamden Kamden, Zeruesenay Desta, David A Flockhart: "Methadone is a potent and mechanism-based inhibitor of metabolism by CYP19 (aromatase)". The 8th Joint Conference of the American Association for Cancer Research and the Japanese Cancer Association: Cancer Genomics, Epigenomics, and the Development of Novel Therapeutics, Waikoloa, HI, February 5-9, 2010. Poster Section D

IRB APPROVED CLINICAL PROTOCOL:

- David A Flockhart and **Wenjie Jessie Lu**. Inhibition of methadone metabolism by the aromatase (CYP19) inhibitor, letrozole. Protocol #1001-13, approved by the Indiana University IRB on February 15, 2010

PATENT:

- **Wenjie Jessie Lu** and David A Flockhart. Materials for inhibiting aromatase and method of using the same to diagnose, treat and monitor breast cancer. March 2011 (IURTC No. 11051, US patent application submitted)

ORAL PRESENTATIONS:

1. **Wenjie Jessie Lu**, Nancy Thong, David A Flockhart. "Reduced methadone clearance during aromatase inhibition". The 32nd Annual Meeting of the Japanese Society of Clinical Pharmacology and Therapeutics (JSCPT) and the JSCPT-KSCPT-ASCPT Joint Conference 2011, Hamamatsu, Japan, December 1, 2011

2. **Wenjie Jessie Lu**. "A structural basis for inhibition of aromatase by tamoxifen metabolites". Graduate Student Symposium in Pharmacokinetics, Pharmacodynamics, and Drug Metabolism and Clinical Pharmacology and Translational Research at the 2011 Annual Meeting and Exposition of the American Association of Pharmaceutical Scientists, Washington, DC, October 25, 2011

3. **Wenjie Jessie Lu**. "New roles of aromatase in xenobiotic metabolism and pharmacokinetic drug interactions". The 2011 Sigma Xi Biomedical Research Day, Indiana University, Indianapolis, IN, August 8, 2011

4. **Wenjie Jessie Lu**, David A Flockhart. "Studies on the mechanism of an adverse reaction to methadone during coadministration of letrozole". Host: Neal Benowitz MD. Division of Clinical Pharmacology, Department of Medicine, University of California, San Francisco, CA, September 30, 2010

SKILL SET

- Measurement of molecules in biological matrices using a range of analytical techniques; pharmacokinetic and pharmacodynamic data analysis
- Protein quantification and proteomic data analysis
- Genetic variant identification, selection and pharmacogenomic genotype-phenotype association analysis
- Basic techniques in studying cellular systems
- Techniques in the design, modeling and conduct of studies in rats and mice
- Development of clinical trial designs that satisfy regulatory requirements
- Fundamental and applied statistics

PROFESSIONAL AFFILIATIONS

- American Association of Pharmaceutical Scientists (AAPS)
- American Association for the Advancement of Science
- Business of Life Sciences Student Associate, Kelley School of Business, Indiana University, USA
- American Association for Cancer Research (AACR)
- American Society for Clinical Pharmacology and Therapeutics (ASCPT)